OPEN ACCESS

5 July 2012
ISSN 1992-2248
DOI: 10.5897/SRE
www.academicjournals.org

ACADEMIC JOURNALS
expand your knowledge

About SRE

Scientific Research and Essays (SRE) is a peer reviewed open access journal with the objective of publishing quality research articles in science, medicine, agriculture and engineering such as Nanotechnology, Climate Change and Global Warming, Air Pollution Management and Electronics etc.

SRE has an h5-index of 12 on Google Scholar Metrics

Indexing

Scientific Research and Essays is indexed in: Abstracts on Hygiene and Communicable Diseases

AgBiotech News and Information, Agricultural Engineering Abstracts, Agroforestry Abstracts, Animal Breeding Abstracts, Animal Production Database, Biocontrol News and Information Biofuels Abstracts, Botanical Pesticides, CAB Abstracts, CABI's Environmental Impact Chemical Abstracts (CAS Source Index), Crop Physiology Abstracts, Crop Science Database Dairy Science Abstracts, Field Crop Abstracts, Forest Products Abstracts Forest Science Database, Forestry Abstracts, Google Scholar, Grasslands and Forage Abstracts Helminthological Abstracts, Horticultural Science Abstracts, Irrigation and Drainage Abstracts Leisure, Recreation and Tourism Abstracts, Maize Abstracts, Matrix of Information for The Analysis of Journals (MIAR), Microsoft Academic, Nematological Abstracts.

Open Access Policy

Open Access is a publication model that enables the dissemination of research articles to the global community without restriction through the internet. All articles published under open access can be accessed by anyone with internet connection.

The Scientific Research and Essays is an Open Access journal. Abstracts and full texts of all articles published in this journal are freely accessible to everyone immediately after publication without any form of restriction.

Article License

All articles published by Scientific Research and Essays are licensed under the Creative Commons Attribution 4.0 International License. This permits anyone to copy, redistribute, remix, transmit and adapt the work provided the original work and source is appropriately cited. Citation should include the article DOI. The article license is displayed on the abstract page the following statement:

This article is published under the terms of the Creative Commons Attribution License 4.0 Please refer to https://creativecommons.org/licenses/by/4.0/legalcode for details about Creative Commons Attribution License 4.0

Memberships and Standards

Academic Journals strongly supports the Open Access initiative. Abstracts and full texts of all articles published by Academic Journals are freely accessible to everyone immediately after publication.

All articles published by Academic Journals are licensed under the Creative Commons Attribution 4.0 International License (CC BY 4.0). This permits anyone to copy, redistribute, remix, transmit and adapt the work provided the original work and source is appropriately cited.

Crossref is an association of scholarly publishers that developed Digital Object Identification (DOI) system for the unique identification published materials. Academic Journals is a member of Crossref and uses the DOI system. All articles published by Academic Journals are issued DOI.

Similarity Check powered by iThenticate is an initiative started by CrossRef to help its members actively engage in efforts to prevent scholarly and professional plagiarism. Academic Journals is a member of Similarity Check.

CrossRef Cited-by Linking (formerly Forward Linking) is a service that allows you to discover how your publications are being cited and to incorporate that information into your online publication platform. Academic Journals is a member of CrossRef Cited-by.

Academic Journals is a member of the International Digital Publishing Forum (IDPF). The IDPF is the global trade and standards organization dedicated to the development and promotion of electronic publishing and content consumption.

COUNTER (Counting Online Usage of Networked Electronic Resources) is an international initiative serving librarians, publishers and intermediaries by setting standards that facilitate the recording and reporting of online usage statistics in a consistent, credible and compatible way. Academic Journals is a member of COUNTER

Portico is a digital preservation service provided by ITHAKA, a not-for-profit organization with a mission to help the academic community use digital technologies to preserve the scholarly record and to advance research and teaching in sustainable ways.

Academic Journals is committed to the long-term preservation of its content and uses Portico

Academic Journals provides an OAI-PMH(Open Archives Initiatives Protocol for Metadata Harvesting) interface for metadata harvesting.

Contact

Editorial Office: sre@academicjournals.org

Help Desk: helpdesk@academicjournals.org

Website: http://www.academicjournals.org/journal/SRE

Submit manuscript online http://ms.academicjournals.org

Academic Journals

73023 Victoria Island, Lagos, Nigeria

ICEA Building, 17th Floor, Kenyatta Avenue, Nairobi, Kenya.

Editor-In-Chief

Editors

Table of Content

Table of Content

Scientific Research and Essays Vol. 7(25), pp. 2168-2173, 5 July, 2012
Available online at http://www.academicjournals.org/SRE
DOI: 10.5897/SRE10.107
ISSN 1992-2248 ©2012 Academic Journals

Review

Pesticide use in agriculture: The philosophy, complexities and opportunities

Kishor Atreya[1*], Bishal Kumar Sitaula[1] and Roshan Man Bajracharya[2]

[1]Department of International Environment and Development Studies (Noragric), Norwegian University of Life Sciences (UMB), Post Box 5003, 1432, Ås, Norway.
[2]Aquatic Ecology Centre, Kathmandu University, Kathmandu, Nepal.

Accepted 30 May, 2012

Exaggerated and incompetent use of chemical pesticides in crop production can have adverse effects on human health, natural ecosystems and social capital. The potential impacts are interconnected and complicated, so the current scientific knowledge base of its understanding seems to be imperfect, and the degree of impacts could be much more; therefore the rationality of pesticide use in agriculture ought to be redefined. The paper highlights how disciplinary sciences professed and interpreted multifaceted impacts of pesticide use over time and it explores the opportunities arising from the complexities of such impacts. The opportunity is explored for Nepal as an example.

Key words: Pesticides, health and environmental impacts, complexities, interconnectedness, interdisciplinary, Nepal.

INTRODUCTION

Pesticides are chemical substances used to control harmful organisms. Its use in agriculture can adversely affect human health, environment and eco-systems. Globally, agriculture sector consumes significant amount of pesticides – approximately 85 percent of the estimated 2.9 million tones used each year (Raven et al., 2008). Pesticide use is increasing worldwide, and at a rapid rate in developing countries. The developing nations utilize only 20% of world total pesticides applied. Despite increasing application of tons of pesticides worldwide, more than 40% of all potential food production and another 20% of the harvested crop is lost to pests (Paoletti and Pimentel, 2000). For example, a 33-fold increase in pesticide use in the United States since the 1940s, crop lost due to pest have not changed significantly (Raven et al., 2008). Only a small amount of the applied pesticide actually reaches the intended target organism and the vast majority ends up elsewhere in the environ-ment (Pimentel, 2005; Pimentel and Burgess, 2012). Less than one percent of pesticides applied to the agriculture reach their target pests, and more than 99% of it adversely affects unintended targets including the public and environmental health (Pimentel, 2005). And pesticides pollute environment and ecosystems and marginalize human populace thus its use and sale is under strict control in many developed countries.

In developing countries, the mechanism for controlling pesticide use and sale are rudimentary because of many reasons. Consequently, pesticide users in developing countries, especially agricultural workers or farmers, are significantly exposed to different kinds of pesticide risks. The magnitude of exposure and associated risks for farmers in developing countries are supposed to be high. But farmers have been using such toxic chemicals in their farm to increase production and to maintain their subsistence for living, and also to increase their income. Ironically, in developing nations, farmers are under increasing pressure to use such toxic chemicals because of various social, economical, political and psychological factors. For example, subsidies in chemicals, lack of alternatives to pesticides, week enforcement of laws and regulations, low levels of education and awareness, and ease in availability are the drivers for using pesticides. Whatsoever the factors exacerbating the pesticide use in developing countries, it is well known that it's exaggerated and incompetent use have negative impacts

*Corresponding author. E-mail: k.atreya@gmail.com.

to human and ecosystems health. The areas where pesticides have negative impacts are diverse and complex. For example, bioaccumulation, biomagnifications, pest resistance and resurgence (Raven et al., 2008) are the hotly discussed and threat to the human society. In addition, dumping of un-used and date-expired highly toxic chemicals into soil is also a major threat to human society (WHO, 2007). Further, few linkages among pesticide use, arctic degradation, international transport, and climate change are the newly born issues. Marla Cone's *Silent Snow* (Cone, 2006) illustrated how such dangerous chemicals are being carried to the Arctic by winds and waves. There are also probable linkages between long-term pesticide exposure and human health problems like neurological effects, endocrine disruption, reproductive health and cancer (EPA, 1999).

The current scientific knowledge on these impacts seems to be imperfect, often estimated and interpreted by a single disciplinary science, and could be much more than we believe today; therefore the rationality of its use in agricultural production ought to be redefined. The main objective of the paper is to highlight how the use of pesticides is perceived and interpreted over time and to make aware scientific communities of the opportunities arise from the complexities of such impacts.

The philosophy of pesticide impacts

Scientific enquiry into a specific subject is not merely for gaining knowledge, but also to transfer new knowledge into practical actions for the improvement of human well-being. However, while doing so, this endeavor presupposes knowledge of the appropriate conceptual framework, which, if originally defective will cause a malfunctioning of the system, impacting negatively on the science and the scientific knowledge (Chalmers, 1999). This is what has been observed for the pesticides knowledge. Until the early 1960s, the scientific community and general public operated on the belief that pesticide use revolutionized food production and human development. They had a uniform understanding of the consequences of pesticide use to humankind, focused only on the positive aspects. The human perception, understanding, and the approach to pesticide science, as well as, methods for problem solving, instruments and techniques were all framed on the positive aspects of pesticides. However, when the book *Silent Spring* (Carson, 1962) was published, a revolutionary shift on human thinking from the benefits of pesticides to its negative consequences occurred. This new thinking was supposed to minimize pesticide use in agriculture, but in reality it did not, because shortly after, there was also a shift in agricultural practices from 'primitive' to the so-called 'green revolution'. This transformation of agricultural practices led further increased use of pesticides, in response to increased population growth, poverty and global demand for food, without regard for its negative externalities. The technology based 'green revolution' demands high inputs and cash investment, and also pollutes the environment and, thus, appears unsustainable for future agriculture (Wilson and Tisdell, 2001). Actually, the original paradigm of the green revolution was intended to generate positive consequences like increased productivity, economy and sustainability. But now many scientists have come to the conclusion that the green revolution technology, including pesticides, has negative consequences for the environment and hence, its proper management has become a bigger challenge for maintaining human and ecosystem health, having major implications for survival and quality of life.

From the 1960s to about 1990, there were many competing theories for and against pesticide use. No single theory was widely accepted during that period, indicating a condition of turmoil. During the 1990s, a school of thought emerged with the widely accepted hypothesis that pesticide use in crop cultivation has mainly two explicit effects. The first is an income gain in the short term. The second is the negative impacts on human and ecosystem health. From 1990 to present, thousands of articles supporting a variety of aspects of the pesticide science according the established rules are available in the peer-reviewed journals, books and other literature. Most of the published articles have either supported beneficial effects of pesticides (Cooper and Dobson, 2007) like income gain, or highlighted its negative effects like environmental pollution and human health problems. In 1994, a small group of scientists proposed a new hypothesis for pesticide use that entails overall lower returns to human (Antle and Pingali, 1994; Pingali et al., 1994) in a long term. Despite much literature in favor of this hypothesis, the larger scientific community and private sector are not in favour of accepting the real consequences of pesticide use for human society. The debates are further confounded due to the as yet incomplete scientific understanding of long-term pesticide exposure on human as well as ecosystem health. Looking at the advancement of knowledge of pesticides it can be concluded that at earlier stages, pesticides were observed to be affecting only a single discipline, for example agriculture and consequent crop production. Later on, human society believed that pesticides not only do benefits but also cause negative consequences to their health. At later stage, or say currently, the use of pesticides is believed to cause multiple consequences on social health, environment and ecosystems.

Figure 1 helps to perceive changing knowledge of pesticide use with time. Its interpretation with time depends on the analytical framework of the scientific communities. The initial set of hypotheses (A_1, A_2, . .) made in the past are replaced by new ones, which result in the stepwise development of the pesticides science. Although it is not possible to claim that hypothesis or

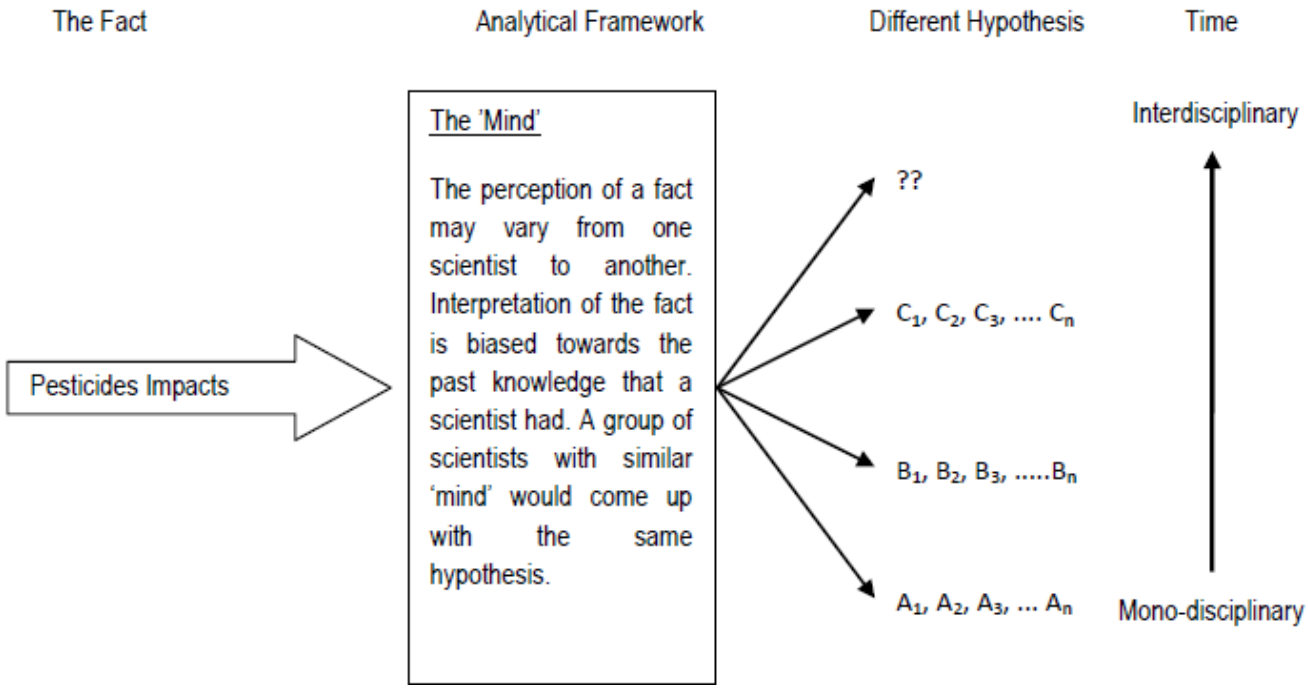

Figure 1. Interpretations of pesticide impacts depend on the analytical framework of the scientific communities and over time changing from mono-disciplinary to interdisciplinary sciences.

theory relating to pesticide use is entirely true, it is plausible to say, for example, that the set of hypotheses (C_1, C_2 . . .) in Figure 1, are closer to the truth than the previous sets (B_1, B_2, . . .) and (A_1, A_2, . . .) and as yet the set C has not been disproved based on the existing knowledge and understanding, but may be replaced in the future.

The hypotheses set C can be considered to be the best based on the current 'mind' on pesticide science, but is not the absolute truth regarding pesticide use because the 'mind' could interpret facts based on different framework in future. The 'fact' is basically constant, but our knowledge and understanding changes due to the changing 'mind', thus the dynamic nature of our 'mind' with reference to perceptions and interpretation of the facts in light of new information will enhance the pesticide knowledge. A chapter of a book (Pimentel and Lehman, 1993) entitled "*The Benefits and Risks of Pesticides: Two Views"* illustrate, for example, how a single fact is interpreted by an industrialist and environmentalist. An industrialist suggests more research on the benefits of pesticides while an environmentalist suggests just opposite. But both realize positive and negative multiple effects of pesticides. And the understandings on the pesticide impacts are shifting from single disciplinary science to multidisciplinary and interdisciplinary. Realization of the multiple impacts of pesticide use either by an 'industrialist' or an 'environmentalist' not only established the interconnectedness and complexities of such impacts into their own defined disciplinary sciences, but also expanded an opportunity for these individual to scientific inquiry into its possible solutions.

The complexity - an opportunity for scientific inquiry

Use of chemical pesticides not only increases crop production and income but also negatively affects human health, pollute soil, water, air; and ultimately the ecosystems as a whole may be collapsed. Although, at the outset, the use of pesticides was believed to be beneficial for human society, it has now become amply evident that this technology may be more of a curse than a boon. The road we passed through was initially attractive (income gain for example) but it appears to be disaster in a long run. It can, some ways, be compared with the invention of nuclear weapons. Despite many positive uses of nuclear power, the two atom bombs detonated in Japan, at the end of the World War II, resulted in the immediate deaths of around 120 thousand people and eventually countless others, had been developed using the same as researched for nuclear energy production. The point here is neither to equate pesticides with nuclear weapons, nor to discount the value of nuclear power, but to illustrate that just as human still suffer from the long-term effects of radiation, agrarian societies that applied persistent chemical pesticides like DDT and BHC in the past, will continue to face health problems from exposure through contaminated soil, water and air. The World Health Organization

(WHO) of the United Nations has estimated that use of pesticides cause 3 million poisonings and 220 thousand deaths and about 750 thousand chronic illnesses every year worldwide (WHO, 2006).

In long-term, the benefits received by the use of pesticides could outweigh by its impacts. Therefore, pesticide use in agricultural farms cannot be viewed in part, rather should addressed the whole system. So the impacts of pesticide use estimated by the single disciplinary science at different levels are minimal and underestimated because they seldom incorporate the whole system approach. Many scientists and scholars (not all) are still working with its own defined field not even interested or willing to see how things interact in a system. It seems that the traditional structures make it hard for researchers to be interdisciplinary and much easier for people to get published in traditional disciplinary settings. However, the use of pesticides in agriculture could be a complex example where scientists may begin to look beyond their boundaries of their own disciplines and try to understand what they are seeing and experiencing. These people will find new ways of thinking and new methodological approaches to gain a better understanding of the pesticide use. As a result, much literature will be emerged in favor of inter-disciplinary science (or whole system approach) for dealing with pesticide dilemma. This is an opportunity for the current scientific world. Integration of knowledge for a complex phenomenon requires close collaboration among scholars from different disciplines. Identifying the full impacts of pesticide use on both physical and biological interacting factors is much more complicated, probably not possible with the current 'mind', thus there is an opportunity to our 'mind' to rethink on the possible methodologies for identifying impacts. For this, (re)examination of the pesticide issues in the broader context of social, environmental, and ecological implications in alliance with many disciplinary sciences and in conjunction with local stakeholders is recommended.

Exploring opportunity- an example of Nepal

At national level, pesticides import substantially increasing in 2007 and 2008, following a general trend of decline since 2002 (Figure 2). According to the Central Bureau of Statistics (CBS, 2003), 25% of Terai land holdings use chemical pesticides, 7% of Mountain, and 9% of Mid-hills. There has been a clear trend towards the increased use of chemical pesticides, especially in semi-rural and peri-urban areas that have easy access to urban markets where a high demand for vegetables, fruits and other fresh produce exists year-round. Chemicals are readily available in the local markets now-a-days. The initial use of chemicals by a few progressive farmers has increased pressure for other farmers to also use them. Generally, pesticides in Nepal are used to control pests such as brown plant hopper, fruit flies and diseases like late blight of potato and tomato. High rates of pesticides are applied to cash crops such as potato, tomato and other vegetables. In Nepal, many studies claimed intensive use of pesticide in the market-oriented agricultural production areas with minimal pesticide use hygiene and safety precaution, but very few of them assessed the health and environmental impacts of its use. The scientific studies on pesticide use and farmers' and environmental health in Nepal are extremely few. Why? It is not an easy task to perform a good scientific study by a single 'actor' taking the multitude of interacting factors, for example, health, environment, ecosystems etc. Either different areas of knowledge required for the 'actor' or a close collaboration among different disciplinary 'actors' is needed. Both are very rare in Nepal. Neither the university degree has an interdisciplinary approach of study, nor institutional collaborations among universities, departments, (I) NGOs, etc. along with local stakeholders are established for handling such complicated problems.

Nepal Agricultural Research Council (NARC), an apex body for agricultural research in the country with ultimate goal of poverty alleviation with sustainable growth of agriculture production is still working itself on its pre-defined traditional working fields like pathology, entomology, soil, agronomy; there is possibility to establish new field of study to include such externalities with other disciplinary sciences. Similarly universities are delivering the same traditional disciplinary sciences over significant time. Some of the world's universities have undergone departmental restructuring to promote interdisciplinary research and collaboration (Lok, 2008), but in Nepal no such interdisciplinary department found at Institute of Agriculture and Animal Science (http://www.iaas.edu.np/departments/index.htm) of the Tribhuvan University and Kathmandu University (http://www.ku.edu.np/departments.php) among many others. Districts agricultural offices under the Department of Agriculture control and manage pesticides issues at local levels. These district level staffs manage and report on the integrated pest management (IPM) an approach to minimize pesticide use and a complex in its nature with multiple benefits without taking care of other disciplinary individuals or public-private partnership for research and extension. In other countries, applications of IPM reduced pesticide use without reducing grain yields. For example, Peshin et al. (2009) documented a reduction in pesticide use by 68% and public health poisonings by 77% in Sweden. In Indonesia, pesticide use was reduced by 65% and increased rice yields by 12% (Oka, 1991). For Nepal, district level staffs manage and report on IPM. Therefore, a revision of the current structure of the IPM research and reporting is warranted with a clear responsibility of a collaborative institutions of the concerned disciplines.

The point here is neither to discount these institutions

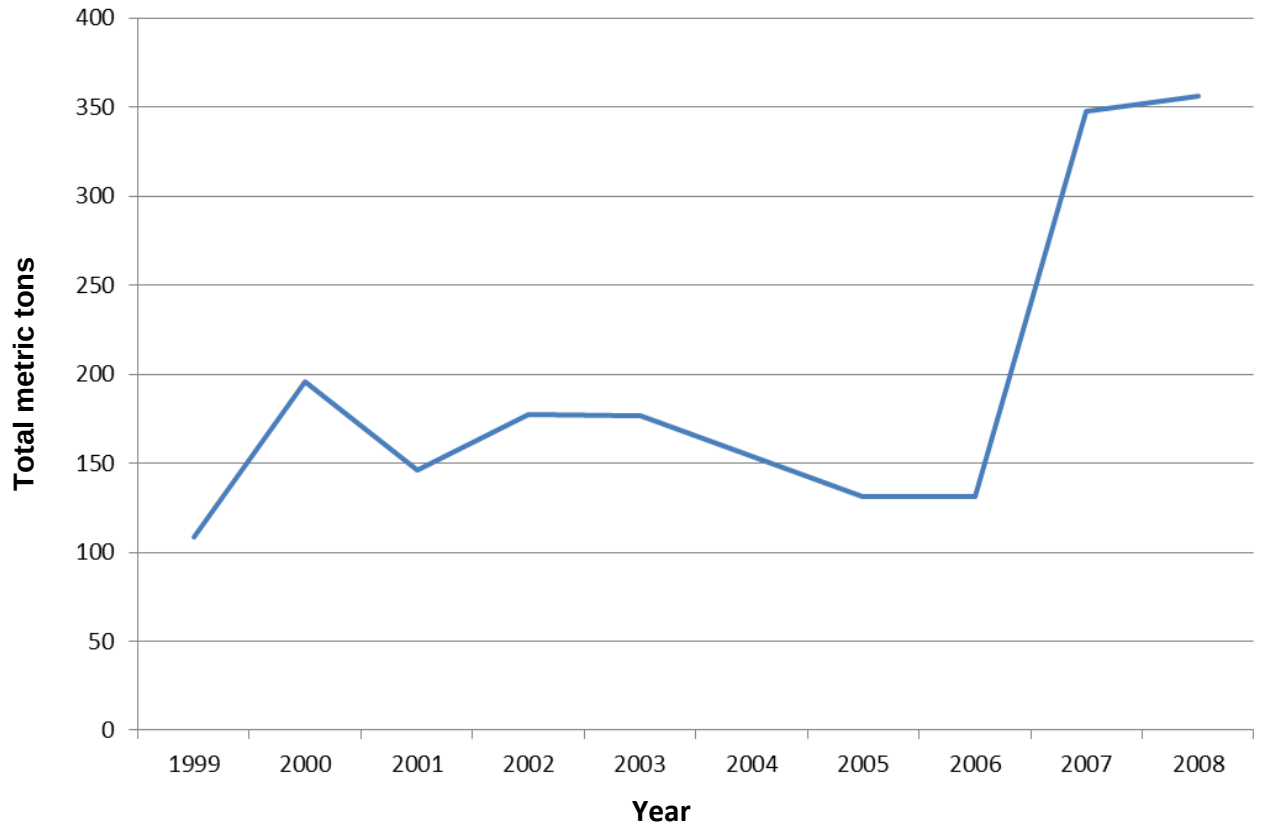

Figure 2. Total metric tons of pesticide's active ingredients import in Nepal during 1999 to 2008.

in their capabilities nor to disqualify their mono-disciplinary functions, rather to suggest incorporation of the global demand of interdisciplinary research and collaboration either by restructuring the present functional mechanisms or by introducing new departments or institutions. Individually these institutions have done number of excellent research in terms of finding impacts and recommending solutions within their disciplinary sciences but no progress be traced for pesticides dilemma because of its multifaceted impacts, and minimal cooperation among different disciplinary individuals/institutions to follow up the recommendations. Therefore, there is a tremendous opportunity to amalgamate these institutions (see Table 1) for studying complex problems like pesticide use, its impacts and management. Adding different ideas from different disciplinary sciences, and sharing knowledge among them is not only a sufficient measure for interdisciplinary approach, rather coming to a consensus through developing a well defined theoretical perspective on the problem analysis (see Table 2) by mutual professional respects and creative 'tension' is warranted.

Because of the complex nature of pesticides impacts, a simple analysis is an insufficient measure of pesticide efficacy. Interdisciplinary holistic systems analyses taking a multitude of interacting factors into account are needed.

CONCLUSION

Single disciplinary sciences seem to have dominated the assessment and evaluation of pesticide use impacts in agriculture. As the pesticides-induced impacts are complex and interconnected in natures, the global know-ledge on pesticides issues over time has been shifting from mono-disciplinary to interdisciplinary sciences. But local efforts to move into new areas of interdisciplinary science are minimal. In Nepal, intensive use of pesticides with minimal hygiene and safety precaution are known but interdisciplinary impacts assessments are extremely few. An alliance with many disciplinary sciences and with local stakeholders either by reorganizing the existing body or by reestablishing new organization/institution is recommended for (re)examine pesticide issues in the broader context of social, environmental, and ecological implications.

ACKNOWLEDGEMENTS

The comments and suggestions received from anonymous reviewers are appreciated. The financial support from the Norwegian Program for Development, Research and Education (Research Grant # NUFUPRO2007/10109) is highly acknowledged.

Table 1. The numbers of 'actors' who ought to work together for problem solving.

1. Governmental Departments – Agriculture, Health, Education etc.
2. Universities – Tribhuvan, Kathmandu, Purbanchal, Pokhara etc.
3. Research Organization – Nepal Academy of Science and Technology (NAST), Nepal Agriculture Research Council (NARC), Nepal Health Research Council (NHRC) etc.
4. (International) non-governmental organizations (I) NGOs – WHO, FAO, ICIMOD, IUCN, Li-Bird, CEPREAD, etc.
5. Local stakeholders – Farmers, pesticide dealers, retailers, etc.

Table 2. Few areas where these 'actors' bring their ideas and knowledge for problem analyses with mutual professional respect.

1. Assessing pesticide use and its health and environmental impacts (farmers, consumers and environmental health) along with social implications.
2. Enforcing rules and regulations of pesticides use and environmental conservation (for example, Pesticides Act 1991, Regulation 1994; Environmental Protection Act 1997, Regulation 1998)
3. Controlling and banning of highly toxic and obsolete pesticides
4. Advocacy for safety precautions while handling and using pesticides
5. Designing and developing new interdisciplinary degrees at university levels to undertake complex problems like pesticides use and climate change
6. Redesigning and redeveloping curriculum of the current university degree focusing on interdisciplinary approach
7. Developing alternatives to chemical pesticides incorporating local knowledge and using local resources, for example integrated pest management
8. Developing mechanisms to inform farmers of the changes in market demands, opportunities, and threats arising from international and national rules, regulations, policies, treaties, etc

REFERENCES

Antle JM, Pingali PL (1994). Pesticides, productivity, and farmer health: a Philippine case study. Am. J. Agric. Econs., 76: 418-430.

Carson R (1962). Silent Spring. Houghton Mifflin Company, New York, USA.

CBS (2003). National Sample Census of Agriculture, Nepal, 2001/02: Highlights. Central Bureau of Statistics, Nepal.

Chalmers AF (1999). What is this thing called sci.? Open Univ. Press, United Kingdom.

Cone M (2006). Silent snow: the slow poisoning of the Arctic. Grove Weidenfeld Publishers, USA.

Cooper J, Dobson H (2007). The benefits of pesticides to mankind and the environment. Crop Prot., 26: 1337-1348.

EPA (1999). Recognition and management of pesticide poisoning. Office of Pesticide Programs, United States Environmental Protection Agency, Washington DC, USA.

Lok C (2008). Harvard under review. Nature, 454: 686-689.

Oka IN (1991). Success and challenges of the Indonesia National Integrated Pest Management Program in the rice-based cropping system. Crop Prot., 10: 163-165.

Paoletti M, Pimentel D (2000). Environmental risks of pesticides versus genetic engineering for agricultural pest control. J. Agric. Environ. Ethics, 12: 279-303.

Peshin R, Bandral RS, Zhang WJ, Wilson L, Dhawan AK (2009). Integrated pest management: a global overview of history, programs and adoption. In Peshin R, and Dhawan AK (Eds.). Integrated pest management: innovation-development process. Springer, India.

Pimentel D (2005). Environmental and economic costs of the application of pesticides primarily in the United States. Environ. Dev. Sustain., 7: 229-252.

Pimentel D, Burgess M (2012). Small amounts of pesticides reaching target insects. Environ. Dev. Sustain., 14(1): 1-2.

Pimentel D, Lehman H (1993). The pesticide question. environment, economics, and ethics. Rutledge, Chapman and Hall, Inc. New York.

Pingali PL, Marquez CB, Palis FG (1994). Pesticides and Philippine rice farmer health: a medical and economic analysis. Am. J. Agric. Econ., 76: 587-592.

Raven PH, Berg LR, Hassenzahl DM (2008). Environ. John Wiley and Sons Inc, USA.

WHO (2006). Preventing disease through healthy environments: Towards an estimate of the environmental burden of disease. World Health Organization of the United Nations Paris, France.

WHO (2007). The World Health Report 2007 - a safer future: global public health security in the 21st century. World Health Organization of the United Nations, Geneva, Switzerland.

Wilson C, Tisdell C (2001). Why farmers continue to use pesticides despite environmental, health and sustainability costs. Ecol. Econ., 39: 449-462.

Scientific Research and Essays Vol. 7(25), pp. 2174-2188, 5 July, 2012
Available online at http://www.academicjournals.org/SRE
DOI: 10.5897/SRE11.619
ISSN 1992-2248 © 2012 Academic Journals

Review

The effect of ceramic in combinations of two sigmoid functionally graded rotating disks with variable thickness

Aidy Ali[1]*, M. Bayat[1], B. B. Sahari[1], M. Saleem[2] and O. S. Zaroog[3]

[1]Department of Mechanical Engineering, Universiti Pertahanan Nasional Malaysia, Kem Sungai Besi, 57000 UPM, Kuala Lumpur ,Malaysia.
[2]Department of Applied Mathematics, Z.H. College of Engineering and Technology, A.M.U., India.
[3]Department of Mechanical Engineering, Universiti Tenaga Nasional, 43009 Kajang, Selangor ,Malaysia.

Accepted 30 May, 2012

This paper present the elastic solutions of the disk made of functionally graded material (FGM) with variable thickness subjected to rotating load. The material properties are presented by combination of two sigmoid FGM (S-FGM) and disk thickness profile are assumed to be represented by power law distributions. Aluminum-ceramic-aluminum FG rotated disk is considered. Hollow disks are considered and the solutions for the stresses and displacements are given under appropriate boundary conditions. The results in metal-ceramic-metal FGMs are presented and compared with the known results in the literature. The solutions for S-FGM are compared with that of non FGM, and for variable thickness and for uniform thickness. The effects of the material grading index, n, and the geometry of the disk on the stress and displacement are investigated. It is found that a FG disk with concave thickness profile has smaller stresses and displacements compared with the concave or linear by variable thickness profile. The results in metal-ceramic or ceramic-metal and metal-ceramic-metal FGMs are compared. These results suggest that a rotating FG disk with metal-ceramic-metal can be more efficient than the one with ceramic-metal or metal-ceramic.

Key words: Rotating disk, variable thickness, elasticity, sigmoid functionally graded material.

INTRODUCTION

Functionally graded materials (FGMs) are defined as those materials in which the volume fraction of the two or more materials is varied, as a power-law, sigmoid or exponential distribution, continuously as a function of position along certain dimension(s) of the structure (Reddy, 2000; Suresh and Mortensen, 1998). These materials are mainly constructed to operate in high temperature environments.

Rotating disks have many practical engineering applications such as in steam and gas turbine rotors, turbo generators, internal combustion engines, fly wheels, turbojet engines, reciprocating and centrifugal compressors just to mention a few. Brake disk can be an example of solid rotating disk where only body force is involved. Solid disks can also be found in components such as cover plates of rotating components and idlers used in belt assemblies.

In a turbine rotor, there is always a possibility that the heat from the external surface transmits to the shaft and from it to the bearings causing adverse effects on its function and efficiency. To deal with this situation and to prevent heat from being transferred to the shaft and bearings, the disk can be made of FGM with ceramic-rich at the outer surface and metal-rich at the inner surface. While the heat resistant property of the ceramic at the outer surface prevents heat from being transferred, the metal at the inner surface helps carry the stress for the transmission of torque from the disk to the shaft.

The boundary conditions of the disk depend on the way

*Corresponding author. E-mail: aidyali@.upnm.edu.my. Tel: +60172496293. Fax: +60 3 86567122.

the disk is attached to the shaft. For a disk connected rigidly to the shaft (by means of welding or shaft and rotor disk cast together), a fixed-free condition applies. On the other hand, for the disk connected to the shaft by means of splines where small axial movement is allowed, a free-free condition applies. Flywheels and gear wheels are other examples of fixed-free conditions usually used for storing kinetic energy and transmitting mechanical power, respectively.

In any of the mentioned applications, the performance of the component in terms of efficiency, service life and power transmission depends on the material, speed of rotation and operating conditions. Normally, a component can be fabricated using any metal. However, for some specific applications such as in aerospace engineering where the component's weight and durability in high temperature environment are so crucial, the components need to be fabricated using special material such as a FGM. FGMs are usually made of a mixture of ceramic and metals. The ceramic constituent of the material provides the high temperature resistance due to its low thermal conductivity. The ductile metal constituent, on the other hand, prevents fracture caused by stress due to high temperature gradient in a very short period of time (Reddy et al., 1999).

Fukui et al. (1993) considered a thick-walled FG tube under uniform thermal loading and investigated the effect of graded components on residual stresses. They further estimated the optimum composition gradient generated by compressive circumferential stress at the inner surface. Boussaa (2000) investigated the problem of optimizing the composition profile of a FG interlayer inserted between a metallic tube and a ceramic coating so as to alleviate the thermal stresses occurring at the metal–ceramic interface. Jabbari et al. (2003) presented the general theoretical analysis of two-dimensional steady-state thermal stresses for a hollow thick cylinder made of FGM.

Horgan and Chan (1999) investigated the effects of material inhomogeneity on the response of linearly-elastic isotropic solid circular disks or cylinders rotating at constant angular velocity about its axis of symmetry. A special case of a body with Young's modulus depending on the radial coordinate only and constant Poisson's ratio was examined. For the case when the Young's modulus had a power-law dependence on the radial coordinate, explicit exact solutions were obtained.

Many studies conducted on FGMs were related to the analysis of thermal stresses and deformations (Liew et al., 2003; Ootao and Tanigawa, 1999; Ootao and Tanigawa, 2004; Shahsiah and Eslami, 2003). Ruhi et al. (2005) presented a semi-analytical thermo elastic solution for finitely long thick-walled cylinders made of FGMs.

Durodola and Attia (2000a, b) presented a finite element analysis for FG rotating disks using comercial software package. The disks were modeled as non-homogeneous orthotropic materials such as those obtained through non-uniform reinforcement of metal matrix by long fibers. They considered three types of gradation distributions of the Young's modulus E in the hoop direction relative to matrix material modulus. Kordkheili and Naghdabadi (2007) presented semi-analytical thermo elastic solutions for hollow and solid rotating axisymmetric disks made of FGMs under plane stress condition. They compared their results with those of Durodola and Attia (2000a, b) under the centrifugal loading.

Although many earlier studies on rotating disks (Tutuncu, 1995) have considered disks with uniform thickness, several authors have emphasized the importance of variable thickness in the rotating disks (Eraslan, 2003; Eraslan and Argeso, 2002; Guven, 1992; Reddy and Srinath, 1974). Recent studies (Eraslan and Orcan, 2002; Orcan and Eraslan, 2002) indicated that stresses in rotating disks (annular or solid) with variable thickness are much lower than those in a uniform-thickness disk at the same angular velocity. Jahed at al. (2005) analyzed an inhomogeneous disk model with variable thickness to achieve minimum weight of disk. Using the variable material properties method, stresses were obtained for the disk under rotation and a steady temperature field. Bayat et al. (2008) analyzed the FG gear wheel with variable thickness using material properties as a single power-law FGM (P-FGM).

To the best of authors' knowledge, no work has been reported to date which concerns with the analysis of the combination of two sigmoid FG (S-FG) disks with variable thickness. This very fact motivates the present study. In this paper, a thin FG disk with variable thickness (Figure 1) subjected to centrifugal loading due to constant angular velocity is considered. The thickness of the disk is assumed to be sufficiently small compared to its diameter and plane stress condition is applied. The symmetry with respect to the rotational axis and the mid-plane is assumed. This work aims to investigate the effect of combination of two S-FGMs and property gradation and also the geometry of the disk on stresses and displacements in hollow disks under free-free and fixed-free boundary conditions. The non-dimensional stress and displacement components in the radial direction are given using semi-analytical method based on the form of the sigmoid distribution for the mechanical properties of the constituent components and hyperbolic distribution for the thickness profile.

To implement the semi-analytical method in numerical studies, the radial domain of the disk is divided into some virtual sub-domains where, in each sub-domain, the mechanical property is assumed to be constant. This assumption yields the governing equilibrium equations in each sub-domain as ordinary differential equations with constant coefficients whose general solution can be written involving certain unknowns. These unknowns can be determined as solution of systems of linear algebraic

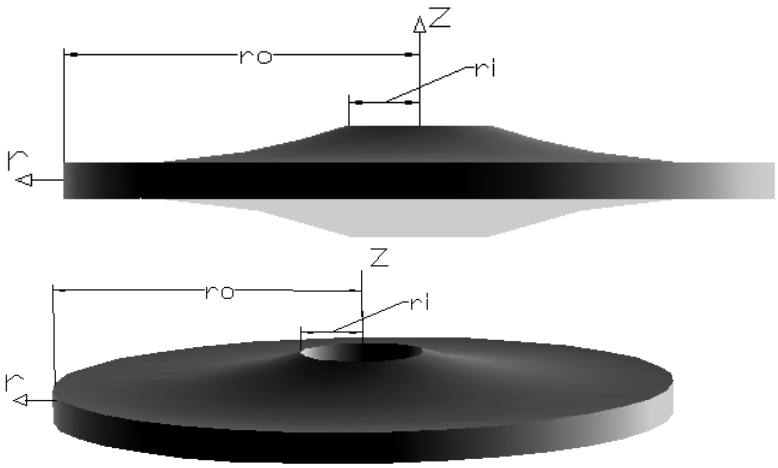

Figure 1. Configuration of a thin disk with variable thickness.

equations obtained by imposing the continuity conditions at the interface of the adjacent sub-domains together with global conditions. Increasing the number of sub-domains (divisions) in the radial direction increases the accuracy in the solution.

GRADATION RELATION

In this study, the property variation P of the material in the FG disk along the radial direction is assumed to be the following form (Chi and Chung, 2006):

$$P(r) = g_1(r)P_1 + (1 - g_1(r))P_2 \;\; ; \quad r_1 < r < \bar{r} \tag{1a}$$

$$P(r) = g_2(r)P_1 + (1 - g_2(r))P_2 \;\; ; \quad \bar{r} < r < r_2 \tag{1b}$$

Where

$$g_1(r) = 1 - \frac{1}{2}\left(\frac{r - r_1}{\bar{r} - r_1}\right)^n \;\; ; \; r_1 < r < \bar{r} \tag{1c}$$

$$g_2(r) = \frac{1}{2}\left(\frac{r_2 - r}{r_2 - \bar{r}}\right)^n \;\; ; \; \bar{r} < r < r_2 \tag{1d}$$

$$\bar{r} = \frac{r_2 + r_1}{2} \tag{1e}$$

Here, P_1 and P_2 are the corresponding properties of materials 1 and 2 of the disk; r_1 and r_2 are the radius that there exist full materials 1 and 2, respectively; $n \geq 0$ is the volume fraction exponent (also called grading index in this paper); $g(r)$ is power low function; $\bar{r}$ is the mean radius of r_1 and r_2. In this study, the Poisson's ratio ν is assumed to be constant and the elastic modulus E and the density ρ are assumed to vary according to the gradation relations (1), for example, the assumed form for the modulus of elasticity E is:

$$E(r) = g_1(r)E_1 + (1 - g_1(r))E_2 \;\; ; \quad r_1 < r < \bar{r} \tag{2a}$$

$$E(r) = g_2(r)E_1 + (1 - g_2(r))E_2 \;\; ; \quad \bar{r} < r < r_2 \tag{2b}$$

By using Equations 1 and considering two types of S-FGMs, first aluminum-ceramic between r_i (inner radius of the disk) and $\frac{r_o + r_i}{2}$ (r_o is outer radius of disk); second ceramic-aluminum between $\frac{r_o + r_i}{2}$ and r_o. The variation of non-dimensional modulus of elasticity, $\frac{E}{E_c}$, with non-dimensional radial distance, $\frac{r}{r_o}$, is shown in Figure 2.

The thickness-profile h of the disk is assumed to vary radially according to the following form:

$$h(r) = h_o\left(1 - \left(\frac{r}{q + r_o}\right)^m\right) \tag{3a}$$

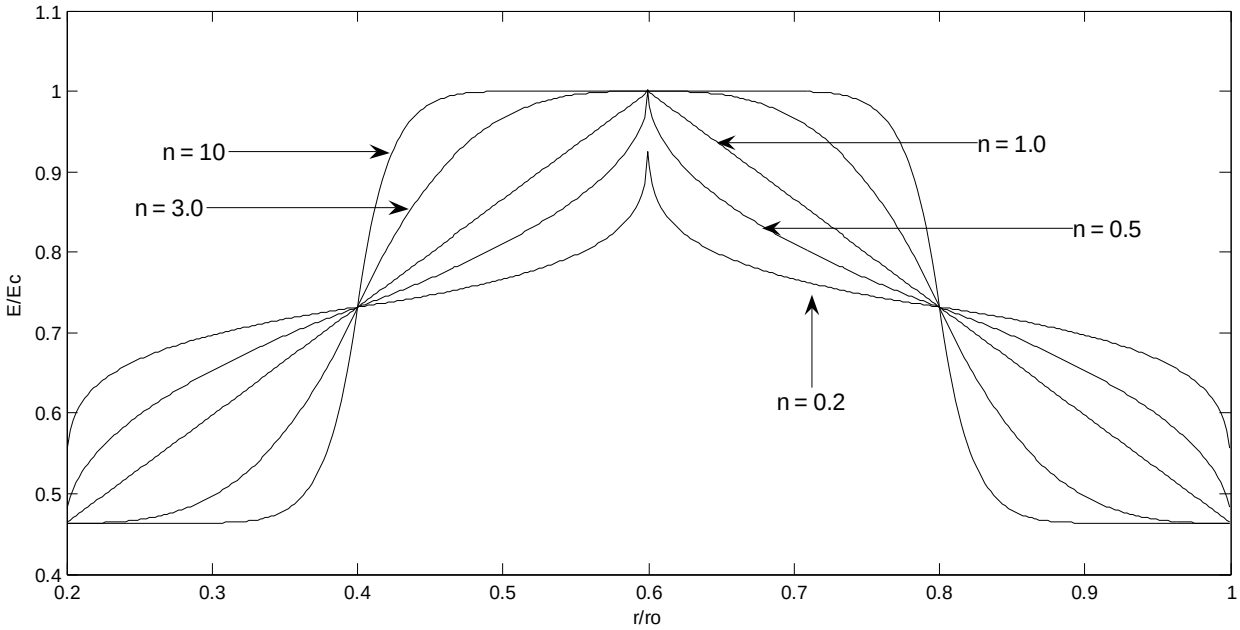

Figure 2. Variation of the non-dimensional elastic modulus versus non-dimensional radius

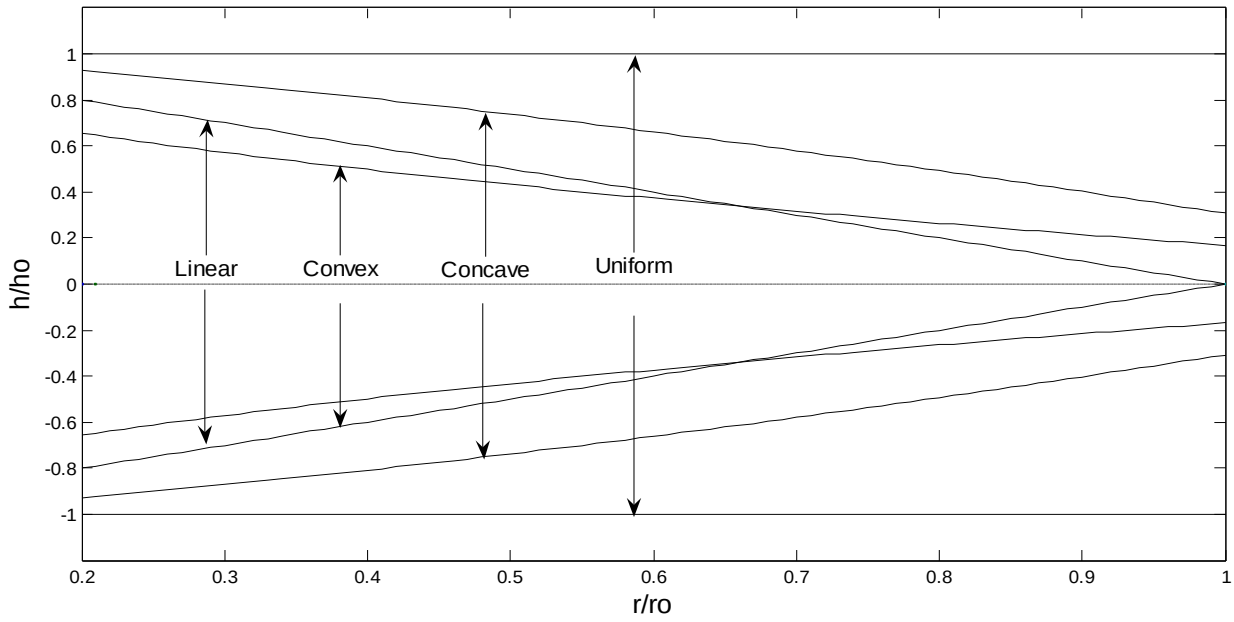

Figure 3. Variation of non-dimensional thickness versus non-dimensional radius.

Here, q and m are geometric parameters such that $0 \le q < 1, m > 0$; h_o is the thickness at the axis of the disk. A uniform thickness disk can be obtained by setting $q \neq 0, m \to \infty$. A linearly decreasing thickness can be obtained for $m = 1$. The profile is concave if $m < 1$ and it is convex if $m > 1$. Different forms of the thickness profiles are shown in Figure 3.

For a future reference, another important parameter that is, the ratio of the weight of the double S-FG disk, W, and the weight of all-ceramic disk of same size, W_{Cer}, denoted by W / W_{Cer} can be defined as:

$$W/W_{Cer}=\left(\int_{r_i}^{\frac{3r_i+r_o}{4}} r\ g_1(r)\rho_{Al}+(1-g_1(r))\rho_{Cer}\left(1-\left(\frac{r}{q+r_o}\right)^m\right)dr\right)/\int_{r_i}^{r_o} r\left(\rho_{Cer}\left(1-\left(\frac{r}{q+r_o}\right)^m\right)\right)dr+$$
$$\left(\int_{\frac{3r_i+r_o}{4}}^{\frac{r_i+r_o}{2}} r\ g_2(r)\rho_{Al}+(1-g_2(r))\rho_{Cer}\left(1-\left(\frac{r}{q+r_o}\right)^m\right)dr\right)/\int_{r_i}^{r_o} r\left(\rho_{Cer}\left(1-\left(\frac{r}{q+r_o}\right)^m\right)\right)dr+$$
$$\left(\int_{\frac{r_i+r_o}{2}}^{\frac{r_i+3r_o}{4}} r\ g_1(r)\rho_{Cer}+(1-g_1(r))\rho_{Al}\left(1-\left(\frac{r}{q+r_o}\right)^m\right)dr\right)/\int_{r_i}^{r_o} r\left(\rho_{Cer}\left(1-\left(\frac{r}{q+r_o}\right)^m\right)\right)dr+$$
$$\left(\int_{\frac{r_i+3r_o}{4}}^{r_o} r\ g_2(r)\rho_{Cer}+(1-g_2(r))\rho_{Al}\left(1-\left(\frac{r}{q+r_o}\right)^m\right)dr\right)/\int_{r_i}^{r_o} r\left(\rho_{Cer}\left(1-\left(\frac{r}{q+r_o}\right)^m\right)\right)dr \quad (3b)$$

with ρ_{Cer} denoting the density of the all-ceramic disk. W/W_{Cer} will be used to compare the weights of FG disks with the weight of all-ceramic disk in the following sections.

THEORETICAL FORMULATION AND EQUILIBRIUM EQUATIONS

Consider a hollow axial symmetric FG disk with variable thickness with inner radius r_i and outer radius r_o, as shown in Figure 1. The disk rotates at an angular velocity ω. The problem is assumed to be plane stress. Due to the axial symmetry assumptions in geometry and loading, cylindrical coordinate system (r,θ,z) is used. The inner and outer surfaces of the FG disk are assumed to be metal-rich and at radius $\overline{r}$ ceramic-rich is assumed. Between these two surfaces, the material properties vary according to Equations 1.

It may be mentioned that although a metal-rich at the inner and outer surfaces and full-ceramic at mid way between inner and outer surfaces, material gradient has been considered for all the disks in this paper. The method of solution that has been followed is independent of such a gradient and may be applied to other gradients as well. However, several applications considered in this paper such as an FG gear wheel mounted on a shaft-support justify consideration of metal-rich inner and outer surface of the disks. Also, for an FG gear wheel mounted on shaft-support ductility plays an important role and thus the metal dominated inner and outer surface of the disk is further justified.

Strains and displacement field

Using the infinitesimal theory of elasticity and the rotational symmetry, the strain-displacement relations are:

$$\varepsilon_r=\frac{du}{dr} \quad (4a)$$

$$\varepsilon_\theta=\frac{u}{r} \quad (4b)$$

Where u is the radial displacement. Also, the linear constitutive elastic equations in the cylindrical coordinate are used in the form of:

$$\sigma_r=\frac{E(r)}{1-\nu^2}(\varepsilon_r+\nu\varepsilon_\theta) \quad (5a)$$

$$\sigma_\theta=\frac{E(r)}{1-\nu^2}(\varepsilon_\theta+\nu\varepsilon_r) \quad (5b)$$

Where E is the modulus of elasticity and ν is the Poisson's ratio.

Equilibrium equations

For a rotating disk, if U_1 is the total strain energy of the body and V_1 is the total potential energy of external force, then the total energy Π can be represented as:

$$\Pi=U_1+V_1 \quad (6)$$

The principle of minimum total potential energy states:

$$\delta(U_1+V_1)\equiv\delta\Pi=0 \quad (7)$$

And this yield

$$\delta U_1=\int_V\sigma_{ij}\delta\varepsilon_{ij}dV=\int_{r_i}^{r_o}\int_{-h(r)/2}^{h(r)/2}2\pi(\sigma_r\delta\varepsilon_r+\sigma_\theta\delta\varepsilon_\theta)rdzdr=\int_{r_i}^{r_o}\int_{-h(r)/2}^{h(r)/2}2\pi(\sigma_r\delta(\frac{du}{dr})+\sigma_\theta\delta(\frac{u}{r}))rdzdr \quad (8)$$

Here, V represents the total volume of disk. For the body force, the potential energy of applied load is given by:

$$\delta V_1=-(2\pi\int_{r_i}^{r_o}\int_{-h/2}^{h/2}\rho r\omega^2 rdzdr)\delta u \quad (9)$$

Substituting for U_1 and V_1 form Equations 8 and 9 into Equation 7, and integrating once, one gets

$$\frac{d}{dr}(h(r)r\sigma_r)-h(r)\sigma_\theta+h(r)\rho(r)\omega^2r^2=0 \quad (10)$$

The equilibrium equation is obtained, the results is the same as Reddy and Srinath (1974) and yields the Navier equation for the radial displacement as follows:

$$rh_r E_r \frac{d^2u}{dr^2} + \left(rE_r \frac{dh_r}{dr} + rh_r \frac{dE_r}{dr} + E_r h_r \right) \frac{du}{dr} +$$
$$\left(\nu E_r \frac{dh_r}{dr} + \nu h_r \frac{dE_r}{dr} - \frac{1}{r} E_r h_r \right) u + \left(1-\nu^2\right) h_r \rho_r r^2 \omega^2 = 0 \qquad (11)$$

Here, for brevity, symbols h_r, E_r and ρ_r have been used for the functions $h(r)$, $E(r)$ and $\rho(r)$, respectively. In Equation 11, the displacement u is a function of r only due to axial symmetry and plane stress condition.

BOUNDARY CONDITIONS

Hollow disk free-free

The following traction conditions on the inner and outer surfaces of the rotating hollow disk must be satisfied.

$$\sigma_r = 0 \quad r = r_i$$
$$\sigma_r = 0 \quad r = r_o \qquad (12)$$

Hollow disk fixed-free

$$u = 0 \quad r = r_i$$
$$\sigma_r = 0 \quad r = r_o \qquad (13)$$

NON-DIMENSIONAL FORM

Navier Equation 11 and the boundary conditions given by Equations 12 and 13 can be written in non-dimensional form using the following set of variables:

$$R = \frac{r}{r_o},\ H_R = \frac{h_r}{h_o},\ \overline{E_R} = \frac{E_r}{E_c},\ U = \frac{u}{u_o},\ \overline{\rho_R} = \frac{\rho_r}{\rho_c}, \qquad (14)$$

Where

$$u_o = \frac{\rho_c r_o^3 \omega^2}{E_c}.$$

The non-dimensional form of Equation 4 is then given by:

$$RH_R \overline{E_R} \frac{d^2U}{dR^2} + \left(R\overline{E_R} \frac{dH_R}{dR} + RH_R \frac{d\overline{E_R}}{dR} + \overline{E_R} H_R \right) \frac{dU}{dR} +$$
$$\left(\nu \overline{E_R} \frac{dH_R}{dR} + \nu H_R \frac{d\overline{E_R}}{dR} - \frac{1}{R} \overline{E_R} H_R \right) U + \left(1-\nu^2\right) H_R \overline{\rho_R} R^2 = 0, \qquad (15)$$

Where

$$\overline{E_R} = g_1(r)\overline{E_{R_i}} - g_1(r) + 1 \ ; \quad r_i < r < \frac{3r_i + r_o}{4}$$

$$\overline{E_R} = g_2(r)\overline{E_{R_i}} - g_2(r) + 1 \ ; \quad \frac{3r_i + r_o}{4} < r < \frac{r_i + r_o}{2}$$

$$\overline{E_R} = g_1(r) + (1 - g_1(r))\overline{E_{R_i}} \ ; \quad \frac{r_i + r_o}{2} < r < \frac{r_i + 3r_o}{4}$$

$$\overline{E_R} = g_2(r) + (1 - g_2(r))\overline{E_{R_i}} \ ; \quad \frac{r_i + 3r_o}{4} < r < r_o$$

$$\overline{E_{R_i}} = \frac{E_{al}}{E_c}$$

$$H_R = R^{-m} \qquad (16)$$

Non-dimensional boundary conditions

Hollow disk free-free

For this case, the boundary conditions of Equation 12 reduce to

$$\overline{\sigma_R} = \frac{\overline{E_R}}{1-\nu^2}\left(\frac{dU}{dR} + \nu \frac{U}{R} \right) = 0 \qquad R = R_i \qquad \overline{\sigma_R} = 0$$
$$R = 1 \qquad (17)$$

Hollow disk fixed-free

Boundary conditions of Equation 13 turn out to be

$$U = 0 \quad R = R_i$$
$$\overline{\sigma_R} = 0 \quad R = 1 \qquad (18)$$

It may be noted that the study of Equation 15 in non-dimensional form makes the absolute values of properties and the loading speed unimportant.

ELASTIC SOLUTION

A closed-form solution of Equation 15 with variable coefficients seems to be difficult, if not impossible, to obtain. The method of analysis is the same as describe in Bayat et al. (2008). However, for completeness of the present paper, the method is also presented here.

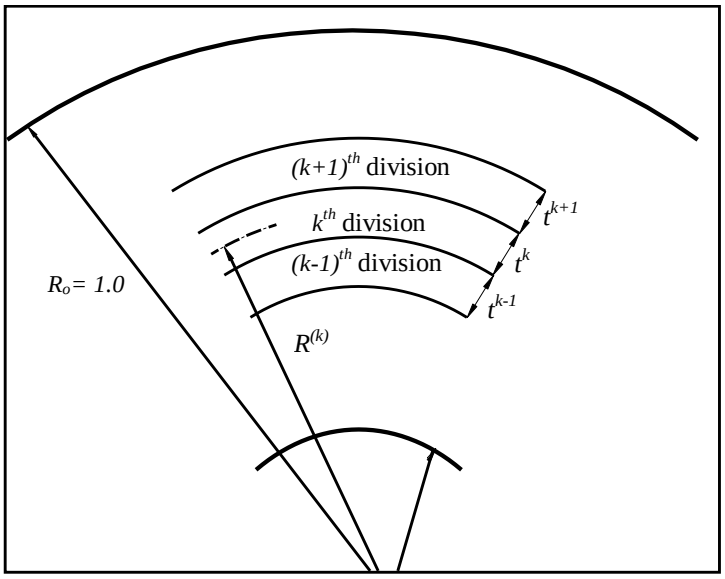

Figure 4. Dividing radial domain into some finite sub-domains.

Hence, in this study a semi-analytical solution of Equation 15 is attempted. In this method, a disk is divided into some virtual sub-domains (say q), with $t^{(k)}$ denoting the radial-width of the k^{th} sub-domain as shown in Figure 4. Evaluating the coefficients of Equation 15 at $R = R^{(k)}$, the mean radius of the k^{th} division, an ordinary differential equation with constant coefficients is obtained which is valid in k^{th} sub-domain. That is:

$$\left(c_1^{(k)} \frac{d^2}{dR^2} + c_2^{(k)} \frac{d}{dR} + c_3^{(k)} \right) U^{(k)} + c_4^{(k)} = 0 , \qquad (19)$$

Where

$$c_1^{(k)} = R^{(k)} H_{R^{(k)}} \overline{E_{R^{(k)}}}$$

$$c_2^{(k)} = R^{(k)} \overline{E_{R^{(k)}}} \left. \frac{dH_R}{dR} \right|_{R=R^{(k)}} + R^{(k)} H_{R^{(k)}} \left. \frac{d\overline{E_R}}{dR} \right|_{R=R^{(k)}} + H_{R^{(k)}} \overline{E_{R^{(k)}}}$$

$$c_3^{(k)} = \nu \overline{E_{R^{(k)}}} \left. \frac{dH_R}{dR} \right|_{R=R^{(k)}} + \nu H_{R^{(k)}} \left. \frac{d\overline{E_R}}{dR} \right|_{R=R^{(k)}} - \frac{1}{R^{(k)}} H_{R^{(k)}} \overline{E_{R^{(k)}}}$$

$$c_4^{(k)} = (1-\nu^2) H_{R^{(k)}} \overline{\rho_{R^{(k)}}} (R^{(k)})^2 . \qquad (20)$$

Using the mentioned technique, Equation 15 with variable Coefficients is changed into a system of q ordinary differential equations with constant coefficients with q being the number of virtual sub-domains.

The solution for Equation 19 can be written in the form of:

$$U^{(k)} = X_1^{(k)} \exp(\lambda_1^{(k)} R) + X_2^{(k)} \exp(\lambda_2^{(k)} R) - \frac{c_4^{(k)}}{c_3^{(k)}} , \qquad (21)$$

Where $X_1^{(k)}$ and $X_2^{(k)}$ are unknown constants for k^{th} sub-domain and

$$\lambda_1^{(k)}, \lambda_2^{(k)} = - \frac{c_2^{(k)} \pm \sqrt{{c_2^{(k)}}^2 - 4 c_3^{(k)} c_1^{(k)}}}{2 c_1^{(k)}}$$

Also, the solution of Equation 21 is valid for

$$R^{(k)} - \frac{t^{(k)}}{2} \le R \le R^{(k)} + \frac{t^{(k)}}{2} . \qquad (22)$$

Where $R^{(k)}$ and $t^{(k)}$ are the mean radius and the radial-width of the k^{th} sub-domain, respectively. The unknowns $X_1^{(k)}$ and $X_2^{(k)}$ can be determined by applying the necessary conditions between each two adjacent sub-domains. For this purpose, the continuity of the radial displacement U as well as radial stress $\overline{\sigma_R}$ is imposed at the interfaces of the adjacent sub-domains. The continuity conditions at interfaces are given by:

Table 1. Different cases of thickness profiles.

Variable	$m<1$	$q\neq 0, m\to\infty$	$m>1$	$m=1$
	Case(a)	**Case (b)**	**Case (c)**	**Case (d)**
Thickness profile (Equation 3a)	Parabolic concave	Constant thickness	Parabolic convex	Linear

Table 2. Variation of non-dimensional weight with grading index n and thickness profile.

Thickness profile (Equation 2) Cases	Values of weight ratio, W/W_c, (Equation 3b)				
	Full-metal	**n = 1**	**n = 5.0**	**Full-metal, full-ceramic, full-metal**	**Full-ceramic**
a) Parabolic concave	0.4737	1194/1580 = 0.7559	1207/1580 = 0.7641	1209/1580 = 0.7652	1
b) Uniform	0.4737	2016/2736 = 0.7368	2016/2736 = 0.7368	2016/2736 = 0.7368	1
c) Parabolic convex	0.4737	684/909 = 0.7525	690/909 = 0.7591	692/909 = 0.7613	1
d) Linear	0.4737	659/851 = 0.7444	673/851 = 0.7908	675/851 = 0.7932	1

$$U^{(k)}\Big|_{R=R^{(k)}+\frac{t^{(k)}}{2}} = U^{(k)}\Big|_{R=R^{(k+1)}-\frac{t^{(k+1)}}{2}}$$
$$\overline{\sigma_R^{(k)}}\Big|_{R=R^{(k)}+\frac{t^{(k)}}{2}} = \overline{\sigma_R^{(k)}}\Big|_{R=R^{(k+1)}-\frac{t^{(k+1)}}{2}} \quad (23)$$

These conditions together with the global boundary conditions of Equation 17 or Equation 18 yield a set of linear algebraic equations in $X_1^{(k)}$ and $X_2^{(k)}$. Solving these equations for $X_1^{(k)}$ and $X_2^{(k)}$ and substituting them in Equation 21, the displacement component, U, is determined in each sub-domain. Increasing the number of divisions improves the accuracy of the results.

NUMERICAL RESULTS

For numerical illustration of the elastic solutions of this study, it is assumed that all the disks considered have the same volume. The same volume of the disks can be achieved by suitably choosing the value of h_o. It can be noted that the results obtained in this study are based on the non-dimensional formulation and thus are independent from the absolute value of h_o.

Two cases namely hollow disk free-free, hollow disk fixed-free are considered. The analysis is conducted using aluminum as the inner-surface metal and Zirconia as outer-surface ceramic the same as that considered by Bayat et al. (2008). The material properties are:

$$E_{Al}=70.0\,GPa \quad , \quad E_{Cer}=151.0\,GPa$$
$$\rho_{Al}=2700.0kg/m^3 \quad , \quad \rho_{Cer}=5700.0kg/m^3 \, , \quad \nu=0.3 \quad (24)$$

A hollow disk with $R_o=5R_i$ or a solid disk rotating at constant angular velocity is considered here. Different cases for the thickness profiles used in numerical illustrations are shown in Table 1.

The following four sets of parameter values for m (each set representing a particular case of Table 1) are considered.

$$a: q=0.30,\ m=1.4$$
$$b: q\neq 0.0,\ m\to\infty$$
$$c: q=0.4,\ m=0.55$$
$$d: m=1.0 \quad (25)$$

The elastic deformation of disk with variable thickness due to rotation is determined. The effect of grading index, n, and variable thickness on the non-dimensional weight of the hallow disk is shown in Table 2. It can be seen that all-ceramic disks are the heaviest whereas full-metal disk is the lightest. The weight of FG disk is in between the all-ceramic and all-metal values.

For the values chosen for q and m as given in Equation 25, each thickness profile of the disk has 70% thickness reduction at the outer surface. The effect of thickness profile on the weight can be shown by comparing the weight values for the same value of grading index n. It can be noted both numerators and denominators are changed, by considering the numerators: it is seen that hollow FG disk with linear thickness profile has smaller weight compared to that with other thickness profiles; Figure 3 may be referred to for more details. To show the effect of grading index n on the weight, disks with the same thickness profile are considered. It is noticed that the weights of FG disks lie in

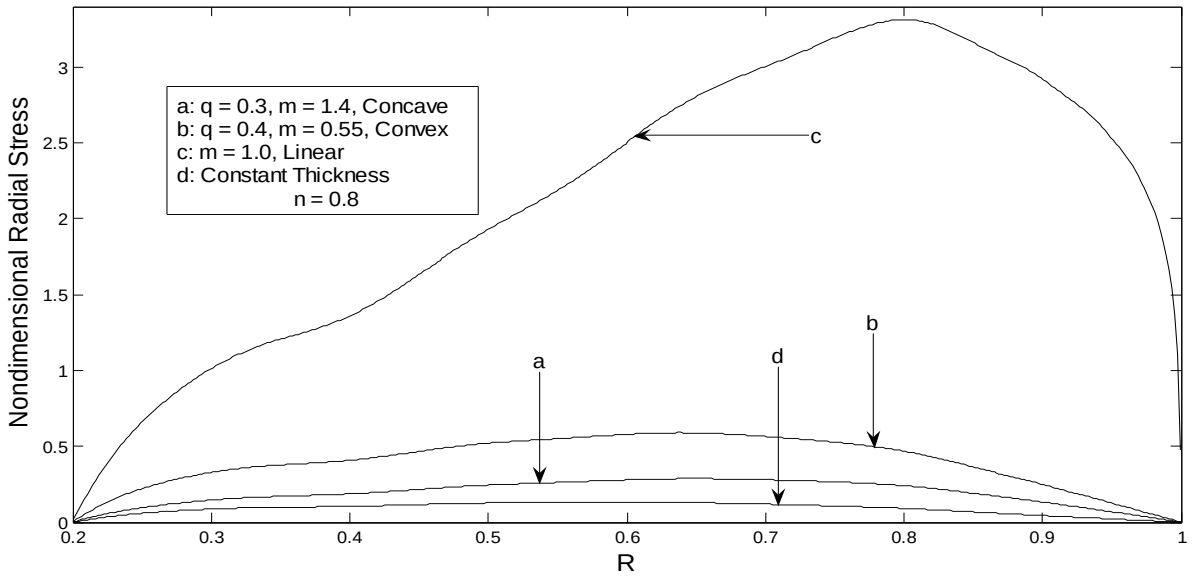

Figure 5. Variation of $\overline{\sigma_R}$ versus R for free-free hollow disk in the FG disk with variable thickness for different values of the geometric parameters q and m .

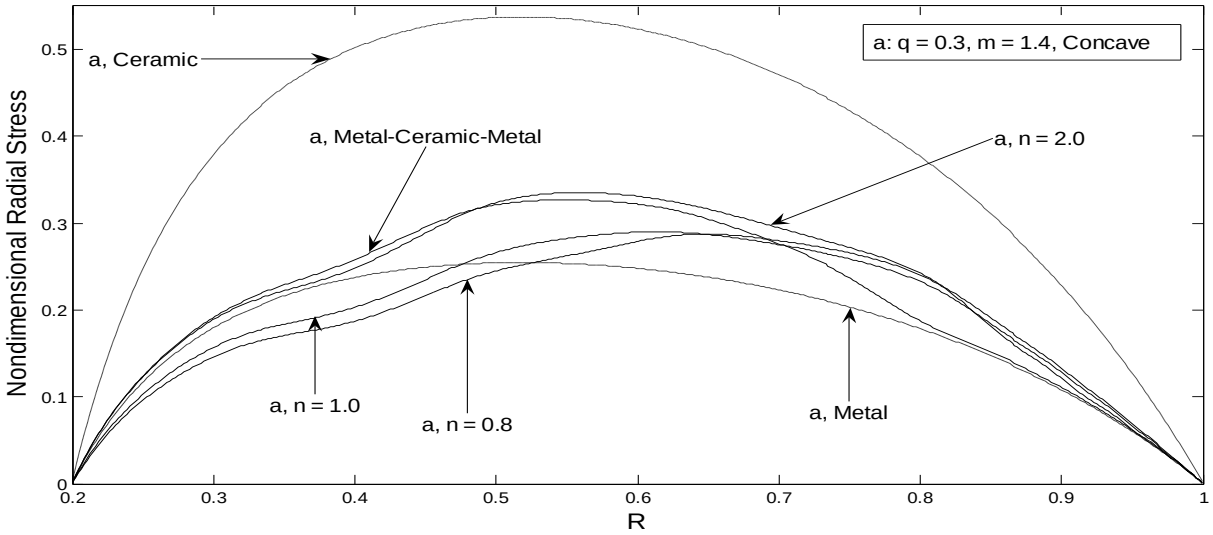

Figure 6. Variation of $\overline{\sigma_R}$ versus R for free-free hollow disk in the disk with concave thickness profile for different values of the grading index n .

between 0.4737 and 1, where $\frac{\rho_m}{\rho_c}=\frac{2700}{5700}=0.4737$. In this study, the density of ceramic is greater than the density of aluminum. It can be noted that for materials such that $\frac{\rho_m}{\rho_c}>1$, the weight of FG disk can be made even lighter than the full-metal disk.

It may be mentioned here that the method of solution considered in this study is general in nature and is not limited to gradients considered in this study only but can be applied to other gradients as well.

Hollow disk (Free-free)

Figures 5 and 6 show the non-dimensional radial stress

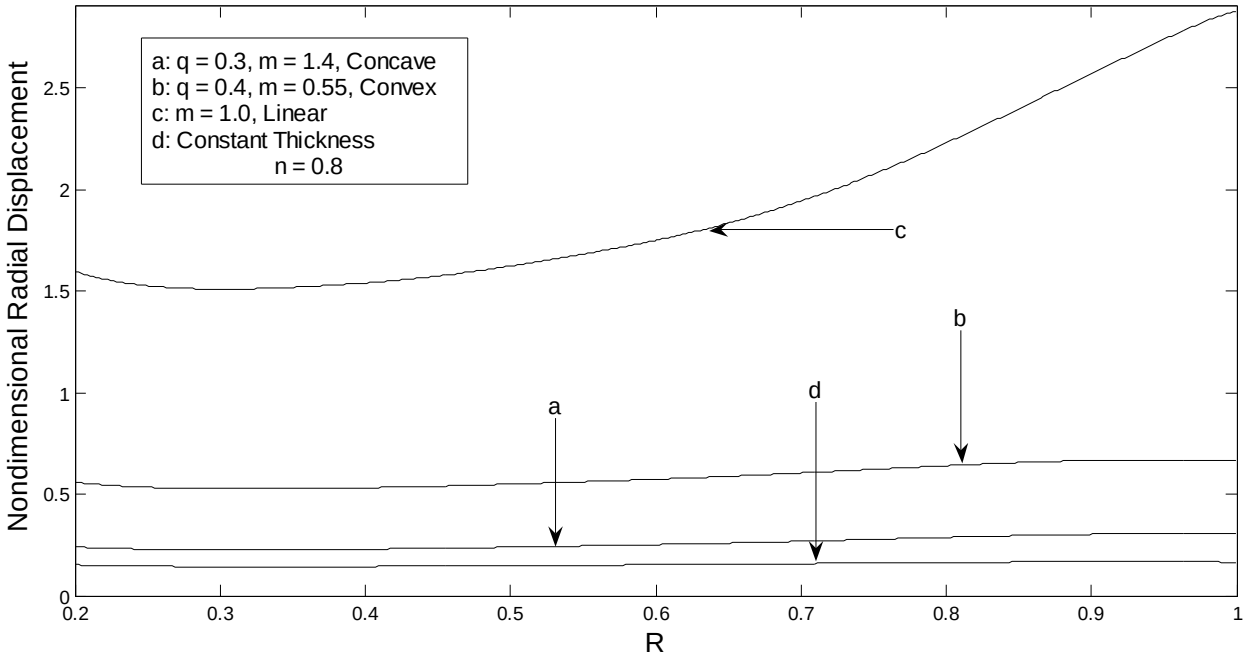

Figure 7. Variation of U versus R for free-free hollow disk in the FG disk with variable thickness for different values of the geometric parameters q and m .

and radial displacement, respectively for different values of the geometric parameters q , m and the grading index n .

In Figure 5, the effect of thickness profile on the radial stress is shown by fixing the value of the grading index, in this case $n=0.8$ and considering different thickness profiles as shown in Figure 2. It is seen that hollow FG disks with uniform-thickness have smaller radial stresses compared to those with variable thickness. FG disk with concave thickness profile is seen to have smaller stress for the chosen values of the geometric parameters q and m in comparison to other variable thickness profiles. Figure 6 shows the effect of grading index n on the stress distributions. It can be seen that the maximum of non-dimensional radial stresses are highest for full-ceramic disk and lowest for full-metal disk and the maximum value of the radial stress for different S-FG disks occur in between. It is noticed that close to the inner surface for the specific values of the grading index n ($n=0.8$), the radial stresses for combination of two S-FG disks may not lie in between the stresses for full-ceramic and full-metal disks but toward the outer surface, the stresses for S-FG disks can be lie in between.

The variation of the radial displacement with radius is shown in Figures 7 and 8. Figure 7 shows the effect of the thickness profile on the radial displacement for the same value of the grading index $n=0.8$ and for different thickness profiles. It is observed that the radial displacement for the S-FG disk with concave profile thickness is smallest in comparison with other thickness profiles that is, linear or convex. Figure 8 shows the effect of grading index, n , on the radial displacement for all the disks with the same concave thickness profile as shown in Figure 2 but having different grading index. As expected, the radial displacement values for full-metal (Aluminum) disk are greater than those for full-ceramic (Zirconia) disk due to higher modulus of elasticity of the latter. It is noticed that close to the outer surface the radial displacements for S-FG disks lie in between the stresses for full-ceramic and full-metal disks but toward the inner surface, for the specific values of the grading index n ($n=2.0$) the displacements for S-FG disks can be even larger than the radial displacement for full-metal disk. It is worth mentioning that near to full metal surface, inner or outer; the radial displacement varies by, increasing or decreasing, the radius, respectively.

The results of Figures 5 to 8 can be summarized to conclude that, for the same value of grading index, n , the hollow S-FG disk with concave thickness profile is better than those with other variable thickness profiles. This result is similar to the one reported by Eraslan (2003).

Hollow disk (Fixed-free)

The stress distributions for S-FG disk with variable thickness mounted on a rigid shaft for different values of

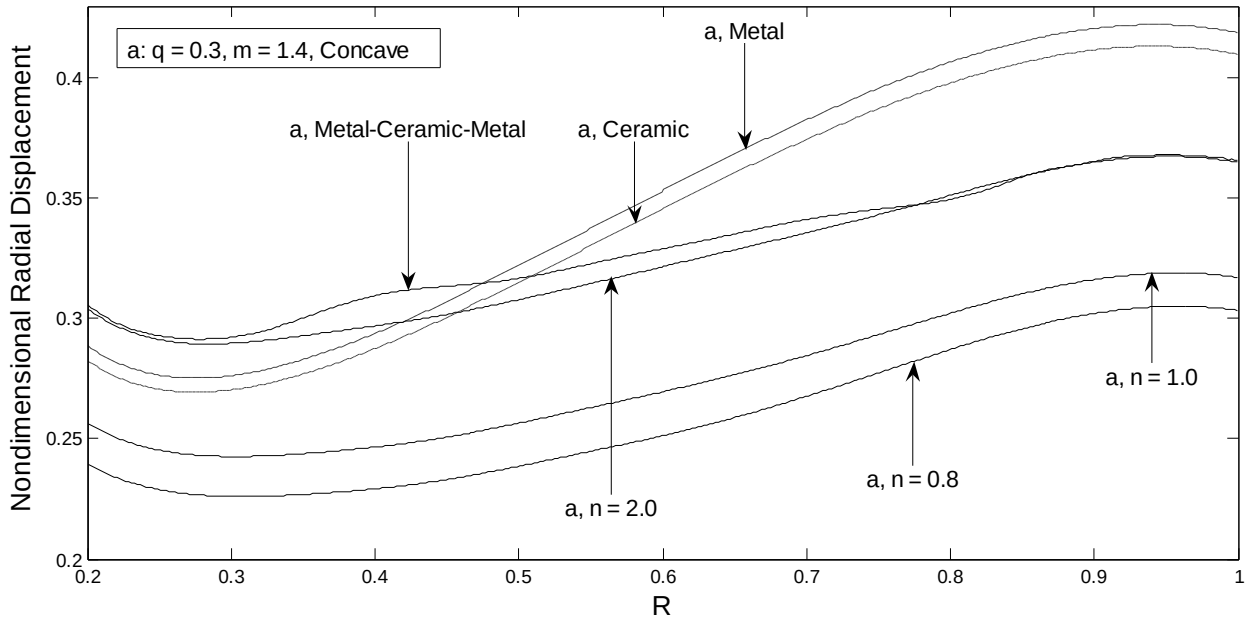

Figure 8. Variation of U versus R for free-free hollow disk in the disk with concave thickness profile for different values of the grading index n .

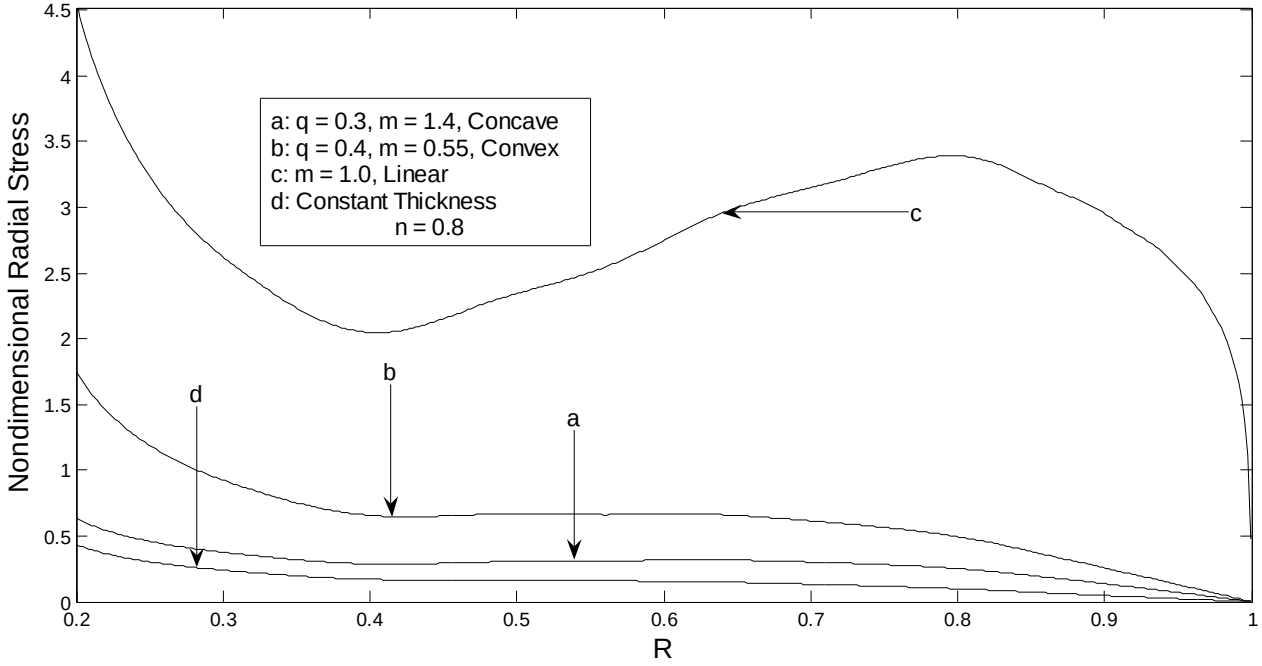

Figure 9. Variation of $\overline{\sigma_R}$ versus R for fixed-free hollow disk in the FG disk with variable thickness for different values of the geometric parameters q and m .

the geometric parameters q , m and the grading index n are shown in Figures 9 and 10.

It is shown in Figure 9 that for the same value of grading index $n\,(n=0.8)$ the maximum value of the radial stress, for each thickness profile from four cases (a) , (b) , (c) and (d) , occurs at the inner surface

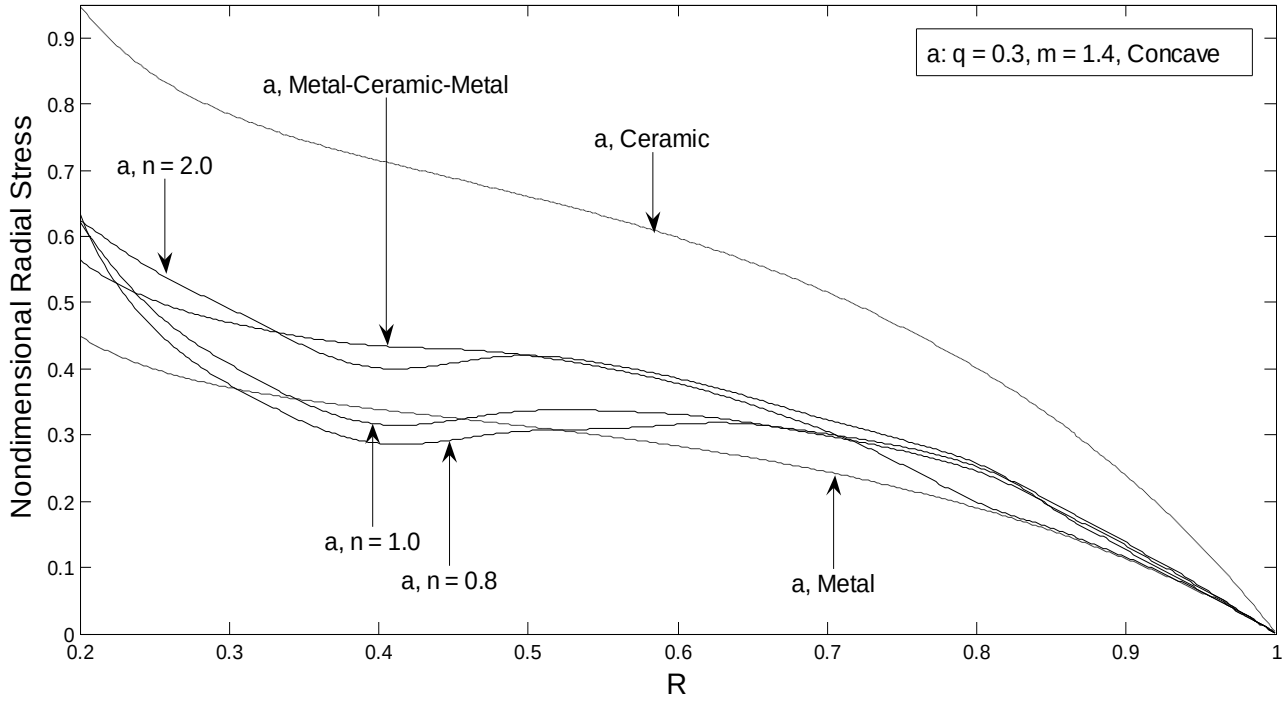

Figure 10. Variation of $\overline{\sigma_R}$ versus R for fixed-free hollow disk in the disk with concave thickness profile for different values of the grading index n.

and each of them is greater than its corresponding value with free-free condition shown in Figure 5. Here again a concave disk is found to have maximum radial stress smaller than other disks with variable thickness. It can also be seen that mounted S-FG disks with uniform-thickness have smaller radial stresses compared to those with variable thickness. Figure 10 shows the effect of grading index n (Figure 4) on the radial stress distributions for S-FG disk with concave thickness profile mounted on a rigid shaft. It is noticed from all the cases considered for different n that for the specific value of the grading index $n=0.8$, the radial stress is smaller than that of full metal disk. Taking into account the boundary condition, this phenomenon can be explained by the presence of interactive effects between stiffness and the centrifugal force due to constant angular velocity of the disk. Figure 2 may be referred to for more details. It is seen near to full-ceramic surface ($r/r_o = 0.6$), the radial stress is constant.

The variation of radial displacements with radius in disks having same grading $n=0.8$ but different thickness profiles (Figure 2) is shown in Figure 11. It is observed that the radial displacement in S-FG disk with concave thickness profile is smaller compared with disks with linear or convex profiles. It is also observed that if the value of n is kept fixed, in the present example, at $n=0.8$ then the FG disks with uniform constant thickness have smaller radial displacements than the disk with variable thickness. It is shown from Figure 12 that the full-ceramic or full-metal mounted disks have smaller or bigger displacements compared to S-FG disks.

Comparison between metal-ceramic, metal-ceramic-metal and ceramic-metal

For a future investigation, another comparison between non-dimensional displacement for one S-FGM (metal-ceramic or ceramic-metal) and two types of S-FGM (metal-ceramic-metal) are shown in Figure 13.

The variation of the radial displacement with radius is shown in Figure 13. It shows the effect of combination two S-FG disks on the radial displacement for the same value of the grading index $n=1.0$ and for concave thickness profiles. It is observed that the maximum radial displacement for the two S-FG disks with concave profile thickness is smallest in comparison with one S-FG disk (meta-ceramic or ceramic-metal). As expected, the radial displacement values for metal-ceramic disk are greater than those for ceramic-metal and metal-ceramic-metal. It is noticed that close to the inner surface the radial displacements for S-FG disks (ceramic-metal) is smaller than metal-ceramic-metal disk but toward the outer surface the displacements for combination of two S-FG disks can be even smaller than the radial displacement

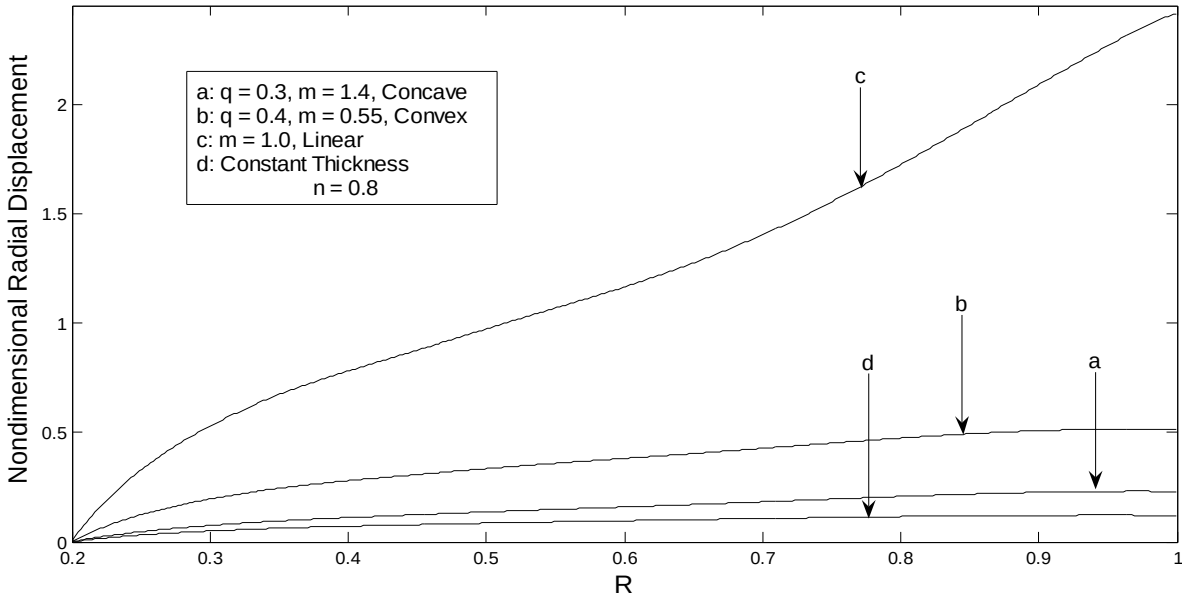

Figure 11. Variation of U versus R for fixed-free hollow disk in the FG disk with variable thickness for different values of the geometric parameters q and m.

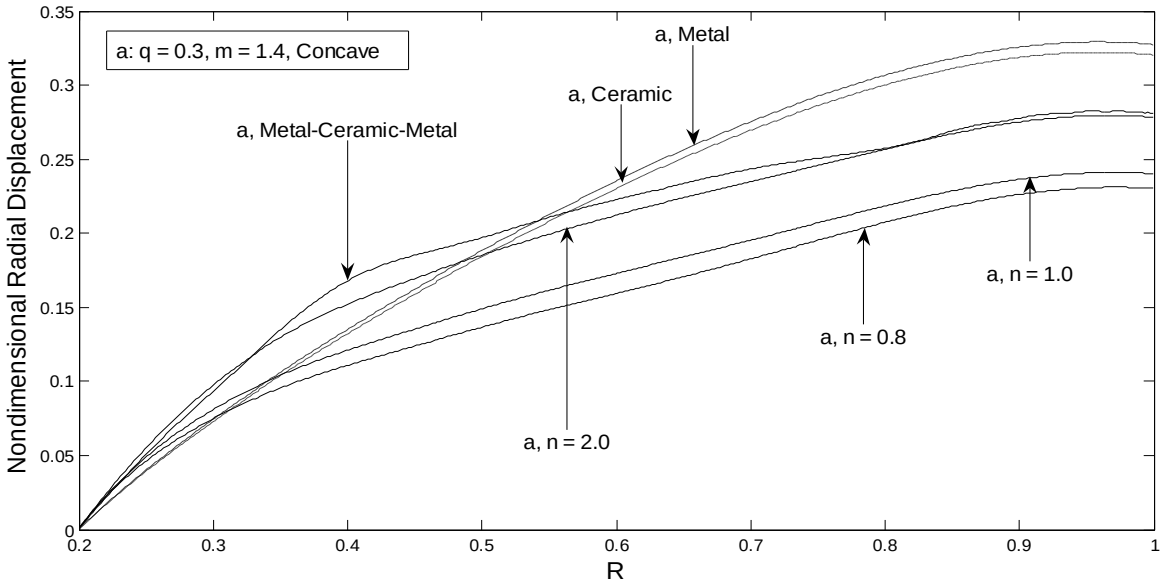

Figure 12. Variation of U versus R for fixed-free hollow disk in the disk with concave thickness profile for different values of the grading index n.

for one S-FG disk.

CONCLUSIONS

An analysis of FG rotating disks with variable thickness is presented. Combinations of two S-FGMs with hyperbolic thickness profile type are considered. Elastic radial stresses and radial displacements for the hollow disks with both free-free and fixed-free boundary conditions are obtained. The effects of the grading index, n, and geometry of the disk based on different thickness profiles

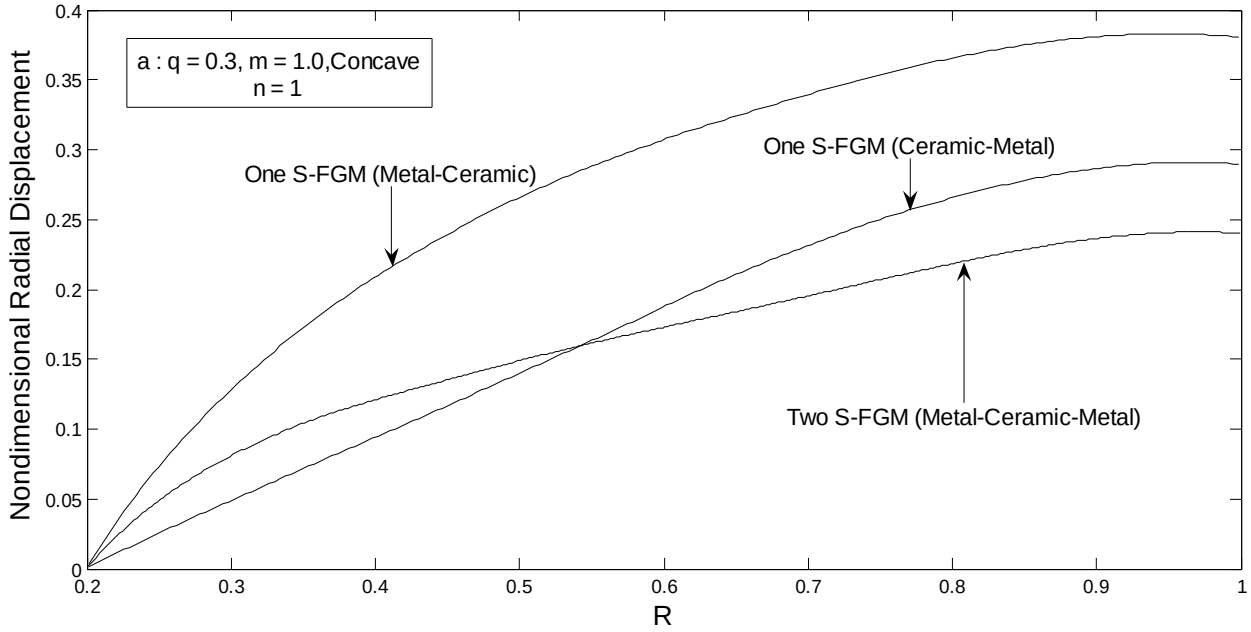

Figure 13. Variation of U versus R for fixed-free hollow disk in the disk with concave thickness profile for different type of S-FGM.

on the stresses and the radial displacements are investigated. Numerical results are presented for the S-FG disk using aluminum as the inner and outer surface-metal and Zirconia at mean radius of disk. These results are compared with those for rotating disks with uniform thickness.

Some salient conclusions of this study can be summarized as follows:

1) For the same grading index, n, linear thickness profile is the lightest disk followed by convex, concave and constant, respectively.
2) The combination of two S-FG disks with concave thickness profile has smaller stresses than with linear or convex thickness profile while the same grading is considered for all the disks.
3) For each of thickness profiles, the radial stress in S-FG disks increases with increase in n by certain radius, after that certain radius the radial stress in S-FG disks decrease with increase in n. Furthermore, for some specific values n ($n=0.8$) the radial stress in S-FG disks are smaller than those in pure material disks.
4) For a given pair of materials, there is a particular volume fraction that maximizes a specific mechanical response under centrifugal loading due to constant angular velocity. In other words, free-free or mounted FG disks can have larger radial displacement than full-metal near to the inner surface for some specific grading while maximum values of radial displacements in S-FG disks with variable thickness are smaller than the maximum values for homogenized disks.
5) Hollow rotating FG disks with uniform-thickness profile have smaller stresses and displacements compared to those with parabolic convergent.
6) Maximum radial displacement for fixed-free rotating disk in combination of two S-FG disks is smaller than those in one S-FG disks.

From the semi-analytical results for combination of two S-FG disks given in this study, it can be suggested that an efficient and optimal design of the FG disk calls for a variable section being thicker at the hub and tapering down to a smaller thickness toward the periphery. And also the combination of two S-FG disks can be more effective in comparison with one S-FG disk.

ACKNOWLEDGEMENTS

The authors wish to thank Universiti Putra Malaysia for the financial support to carry out this research and all mechanical and manufacturing department members for their support and helps.

REFERENCES

Bayat M, Saleem M, Sahari BB, Hamouda AMS, Mahdi E (2008). On the stress analysis of functionally graded gear wheels with variable thicknes. Int. J. Comput. Methods Eng. Sci. Mech., 9(2): 121-137.
Boussaa D (2000). Optimizing a compositionally graded interlayer to reduce thermal stresses in a coated tube. C. R. Acad. Sci. Paris, 328: 209-215.
Chi SH, Chung YL (2006). Mechanical behavior of functionally graded

material plates under transverse load- Part I: Analysis. Int. J. Solids Struct., 43(13): 3657-3674.
Durodola JF, Attia O (2000a). Deformation and stresses in FG rotating disks. Compos. Sci. Technol., 60: 987-995.
Durodola JF, Attia O (2000b). Property gradation for modification of response of rotating MMC discs. J. Mater. Sci. Technol., 16: 919-924.
Eraslan AN, Argeso H (2002). Limit angular velocitiesof variable thickness rotating disks. Int. J. Solids Struct., 39: 3109-3130.
Eraslan AN, Orcan Y (2002). Elastic-plastic deformation of a rotating solid disk of exponentially varying thickness. Mech. Mater., 34: 423-432.
Eraslan AN (2003). Elastic-plastic deformations of rotating variable thickness annular disks with free, pressurized and radially constrained boundary conditions. Int. J. Mech. Sci., 45(4): 643-667
Fukui Y, Yamanaka N, Wakashima K (1993). The stresses and strains in a thick-walled tube for functionally graded material under uniform thermal loading. JSME Int. J. Ser. A, 36: 156-162.
Guven U (1992). Elastic-plastic stresses in a rotating annular disk of variable thickness and variable density. Int. J. Mech. Sci., 34: 133-138.
Horgan CO, Chan AM (1999). The stress response of functionally graded isotropic linearly elastic rotating disks. J. Elastic, 55: 219-230.
Jabbari M, Sohrabpour S, Eslami MR. (2003). General Solution for Mechanical and Thermal Stresses in a Functionally Graded Hollow Cylinder Due to Nonaxisymmetric Steady-State Loads. J. Appl. Mech., Trans. ASME, 70: 111-118.
Jahed H, Farshi B, Bidabadi J (2005). Minimum weight design of inhomogeneous rotating discs. Int. J. Press. Vessels Piping, 82: 35-41.
Kordkheili SAH, Naghdabadi R (2007). Thermo elastic analysis of a functionally graded rotating disk. Compos. Struct., 79: 508-516.
Liew KM, Kitipornachi S, Zhang XZ, Lim CW (2003). Analysis of the thermal stress behavior of functionally graded hollow circular cylinders. Int. J. Solids Struct., 40: 2355-2380.
Ootao Y, Tanigawa Y (1999). Three-dimensional transient thermal stresses of functionally graded rectangular plate due to partial heating J. Therm. Stress, 22: 35-55.
Ootao Y, Tanigawa Y (2004). Transient thermoelastic problem of functionally graded thick strip due to non-uniform heat supply. J. Compos. Struct., 63: 139-149.
Orcan Y, Eraslan AN (2002). Elastic-plastic stresses in linearly hardening rotating solid disks of variable thickness. Mech. Res. Commun., 29: 269-281.
Reddy JN (2000). Analysis of functionally graded plates. Int. J. Numer. Meth. Eng., 47: 663-684.
Reddy TY, Srinath H (1974). Elastic stresses in a rotating anisotropic annular disk of variable thickness ans variable density. Int. J. Mech. Sci., 16: 85-89.
Reddy JN, Wang CM, Kitipornchai S (1999). Axisymmetric bending of functionally graded circular and annular plates. Eur. J. Mech. A/Solids, 18: 185-199.
Ruhi M, Angoshtari A, Naghdabadi R (2005). Thermoelastic analysis of thick-walled finite-length cylinders of functionally graded materials. J. Therm. Stress., 28: 391-408
Shahsiah R, Eslami MR (2003). Thermal buckling of functionally graded cylindrical shell. J. Therm. Stress., 26: 277-294
Suresh S, Mortensen A (1998). Fundamentals of functionally graded materials. Fundamentals of functionally graded materials. IOM Communications Limited, London.
Tutuncu N (1995). Effect of anisotropy on stresses in rotating discs. Int. J. Mech. Sci., 37(8): 873-881.

Scientific Research and Essays Vol. 7(25), pp. 2189-2194, 5 July, 2012
Available online at http://www.academicjournals.org/SRE
DOI: 10.5897/SRE11. 1220
ISSN 1992-2248 ©2012 Academic Journals

Full Length Research Paper

Molecular cloning and analysis of a novel HMW-GS gene *Glu1-St1.5* from *Elymus sibiricus* in Qinghai-Tibetan Plateau

LIU Jin[1,2,3#], ZHANG Bo[1#], LIU Bao-long[1], LI Hong-qin[1,2], WANG Xin[1,2], LIU Qi[1,2], WEI Le[1,2] LIU Deng-cai[1,4] and ZHANG Huai-gang[1]*

[1]Key Laboratory of Adaptation and Evolution of Plateau Biota, Northwest Institute of Plateau Biology Chinese Academy of Sciences, Xining 810008, China.
[2]Graduate University, Chinese Academy of Sciences, Beijing 100049, China.
[3]Yunnan Institute of Tropical Crops, Xishuangbanna 666100, China.
[4]Triticeae Research Institute, Sichuan Agricultural University, Wenjiang, Chengdu 611130, Sichuan, China.

Accepted 30 May, 2012

In the present study, a HMW-GS allele *Glu1-St1.5* was isolated and characterized from *Elymus sibiricus*. Nucleotide sequence analysis indicated that the St1.5 shared the highest similarity with St1.3 from *Elymus canadensis*, but the "TA" insertion mutation at 15 to 16 bp in signal peptide sequence made it an inactive gene, because three premature stop codons were generated by "TA" insertion in signal peptide region, N-terminal region and C-terminal region, respectively. To identify the type of St1.5, the inserted "TA" was eliminated factitiously and the deduced amino acid sequence was analyzed, the result showed that St1.5 was a y-type HMW-GS pseudo gene. Phylogenetic tree demonstrated that St1.5 had the closest relationship to the St1 allele of *Pseudoroegneria stipifolia*, which indicated that St1.5 was a novel gene of St Genome. These results provide insights into the evolutionary biology of *Glu1-St1.5* and other HMW-GS genes.

Key words: *Glu1-1St1.5*, HMW-GS, *Elymus sibiricus*.

INTRODUCTION

The end-use quality of wheat (*Triticum aestivum* L.) flour is largely determined by the composition of storage proteins in seed endosperm (Payne, 1987; Gianibelli, 2001a, b). The high molecular weight glutenin subunit (HMW-GS) is one of most important storage proteins in seed endosperm of wheat and related species and accounting for approximately 10% of the total proteins in wheat seed (Shewry et al., 1995). In hexaploid wheat, HMW-GS is encoded by the *Glu-A1*, *Glu-B1* and *Glu-D1* locus on the long arm of homologous chromosomes 1A, 1B and 1D, respectively (Shewry et al., 1992). There are two tightly linked genes encoding a larger x-type (80-88 kDa) and a smaller y-type (67 to 73 kDa) subunit at each locus. But only three to five HMW-GSs could be detected in hexaploid wheat seed by conventional SDS-PAGE analysis, because the y-type gene of *Glu-A1* locus is often silenced and the x-type gene of *Glu-A1* locus and y-type gene of *Glu-B1* locus are silence occasionally (Harberd et al., 1986; Payne, 1987; Shewry et al., 1992, 2001, 2002).

Elymus L. is the largest genus in the tribe Triticeae with about 150 species distributed in most places of the world, especially in some high altitude, cold and arid areas. (Lu, 1993; Ma et al., 2009). As the type species of the genus *Elymus*, *Elymus sibiricus* L. is a perennial, self-pollinating and allotetraploid grass indigenous to Northern Asia, possessing the St and H genome (Dewey 1974, 1984). Its geographic distribution extends from Sweden to Japan and even to parts of Alaska and Canada (Bowden and

*Corresponding author. E-mail: hgzhang@nwipb.ac.cn. Tel: +86-9716143630.

# These authors contributed equally to this paper.

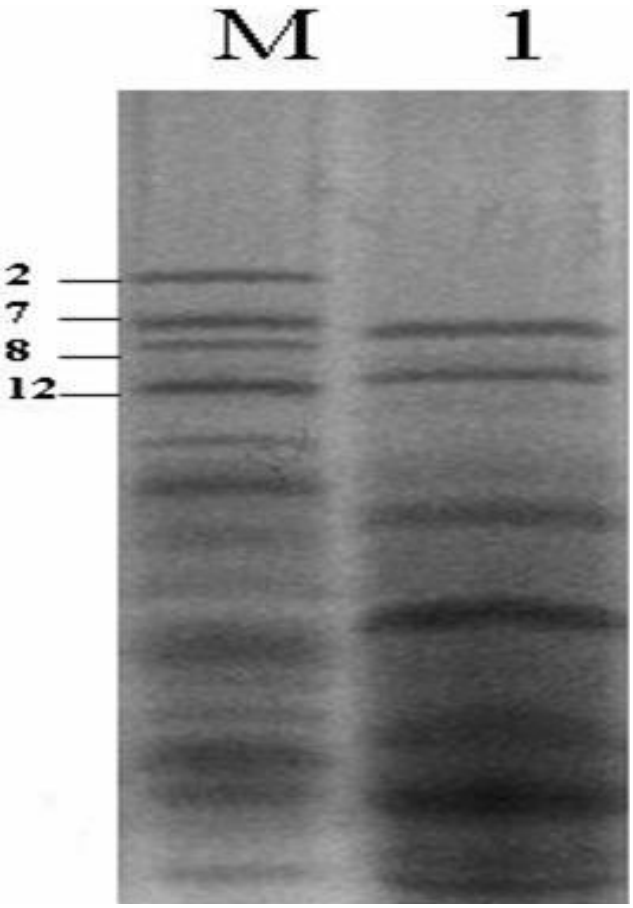

Figure 1. The SDS-PAGE characters of HMW-GS in Elymus sibiricus (lane 1) and the common wheat line Chinese Spring (lane M) with HMW-GS composition 1Dx2, 1Bx7, 1By8 and 1Dy12 was used as control. The Elymus sibiricus posses two glutenin subunits, both of them moved slower than 1Dy12 of the control.

Cody, 1961) and then extends southernly to Qinghai-Tibet Plateau, which is the highest plateau in the world.*E. sibiricus* usually grows on wet meadows, riverside sands and among open forest or shrubs. In the subalpine meadows with less than 4000 meter altitude in Qinghai-Tibet Plateau, *E. sibiricus* usually serves as an important forage species.

Orthologous HMW glutenin subunits have been found in many Triticeae grasses including various *Aegilops* species and rye (De Bustos et al., 2001; De Bustos and Jouve, 2003; Liu et al., 2003; Wan et al., 2002; William et al., 1993). Up to now, no research work has been reported on HMW-GS gene isolation and characterization in *Elymus sibiricus*.

In the present work, a novel HMW-GS gene *Glu1-St1.5* was isolated and chracterized from *Elymus sibiricus*. The gene structure was analyzed by comparation with HMW-GS genes in other wheat related wild species. The results will help us understanding the evolutionary relationship between *Glu1-St1.5* and other HMW-GS genes.

MATERIALS AND METHODS

Plant material

SDS-PAGE analysis of 105 individual plants of *Elymus* L. distributed in 56 different longitude and dimensionality using seed protein extracts, revealed the presence of two putative HMW glutenin subunits in one of the *Elymus sibiricus* collected from Qinghai-Tibetan Plateau (Figure 1). The longitude and dimensionality of collected site was E 100.913663 and N 36.372140, respectively and the altitudes was 3535.16 m. Therefore the *Elymus sibiricus* was chosen as the material for the follow-up experiment. SDS-PAGE analysis was conducted according to Wan et al. (2002).

Genomic DNA extraction and PCR amplification

Seeds of *Elymus sibiricus* were germinated under the dark at room temperature for two weeks. Genome DNA was extracted from young leaves by conventional CTAB method with some modifications, ethanol precipitated, re-suspended in 50 ul of sterile distilled water and then stored at -20°C.

In order to amplify HMW-GS genes by genomic PCR, a pair of degenerated primers P1 (5'-ATGGCTAAGCGGC /TTA/GGTCCTCTTTG-3') and P2 (5'-CTATCACTGGCTA/ GGCCGACAATGCG-3'), which could amplify the complete ORFs of HMW-GS genes of wheat related species were used (Liu et al., 2003; Li et al., 2008). Primer P1 contains the start codon of the HMW-GS ORF whereas primer P2 contains the two tandem stop codons that are conserved in the HMW-GS ORFs characterized so far (Liu et al., 2003). PCR were carried out using ABI Gene Amp PCR System 9700, the high fidelity polymerase HiFi Taq with GC buffer (TransGen Biotech, Beijing, China) were used. Different annealing temperatures were tested and 65°C appeared to be optimal for PCR amplification of the complete ORFs of HMW-GS genes. The PCR reaction programmed at 94°C for 5 min to denature the DNA, followed by 30 cycles each with a 50 s denaturing step at 94°C, a 1 min annealing step at 65°C and a 1.5 min extension step at 72°C. The final extension step was for 10 min, followed by a 4°C soak step. PCR products were separated by 1% agarose gel electro-phoresis in TAE buffer.

DNA cloning, sequencing and phylogenetic analysis

The PCR product of expected size was extracted from agarose gel; the fragment was ligated into the pEASY-T1 vector (TransGen Biotech, Beijing, China) and transformed into competent cells of *Escherichia coli* DH-10B strain. The positive clones were identified using blue/white screening and colony PCR. The complete sequence was acquired by sequencing three different positive clones; the sequencing was performed by AUGCT Biotechnology Company (Beijing, China). Nucleotide sequences assemble and phylogenetic analysis were carried out by Invitrogen Advance 10 program.

RESULTS

Isolation and sequencing of HMW-GS gene *Glu1-St1.5*

PCR amplification was carried out using the two degenerated primer P1 and P2 which could amplify the complete ORFs of HMW-GS genes in all of the wheat

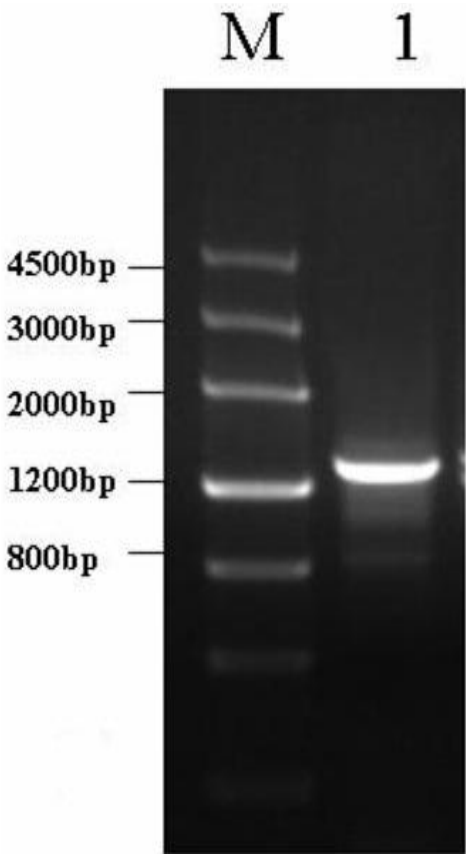

Figure 2. Agarose-gel separation of amplified products of *Elymus sibiricus* using primers P1+P2 (lane 1) and DNA size makers (lane M).

related species. The agarose electro-phoresis analysis of the PCR products showed that only one fragment have been amplified, the size of the fragment was just approximate 1300bp (Figure 2). Previous studies showed that the DNA sequence length of 1Dy12 in the control Chinese Spring was 1977 bp (Cunsolo et al., 2003), so the PCR fragment was not correspondent with the two subunit in SDS-PAGE, the PCR fragment may be another HMW-GS gene which have not been detected by SDS-PAGE.

To elucidate whether the PCR fragment in Figure 2 was a HMW-GS gene and whether it could translate into glutenin subunit, the fragment was cloned into the pEASY-T1 vector and sequenced. The sequence was deposited in GenBank under the accession number HM804857.

Characterization of St1.5 gene

BLAST analysis in NCBI revealed that the DNA sequence of St1.5 showed very high homology to that of previously cloned HMW-GS genes in all kinds of wheat related species, *Glu1-St1.3* in *Elymus canadensis* was the highest one, coefficient of similarity between these two genes was 94.50%, so the St1.5 was a family member of high molecular weight glutenin subunit genes.

Compared the DNA sequences of St1.5 and St1.3, 29 different sites were observed, two sites were nucleotide insertion, others were nucleotide substitution or deletion mutation (boxed in Figure 3). The most crucial difference of these two sequences was the “TA” insertion mutation at 15 to 16 bp downstream the start codons of St1.5, which caused three stop codons at 34 to 36 bp, 397 to 399 bp, 1237 to 1239 bp downstream the start codons, these stop codons made St1.5 could not be translated into protein normally. The other nucleotide insertion occurred at the central repetitive domain, but it did not caused any mutation of the reading frame of St1.5.

Regardless of its inactivation, elucidating whether St1.5 had the typical HMW-GS structure before the “TA” insertion in its evolutionary processing was much more valuable to us. So the inserted “TA” of St1.5 was eliminated factitiously, the deduced amino acid sequences of St1.5 (TA) and St1.3 were compared.

The deduced amino acid sequences of both St1.5 (TA) and St1.3 shared the typical HMW-GS structure, including the signal peptides, N-terminal region, central repetitive domain and C-terminal region (Figure 4). The signal peptides, N-terminal region and C-terminal region were conservative, but the central repetitive domain which consisted of nonapeptide (GYYPTSP/LQQ) and hexapeptide (consensus PGQGQQ) was semi-conservative. There were eleven different sites between the deduced amino acid sequences of St1.5 (~~TA~~) and St1.3, seven of them were amino acid substitution, and the other four were amino acid insertion or deletion.

Both of St1.5 (TA) and St1.3 had six cysteine residues, five in N-terminal region and the other one in C-terminal region. Previous studies showed that x-type HMW-GS has three conservative cysteine residues in its N-terminal region and one in its C-terminal region, but the y-type HMW-GS has five conservative cysteine residues in its N-terminal region and one in its C-terminal region, both of them have a semi-conservative cysteine residue the central repetitive domain (Shewry and Tatham, 1997; Belton, 1999; Veraverbek and Delcour, 2002; Wieser, 2007). So it was obvious that St1.5 was a y-type HMW-GS gene.

Phylogenetic analysis of HMW-GS genes

Sequence comparisons among different HMW-GS alleles could provide useful information relevant to the evolutionary relationship among them. There are nearly two hundred HMW-GS genes from more than thirty different wheat related species which belong to 12 different genera have been cloned till now (www.ncbi.nlm.nih.gov), it was difficult to analyze the phylogenetic relationship of all the cloned genes, so 23 x-

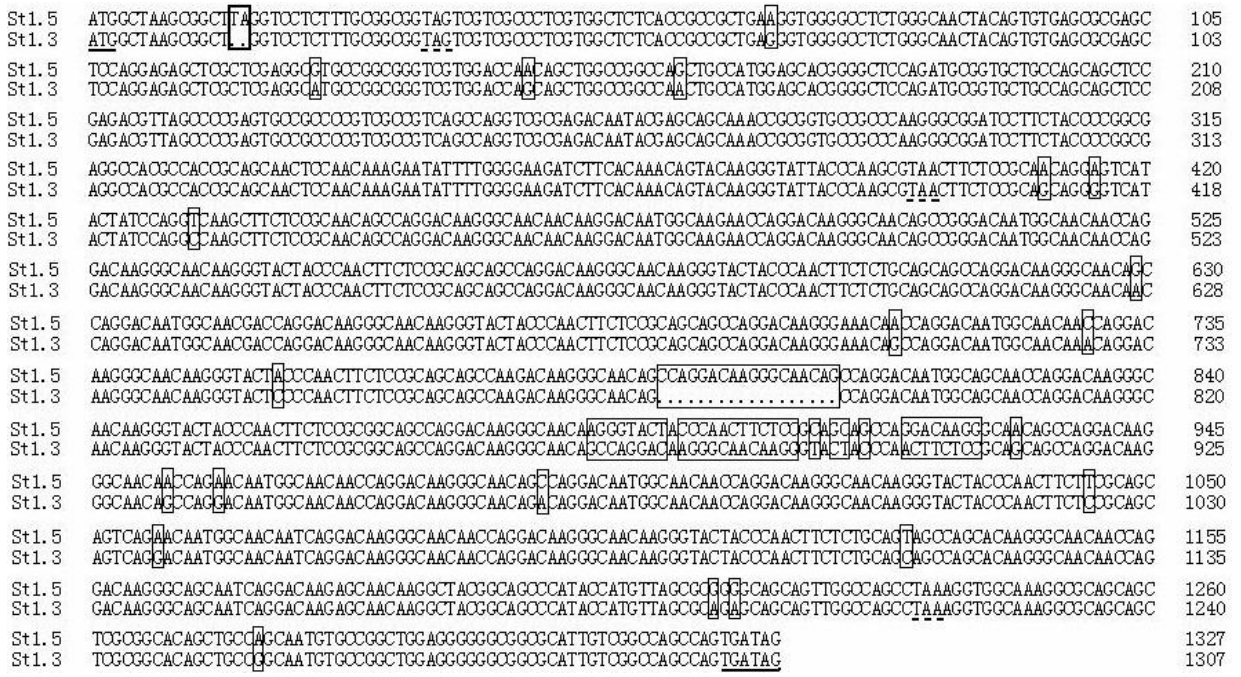

Figure 3. Nucleotide sequences of the novel inactive HMW-GS gene St1.5 compared with the ORFs of another active gene St1.3 which came from *Elymus canadensis*, the GenBank accession number for St1.5 and St 1.3 were HM804857 and GU998882.1, respectively. Solid boxes point out the sites of difference among the two nucleotide sequences, the start codons and stop codons are marked by bold line, the "TA" insertion of St1.5 was marked by a bold box. Broken bold line point out the stop codons induced by the "TA" insertion mutation in St1.5.

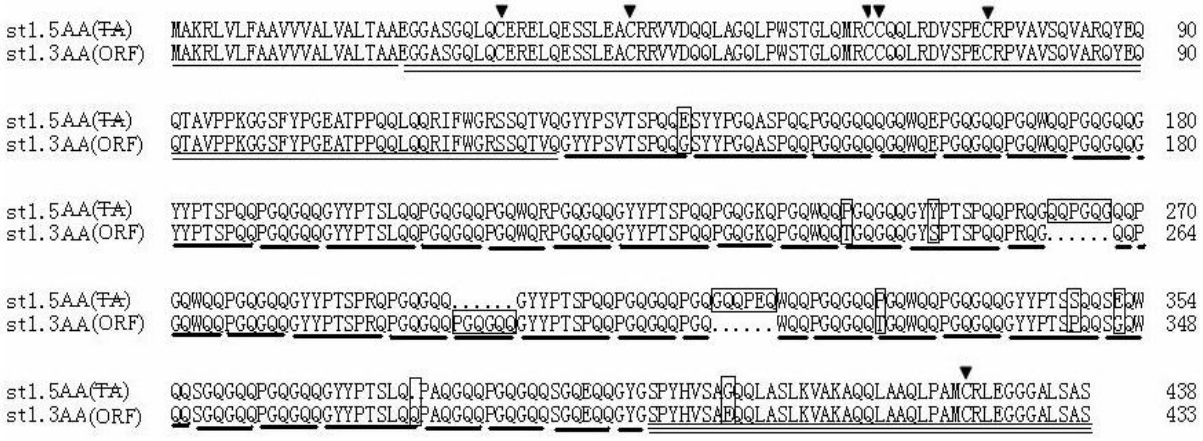

Figure 4. The deduced amino acid sequences of St1.5 while eliminated the inserted "TA" factitiously, compared with the deduced amino acid sequences of the ORFs of St1.3. Solid boxes point out the sites of difference among the two sequences, the signal peptides are underlined with solid line, while the N-terminal region and the C-terminal region are underlined with double lines and triplicate lines, respectively. The central repetitive domain which consisted of nonapeptide (GYYPTSP/LQQ) and hexapeptide (consensus PGQGQQ) are indicated by bold line and cysteine residues are indicated by black trigones.

and y-type genes from 12 different genera of *Triticeae* were chosen to analyze the phylogenetic position of the novel gene- St1.5 in this study.

As shown in Figure 5, the phylogenetic tree was obviously divided into two halves. The y-type subunit genes were clustered into one subclass and the x-type ones were clustered into another. The newly cloned *Glu1-St1.5* gene from *Elymus sibiricus* was a y-type gene.

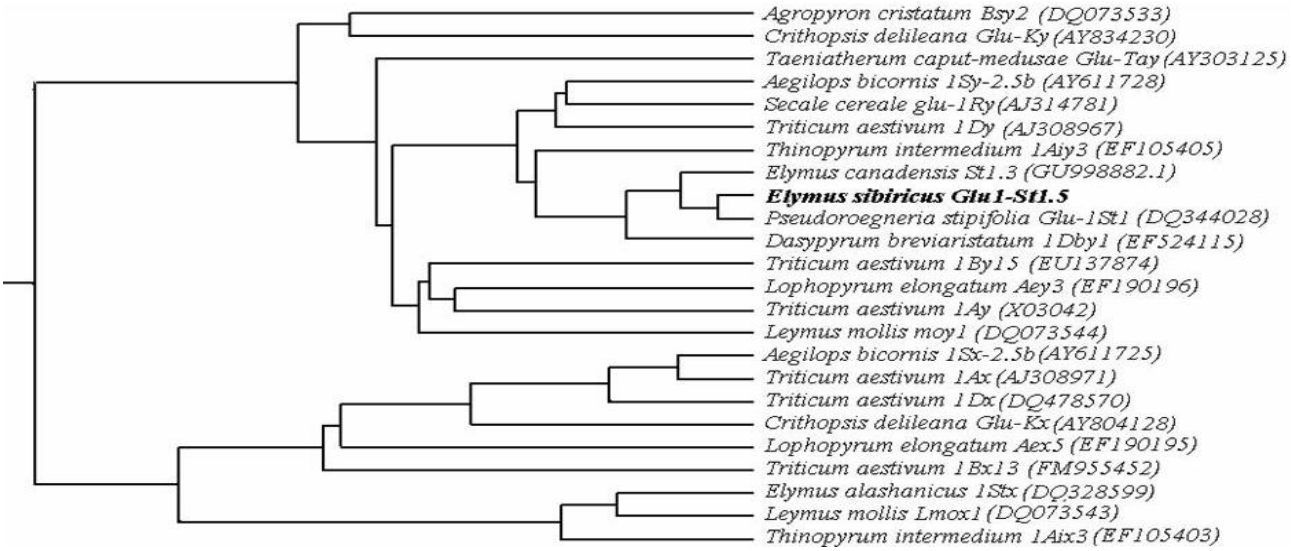

Figure 5. A phylogenetic tree derived from the sequences alignment of 24 HMW-GS genes from different wild species of 12 different genera of Triticeae.

St1.5 of *Elymus sibiricus* and St1 of *Pseudoroegneria stipifolia* were clustered into one group inferring their closest relationship. It is known that *Pseudoroegneria stipifolia* was one of wild wheat related species with the genome of St (2n = 2x = 14), so we speculated St1.5 was a novel HMW-GS allele in St Genome.

DISCUSSION

In the present study, a novel HMW-GS gene *Glu1-St1.5* was isolated and characterized, the insertion mutation of "TA" at signal region resulted three stop codons in N-terminal region, central repetitive domain and C-terminal region, respectively, which made St1.5 gene not being translated into protein. Previous studies showed that not all HMW-GS genes could be translated, the representative case is *Glu1-Ay* in common wheat (Harberd et al., 1987; Halford et al., 1989; Sun et al., 2004) and the main reason of HMW-GS gene silence was the insertion transposon element or the presence of stop codon (Xiang et al., 2010). So the St1.5 represented a new silence mechanism compared with the previous published inactive HMW-GS genes.

The molecular size of x-type HMW-GS genes was bigger than y-type genes, but the cysteine number of y-type was more than x-type (Shewry and Tatham, 1997; Belton, 1999; Veraverbek and Delcour, 2002; Wieser, 2007) and they were useful significant characteristics to distinguish the x- and y-type HMW-GS alleles. Wheat flour quality was affected by the different composition of HMW-GS alleles because cysteine number affected the volume and quantity of glutenin macro polymer, which positively correlated with the visco-elastic property of wheat dough, so the y-type genes were more important than x-type for wheat flour quality. Although the St1.5 was an inactive y-type gene, but more research should been carried out in other y-type alleles of *Elymus sibiricus* and if there existed active y-type allele, it could be used as a target gene to modified the quality of wheat flour by transgenic approach.

The evolutionary origin of different HMW-GS alleles from different Triticeae grasses and genome was an interesting issue for scientists. The St Genome of *Elymus* L. was probably derived from *Pseudoroegneria* (Nevski) A. Love, which only has the St Genome. The phylogenetic tree of 24 HMW-GS genes from different genome showed that the alleles from St (*Elymus sibiricus*, *Elymus canadensis*, *Pseudoroegneria stipifolia*, *Thinopyrum intermedium*) have closer relationship with those from V genome (*Dasypyrum breviaristatum*), R genome (*Secale cereale*) and D genome (*Triticum aestivum 1Dy*) than those from P genome (*Agropyron cristatum*), K genome (*Crithopsis delileana*), B genome (*Triticum aestivum 1By*), E^e genome (*Lophopyrum elongatum*) and Ns genome (*Leymus mollis*). Interestingly, the "TA" insertion resulted gene silence was observed in the present study. The silence mechanism of St1.5 was different from the previous studies. Further investigations are underway to examine if the above feature is common to the HMW glutenin subunits encoded by other species in *Elymus* L. from Qinghai-Tibetan Plateau.

ACKNOWLEDGEMENTS

The work was supported by grants from Project of

Knowledge Innovation Engineering, CAS (KSCX3-EW-N-02), the Ministry of Agriculture of China (2008ZX08002-004) and National Natural Science Foundation of China (31101140).

REFERENCES

Belton PS (1999). On the elasticity of wheat gluten. J. Cereal Sci., 29(2): 103-107.

Bowden WM, Cody WJ (1961). Recognition of *Elymus sibiricus* L. from Alaska and the district of Mackenzie. Bulletin of the Torrey Botanical Club, New York. 88: 153-155.

Cunsolo V, Foti S, Saletti R, Gilbert S, Tatham AS, Shewry PR (2003). Structure studies of glutenin subunits 1Dy10 and 1Dy12 by matrix-assisted laser desorption/ionization mass spectrometry and high-performance liquid chromatography/electrospray ionization mass spectrometry. Rapid Commun. Mass Spectrom, 17(5): 442-454.

De Bustos A, Jouve N (2003). Characterization and analysis of new HMW-glutenin alleles encoded by the Glu-R1 locus of *Secale cereale*. Theor. Appl. Genet., 107(1): 74-83.

De Bustos A, Rubio P, Jouve N (2001). Characterization of two gene subunits on the 1R chromosome of rye as orthologs of each of the Glu-1genes of hexaploid wheat. Theor. Appl. Genet., 103(5): 733-742.

Dewey DR (1974). Cytogenetics of *Elymus sibiricus* and its hybrids with *Agropyron tauri*, *Elymus canadensis*, and *Agropyron caninus*. Bot. Gaz., 135(1): 80-87.

Dewey DR (1984). The genomic system of classification as a guide to intergeneric hybridization with the perennial Triticeae. In: Gustafson, JP (Ed.), Gene Manipulation in Plant Improvement. Plenum, New York. pp. 209-279.

Gianibelli MC, Gupta RB, Lafiandra D, Margiotta B, MacRitchie F (2001a). Polymorphism of high Mr glutenin subunits in *Triticum tauschii*: characterization by chromatography and electrophoretic methods. J. Cereal Sci., 33(1): 39-52.

Gianibelli MC, Larroque OR, MacRitchie F, Wrigley CW (2001b). Biochemical, genetic, and molecular characterization of wheat endosperm proteins. Cereal Chem., 78(6): 635- 646.

Halford NG, Forde J, Shewry PR, Kreis M (1989). Functional analysis of the upstream regions of a silent and an expressed member of a family of wheat seed protein genes in transgenic tobacco. Plant Sci., 62: 207-216.

Harberd NP, Bartels D, Thompson RD (1986). DNA restriction fragment variation in the gene family encoding high-molecular-weight (HMW) glutenin subunits of wheat. Biochem. Genet., 24: 579-592.

Harberd NP, Flavell RB, Thompson RD (1987). Identification of a transposon-like insertion in a *Glu-1* allele of wheat. Mol. Gen. Genet., 209(2): 326-332.

Li ZX, Zhang XQ, Zhang HG, Cao SH, Wang DW, Hao ST, Li LH, Li HJ, Wang XP (2008). Isolation and characterization of a novel variant of HMW glutenin subunit gene from the St genome of *Pseudoroegneria stipifolia*. J. Cereal Sci., 47(3): 429-437.

Liu ZJ, Yan ZH, Wan YF, Liu KF, Zheng YL, Wang DW (2003). Analysis of HMW glutenin subunits and their coding sequences in two diploid Aegilops species. Theor. Appl. Genet., 106(8): 1368-1378.

Lu BR (1993). Meiotic studies of *Elymus nutans* and *E. jacquemontii* (Poaceae: Triticeae) and their hybrids with *Pseudoroegneria spicata* and seventeen *Elymus* species. Plant Syst. Evol., 186: 193-212.

Ma X, Zhang XQ, Zhou YH, Bai SQ, Liu W (2009). Assessing genetic diversity of *Elymus sibiricus* (Poaceae: Triticeae) populations from Qinghai-Tibet Plateau by ISSR markers. Biochem. Syst. Ecol., 36(7): 514-522.

Payne PI (1987). Genetics of wheat storage protein and the effect of allelic variation on bread making quality. Ann. Rev. Plant Physiol., 38: 141-153.

Shewry PR, Halford NG, Belton PS, Tatham AS (2002). The structure and properties of gluten: an elastic protein from wheat grain. Philosophical Transactions of the Royal Society of London Series b.Biological Sciences 357(1418): 133-142.

Shewry PR, Halford NG, Tatham AS (1992). The high molecular weight subunits of wheat glutenin. J. Cereal Sci., 15(2): 105-120.

Shewry PR, Popineau Y, Lafiandra D, Belton P (2001). Wheat glutenin subunits and dough elasticity findings of the EUROWHEAT project. Trends Food Sci. Technol., 11(12): 433-441.

Shewry PR, Tatham AS (1997). Disulphide bonds in wheat gluten proteins. J. Cereal Sci., 25(3): 207-227.

Shewry PR, Tatham AS, Barro P, Lazzeri P (1995). Biotechnology of breadmaking: unraveling and manipulating the multi-protein glutencomplex. Nat. Biotechnol., 13: 1185-1190.

Sun MM, Yan YM, Jiang Y, Xiao YH, Hu YK, Cai MH, Li YX, Hsam SLK, Zeller FJ (2004). Molecular cloning and comparative analysis of a y-type inactive HMW glutenin subunit gene from cultivated emmer wheat (*Triticum dicoccum* L.). Hereditas, 141(1): 46-54.

Veraverbek WS, Delcour JA (2002). Wheat protein composition and properties of wheat glutenin in relation to breadmaking functionality. Crit. Rev. Food Sci. Nutr., 42(3): 179-208.

Wan YF, Wang DW, Shewry PR, Halford G (2002). Isolation and characterization of five novel high molecular weight subunit of glutenin genes from *Triticum timopheevi* and *Ageilops cylindrical.* Theor. Appl. Genet., 104(5): 828-839.

Wieser H (2007). Chemistry of gluten proteins. Food Microbiol., 24(2): 115-119.

William MD, Pena RJ, Mujeeb-Kazi A (1993). Seed protein and isozyme variations in *Triticum tauschii* (*Aegilops squarrosa*). Theor. Appl. Genet., 87: 257-263.

Xiang WW, Liu BL, Zhang HG (2010). Cloning and characterization of a y-type inactive HMW glutenin subunit gene from *Triticum durum* cultivar youmangbingmai. Afr. J. Biotechnol., 9(7): 967-971.

Scientific Research and Essays Vol. 7(25), pp. 2195-2204, 5 July, 2012
Available online at http://www.academicjournals.org/SRE
DOI: 10.5897/SRE11.1329
ISSN 1992-2248 © 2012 Academic Journals

Full Length Research Paper

Growth, phosphorus status, and nutritional aspect in common bean exposed to different soil phosphate levels and foliar-applied phosphorus forms

Fabrício William Ávila[1]*, Valdemar Faquin[1], Allan Klynger da Silva Lobato[2], Danielle Pereira Baliza[3], Douglas José Marques[1], Alexandre Martins Abdão dos Passos[4], Carla Elisa Alves Bastos[5] and Elaine Maria Silva Guedes[2]

[1]Departamento de Ciência do Solo, Universidade Federal de Lavras, Lavras, Brazil.
[2]Núcleo de Pesquisa Vegetal Básica e Aplicada, Universidade Federal Rural da Amazônia, Paragominas, Brazil.
[3]Instituto Federal de Educação, Ciência e Tecnologia do Sudeste de Minas Gerais, Rio Pomba, Brazil.
[4]Empresa Brasileira de Pesquisa Agropecuária/Rondônia, Porto Velho, Brazil.
[5]Departamento de Ciência do Solo, Escola Superior de Agricultura Luiz de Queiroz/USP, Piracicaba, Brazil.

Accepted 30 May, 2012

This study aimed to investigate the effect of the foliar application of phosphite and phosphate on growth, phosphorus (P) status, and nutritional aspect of common bean (*Phaseolus vulgaris* cv. Radiante) plants grown under different soil phosphate levels. Experiment was organized in factorial scheme completely randomized using 2 soil phosphate levels (Pi-starved and Pi-sufficient plants), combined with 3 nutrient sources supplied via foliar application (KH_2PO_3, KH_2PO_4, and KCl used as control), and 2 foliar application numbers (single and two applications). In this study were measured root dry weight, shoot dry weight, and root to shoot ratio, as well as shoot P concentration, root P concentration, accumulated P in shoot, accumulated P in root, P uptake efficiency, P utilization efficiency, P translocation, and macro and micronutrients in shoot. Common bean growth under limiting phosphate availability in soil exhibited lower biomass yield and higher concentration of nutrients in shoot tissues. The results exhibit foliar-applied KH_2PO_3 causes harmful effects in phosphate-starved common bean. Either one or two foliar sprays of KH_2PO_4 were not sufficient to affect the growth and nutrition of the common bean plants, regardless of soil P status.

Key words: *Phaseolus vulgaris*, phosphorus, phosphate and phosphite anions, foliar application.

INTRODUCTION

Limited phosphorus (P) availability in Ultisols and Oxisols has been identified as one of the major problems for plant growth in tropical and subtropical regions of the world. High rate P "fixation" and formation of insoluble complexes with aluminum and iron under acid conditions are recognized as an important factor contributing to the low P availability. Thus, application of P-containing fertilizers in these soils is a necessary practice for adequate crop yields in many instances (Vance et al., 2003) and foliar-applied P may increase use efficiency by minimizing soil supply (Girma et al., 2007; Mosali et al., 2006).

Phosphate anions ($H_2PO_4^-$, HPO_4^{2-} and PO_4^{3-}) are considered as the main phosphorus forms assimilated by plants and these can induce adequate growth and development with consequences in yield. However, another P form known as phosphite has been widely marketed either as fungicide or as a superior P source for plant nutrition (McDonald et al., 2001; Thao and Yamakawa, 2009; Deliopoulos et al., 2010). Phosphite anions ($H_2PO_3^-$ and HPO_3^{2-}) are reduced forms of phosphate anions, in which one hydroxyl group is substituted by hydrogen (Danova-Alt et al., 2008).

Several studies conclusively indicate that phosphite is

*Corresponding author. E-mail: fabriciowilliamavila@yahoo.com.br. Tel: +55 35 38291252.

effective in controlling some important plant diseases caused by pathogens belonging to the class Oomycetes (phylum Oomycota), such as *Phytophthora* sp. Action of phosphite anion is based on two mechanisms: the first is a direct toxic action on the pathogen and the second in indirect action due to phosphite anion activates plant defence responses (McDonald et al., 2001; Wilkinson et al., 2008; Shearer and Fairman, 2007; Orbovic et al., 2008; Cook et al., 2009; Moor et al., 2009). Thus, phosphite has been used as active ingredient in several fungicides.

In terms of plant nutrition, phosphite-based products have been recommended as fertilizers for foliar application, and number of foliar fertilizers containing the phosphite anion has recently increased (Moor et al., 2009). Phosphite salts are recommended as fertilizer because they contain a cation that may be plant nutrient, such as K^+, NH_4^+, Ca^{2+}, Mg^{2+}, Cu^{2+} or Zn^{2+}, and the P in form of phosphite anion. However, results of studies that investigated nutritional value of phosphite anion as a P nutrient are inconclusive. In the year 1990, it was reported foliar application of potassium phosphite improved set fruit and yield of avocado, and restored normal growth of phosphate-starved citrus (Lovatt, 1990; Lovatt, 1990). Similarly, positive effects of phosphite on plant P nutrition or crop yields also were demonstrated in other works (Albrigo, 1999; Rickard, 2000; Watanabe, 2005). On the other hand, recent studies have indicated phosphite anion may not be used by plants as a P nutrient, even though it is well absorbed by leaves and roots. Moreover, there are indications phosphite supply causes growth depression in phosphate-starved plants (McDonald et al., 2001; Schroetter et al., 2006; Thao et al., 2008, 2009). In this case, it appears that phosphite inhibits the gene expression related to the responses for overcoming P starvation, such as increased phosphatase activity, synthesis of high affinity transporters for P and elongation of the root system (Varadarajan et al., 2002; Ticconi et al., 2001; Lee et al., 2005).

The aim of this study was to investigate (i) interference produced by different soil phosphate levels, to evaluate (ii) action produced by foliar-applied phosphorus forms (phosphite and phosphate), and to measure (iii) as number of foliar application can act on growth, phosphorus status, and nutritional aspect in common bean (*Phaseolus vulgaris* cv. Radiante) plants.

MATERIALS AND METHODS

Growth conditions, substrate, and plant material

Study was implemented in Departamento de Ciência do Solo of the Universidade Federal de Lavras, Brazil (21°14' S; 45°00' W; 915 m asl). Plants remained in glasshouse environment under natural conditions day/night. Substrate used was composed by low-fertility Oxisol (Typic Haplustox) placed in plastic pots with capacity of 6 L (Table 1). For plant material, common bean (*Phaseolus vulgaris* cv.Radiante) was used.

Substrate preparation

Surface soil with depth from 0 to 20 cm was collected from a non-cultivated field with natural Brazilian cerrado vegetation, allowed to dry, crushed to pass through a 4-mm sieve and then mixed with $CaCO_3$ and MgO (4:1 stoichiometric ratio of Ca:Mg) to raise soil base saturation to 60% of cation exchange capacity at pH 7.0. After 30 days of incubation, a basal nutrient solution was applied and was thoroughly mixed with the soil. Nutrients without P treatments were supplied at the following rates of 90 N, 80 K, 30 S, 5 Zn, 5 Mn, 2 Cu, 1 B and 0.25 Mo mg dm^{-3} of dry soil.

Experimental application

Experiment was organized in factorial scheme completely randomized using 2 soil phosphate levels (Pi-starved and Pi-sufficient), combined with 3 nutrient sources supplied via foliar application (KH_2PO_3, KH_2PO_4, and KCl used as control), and 2 foliar application numbers (single and two applications). For soil phosphate levels, Pi-starved and Pi-sufficient corresponded to 40 and 200 mg of P per dm^3 of dry soil, respectively, applied together with the basal nutrient solution. This study had 3 replicates, and each experimental unit consisted of one pot containing two plants, and all variables measured were expressed as mean of two plants.

Nutrient solutions and foliar applications

Solutions of KH_2PO_3 (monobasic potassium phosphite pa), KH_2PO_4 (monobasic potassium phosphate pa) and KCl (potassium chloride pa) were sprayed at concentration of 40 µM, using a manual backpack sprayer. Concentration of P equals the used dose of approximately 3 L of commercial potassium phosphate to 400 L of water, which is usually recommended for growing beans. And KH_2PO_3 was obtained by reaction of H_3PO_3 (phosphorous acid pa) with KOH (potassium hydroxide pa). Single application was implemented when plants presented fourth trifoliate leaf stage, and two applications was carried out in stage of fourth trifoliate leaf and another application in the beginning of flowering stage.

Fertilization as top dressing, irrigation, and harvest

During the soil pot experiment, fertilizations with 240 N, 210 K, and 45 S mg dm^{-3} of dry soil were supplied as top dressing. These fertilizations were split among into three applications throughout the experiment. Soil moisture was maintained at 60% of the total soil pore space occupied by water through daily irrigation. Plants were harvested at full flowering stage and separated into shoot and root. Both shoot and root were rinsed in deionized water and dried at 60°C for 72 h prior to dry weight determination.

Phosphorus determinations

Shoot and root dry mass were ground and analyzed for total P content colorimetrically (Murphy and Riley, 1962) after nitric-perchloric digestion of the plant material (Johnson and Ulrich, 1959). Data from shoot and root dry wt and total P concentration were used to calculate the P accumulation, P uptake efficiency (Swiader et al., 1994) (P total accumulation in plant / root dry wt), P utilization efficiency (Siddiqi and Glass, 1981) [(plant dry wt)^2/ (P total accumulation in plant)], and P translocation from root to shoot (P total accumulation in shoot / P total accumulation in plant)

Table 1. Chemical, physical and mineralogical compositions of Oxisol.

Chemical compositions[1]															
pH	P	K	Zn	Cu	Mn	Fe	EP	Ca	Mg	Al	H+Al	T	m	V	MPAC
	(mg dm^{-3} of soil)						(mg L^{-1})	(cmol$_c$ dm^{-3} of soil)					(%)		(mg kg^{-1})
5.4	0.9	22	0.5	0.7	0.4	27.4	20.5	0.1	0.1	0.1	1.7	2	28	13.3	396

Physical compositions (%)[2]			
Sand	Silt	Clay	OM
60	17	23	0.8

Mineralogical compositions (g kg^{-1} of clay)[3]										
SiO_2	Al_2O_3	Fe_2O_3	TiO_2	P_2O_5	Fe_d	Fe_o	Ct	Gb	Ki	Kr
95.1	97.4	36.2	6.2	0.0	10.8	0.1	752.0	63.0	0.98	0.71

[1] pH in water (1:2.5), P and K by Mehlichl extraction, Mg and Al extractable by 1 M KCl solution (Thomas, 1982); P in the equilibrium solution (EP) according to Alvarez et al. (2000); level of organic matter (OM) according to Anne (1945). T = Cation exchange capacity at pH 7.0; m = Aluminum saturation index; V = Base saturation index and MPAC = maximum P adsorption capacity (Ohtake et al., 1996).[2] The soil granulometry was determined by the pipette method of Day (1965). [3] SiO_2, Al_2O_3, Fe_2O_3, TiO_2 and P_2O_5 were determined according to Vettori (1969) with modifications (Embrapa ,1997); Fe_d, according to Mehra and Jackson (1960); Fe_o, according to Schwertmann (1964) and Ct (kaolinite) and Gb (gibbsite) according to Klug and Alexander (1974). Ki = SiO_2 / Al_2O_3 and Kr = SiO_2 / (Al_2O_3 + Fe_2O_3).

Macro and micronutrients

Concentrations of nutrients in shoot were determined after nitric-perchloric digestion as follows: S by turbidimetry; K by flame photometry; Ca, Mg, Cu, Mn, Fe, and Zn by flame atomic absorption spectroscopy. Total N was determined using the Kjeldahl method after sulphuric digestion, and B by colorimetry using the Azomethine-H method after dry digestion, with ash content obtained in muffle furnace by 1 h at 550°C.

Data analysis

Results were submitted to variance analysis (F teste, $p \leq 0.05$), and when significant differences occurred were applied to Tukey test at 5% level of error probability ($p \leq 0.05$), standard errors were calculated in all evaluated points. The statistical analyses were carried out with the Sisvar software (Ferreira, 2008).

RESULTS AND DISCUSSION

Biomass yield

Most variables in this study were not significantly affected ($p > 0.05$) by foliar application numbers during single application timing and two application timings (Figure 1). As expected, common bean plants grown under limiting phosphate availability (Pi-starved) showed considerable reductions in the root and shoot dry wt and increased root to shoot ratio. The increase root to shoot ratio by phosphate-starved plants is a mechanism for overcoming P deficiency (Clarkson, 1985).

Foliar application of potassium phosphite (KH_2PO_3) and potassium phosphate (KH_2PO_4) had no significant effect ($p > 0.05$) on biomass yield of phosphate-sufficient common bean, when compared with the control (foliar application of potassium chloride). However, for plants grown under limiting phosphate availability, shoot and root dry weight were significantly decreased by foliar-applied potassium phosphite. In addition, root to shoot ratio also was increased with two foliar applications of potassium phosphite (an application in the fourth trifoliate leaf stage and another application in the beginning flowering stage) due to the strong inhibition of shoot dry mass yield. This same behavior also occurred for a single foliar application of potassium phosphite (in the fourth trifoliate leaf stage) but in this case there was no significant difference by Tukey's test ($p > 0.05$). Hence, our results showed phosphite may not be used by common bean as a P nutrient, and that this anion inhibits biomass yield

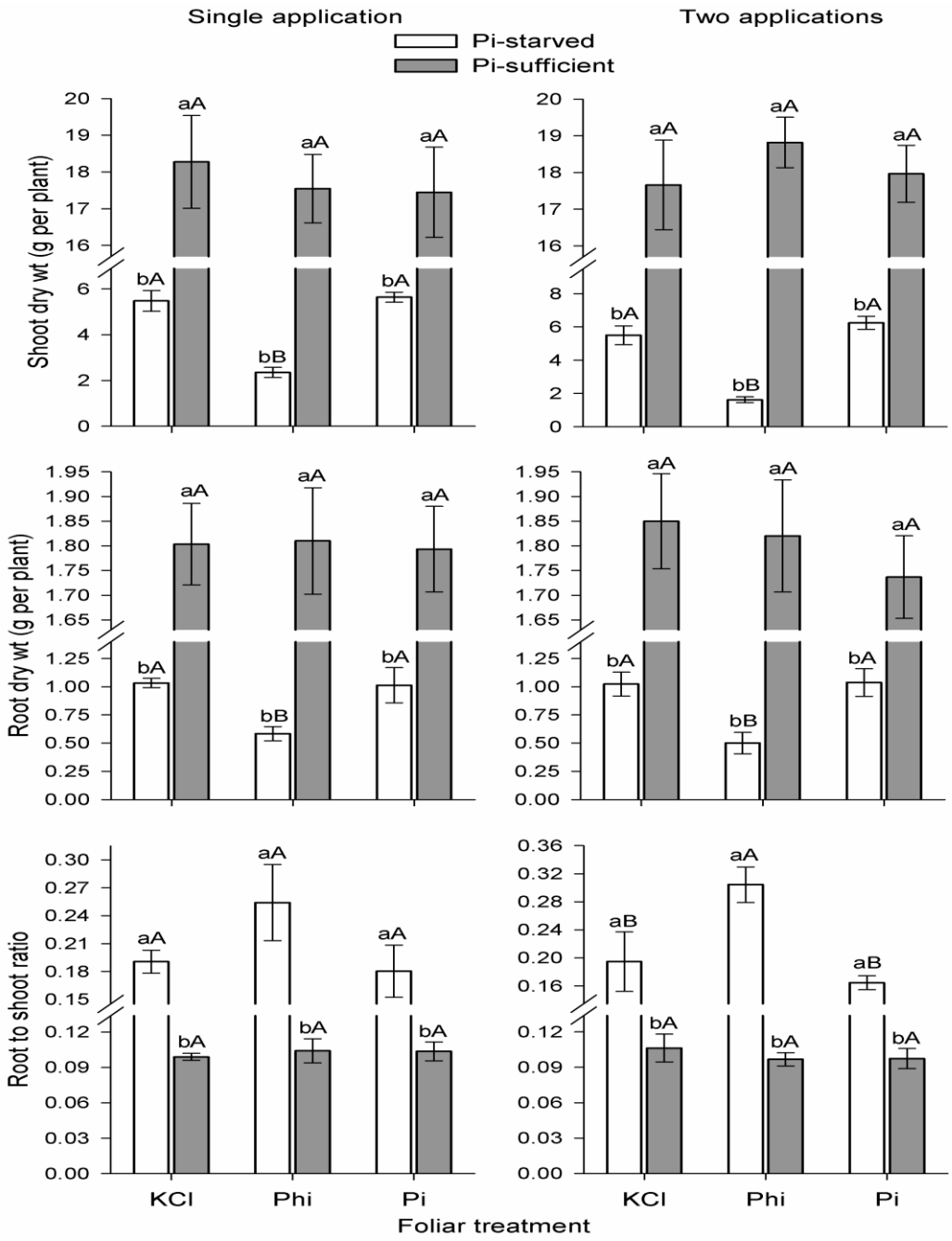

Figure 1. Root dry weight, shoot dry weight, and root to shoot ratio in common bean grown in Oxisol under 2 phosphate levels (Pi-starved and Pi-sufficient), 3 nutrient sources supplied via foliar application (KH_2PO_3, KH_2PO_4, and KCl), and 2 foliar application numbers (single and two applications). Averages followed by the same lowercase letter within soil phosphate levels and uppercase letter among foliar application for each phosphate level, do not differ among themselves by the Tukey test at 5% of probability. The bars represent the mean standard error.

under phosphate-deficient conditions.

The inhibiting effect of the phosphite anion on growth of phosphate-starved plants has been reported by different workers (Thao and Yamakawa, 2009). The causes of this effect are not well understood. The most plausible hypothesis to date is that plants do not metabolize phosphite anion, which, after uptake, remains stable in the cell compartments. Furthermore, phosphite anion inhibits some mechanisms involved in overcoming of phosphate deficiency, such as increased synthesis of phosphatases, phosphodiesterases, nucleases, and high-affinity P transporters. Most likely, the molecular mecha-

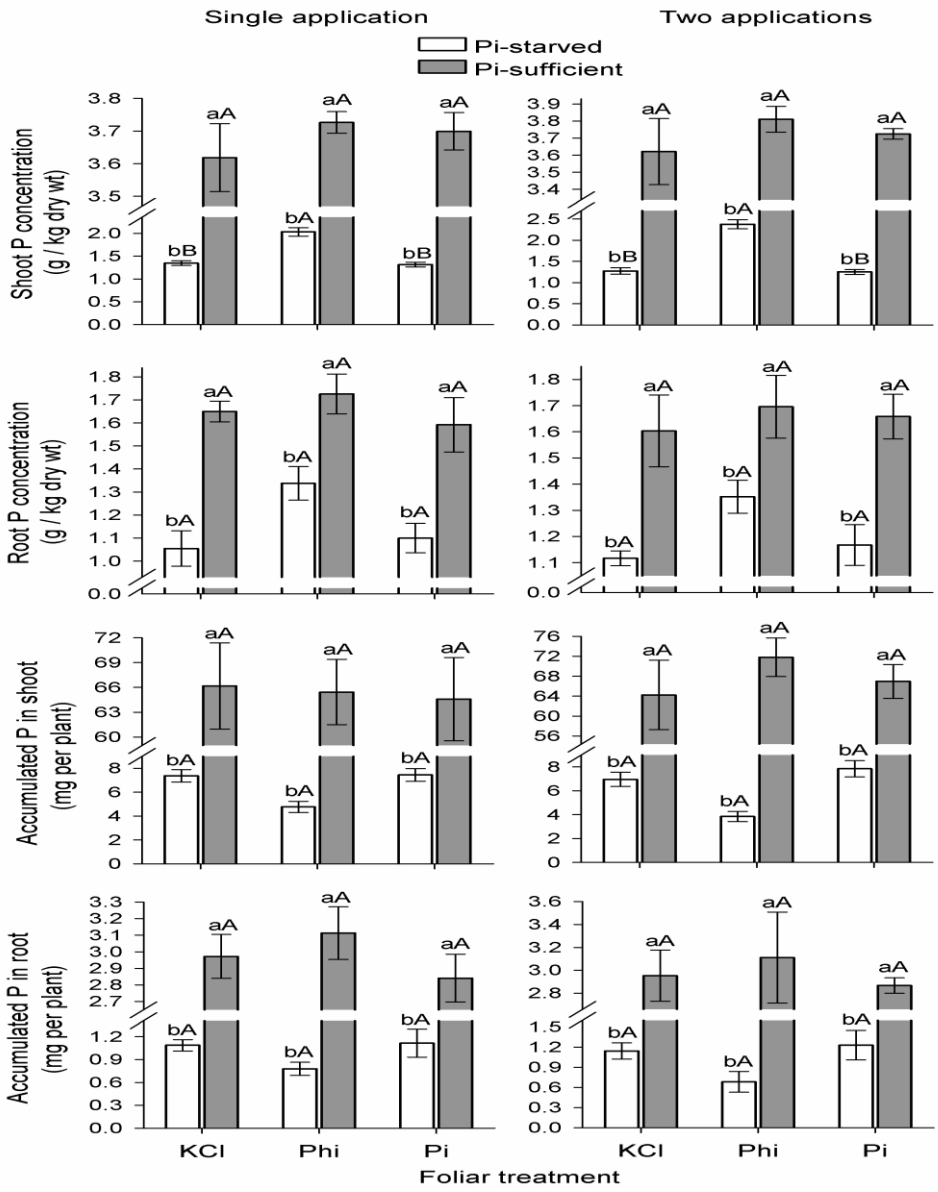

Figure 2. Shoot P concentration, root P concentration, accumulated P in shoot, and accumulated P in root in common bean grown in Oxisol under 2 phosphate levels (Pi-starved and Pi-sufficient), 3 nutrient sources supplied via foliar application (KH_2PO_3, KH_2PO_4, and KCl), and 2 foliar application numbers (single and two applications). Averages followed by the same lowercase letter within soil phosphate levels and uppercase letter among foliar application for each phosphate level, do not differ among themselves by the Tukey test at 5% of probability. The bars represent the mean standard error.

nisms responsible for signaling P deficiency do not discriminate phosphate from phosphite. Thus, there is no expression of genes responsible for proteins involved in P starvation responses (Varadarajan et al., 2002; Ticconi et al., 2001; Lee et al., 2005).

We also found that one and two foliar applications of potassium phosphate had no significant effect ($p > 0.05$) on biomass yield of phosphate-starved common bean, when compared with the control. Thus, these results suggest that several foliar applications of phosphate may be necessary to adequately correct a P deficiency, impractical in most cases.

Concentrations and accumulations of P in shoot and root

Common bean plants grown under limiting phosphate availability (Pi-starved) showed decreased concentrations and accumulations of P in shoot and root (Figure 2).

Foliar-applied potassium phosphite did not affect P nutrition of phosphate-sufficient plants, but increased concentration of P in shoot of phosphate-starved plants. However, accumulation of P was not significant varied among foliar application treatments ($p > 0.05$), showing that this increased concentration of P was not due directly to the P from the foliar-applied phosphite, but likely to concentration effect, which is confirmed by the lower shoot dry weight. When biomass yield decreases, this concentration effect for some nutrients may occur (Crusciol et al., 2008; Marschner, 1995), which is the elevation of their concentration in the tissues without there being an alteration in the quantity of nutrient taken up.

In this study, foliar-applied potassium phosphate did not significantly affect ($p > 0.05$) concentrations and accumulations of P in common bean, when compared with the control. This shows that either one or two foliar applications of phosphate were not sufficient to affect the plant P status. Several attempts to use foliar-applied phosphate in plant nutrition are known, but results are inconclusive. It was recorded that phosphate uptake by leaves after the foliar spray is about 50% (Kannan, 1990). A previous study reported that P concentration in grain of common bean grown under field conditions was not affected by three foliar application timing of phosphate anion (Contee Castro and Boaretto, 2001). On the other hand, Girma et al. (2007) found effect of foliar-applied phosphate on forage and grain P concentrations of maize varied with both applied P levels and plant growth stage. Another study by Mosali et al. (2006) on winter wheat indicated foliar application of phosphate generally increased grain yield, P uptake and P use efficiency, suggesting the authors that low rates of foliar-applied phosphate might correct mid-season P deficiency.

Effects on P uptake efficiency, P utilization efficiency, and P translocation

Either one or two foliar applications of potassium phosphate and phosphite had no significant effects ($p > 0.05$) on P uptake efficiency such as ability to take up P from soil, and also P translocation such as ability to transporter P from root to shoot (Figure 3). Nevertheless, regardless of the foliar-applied treatments, limiting phosphate availability in soil reduced P uptake efficiency and P translocation by common bean. This was principally due to decreased P uptake by phosphate-starved plants according to the Figure 2, although the root dry weight (Figure 1) also was reduced, but in lower magnitude. To reiterate, in this study the P uptake efficiency represent the P-uptake amount per root dry weight unit, and the P translocation from root to shoot represent the ratio between accumulated P in shoot and accumulated P in plant. When the phosphate availability to plants is insufficient, P translocation from root to shoot decreases, increasing the root growth rate to the detriment of shoot growth rate. Thus, phosphate-starved plants commonly have higher root dry weight to shoot dry weight ratio, a response that enhances the P uptake efficiency (Raghothama, 1999; Schenk, 2006).

Foliar-applied treatments did not affect P utilization efficiency (that is, ability to yield biomass for a given plant P concentration) (Siddiqi and Glass, 1981) of phosphate-sufficient plants, whereas under limiting phosphate availability in soil, foliar-applied phosphite decreased P utilization efficiency of common bean. This result was due to the inhibitory effect of phosphite on biomass yield of the phosphate-starved plants (according to the Figure 1), since accumulated P of the plants was not affected by the treatments. In contrast, when compared with the control, either one or two application timings of foliar potassium phosphate had no significant effect ($p > 0.05$) on P utilization efficiency. Other studies had shown phosphate-starved plants exhibit more P utilization efficiency, as response to soil phosphate deficiency, but this more P utilization efficiency varies among cultivars of the same species. Akhtar et al. (2008) found *Brassica* cultivars differ substantially in P utilization efficiency when grown with sparingly soluble P-forms ($Ca_3(PO_4)_2$ and Jordan rock-P). These investigators suggested the existence of useful genetic differences among cultivars for mobilization of P from sparingly soluble P-sources. In spite of phosphate-starved plants tend to increase the P utilization efficiency; the results of this study may have been a reflection of the strong P uptake decrease of the plants grown under phosphate deficient Oxisol.

Concentrations of nutrients in shoot

Likewise for shoot P concentration, concentrations of other nutrients in plant shoot tissues were not significantly affected ($p > 0.05$) by foliar application numbers (Table 2). Apart from the K, common bean grown under limiting phosphate availability exhibited higher concentrations of nutrients in shoot, regardless of the foliar-applied treatments. Foliar application of potassium phosphite also increased concentrations of N, K, Mg, B, Cu, Mn and Fe in shoot tissues of phosphate-starved plants. However, this increased concentration of nutrients coincides with the decreased shoot dry weight (Figure 1), which may suggest that it is involved with the concentration effect, as mentioned above in the presentation of P concentration. Indeed, the applied treatments did not increase accumulation of nutrients in shoot (data not shown), supporting the suggestion above. On the contrary, plants grown under limiting phosphate availability exhibited lower accumulations for all nutrients measured in shoot, regardless of the foliar-applied treatments, due the strong inhibition of shoot biomass yield. Likewise, foliar application of potassium phosphite decreased the accumulation for the majority of nutrients

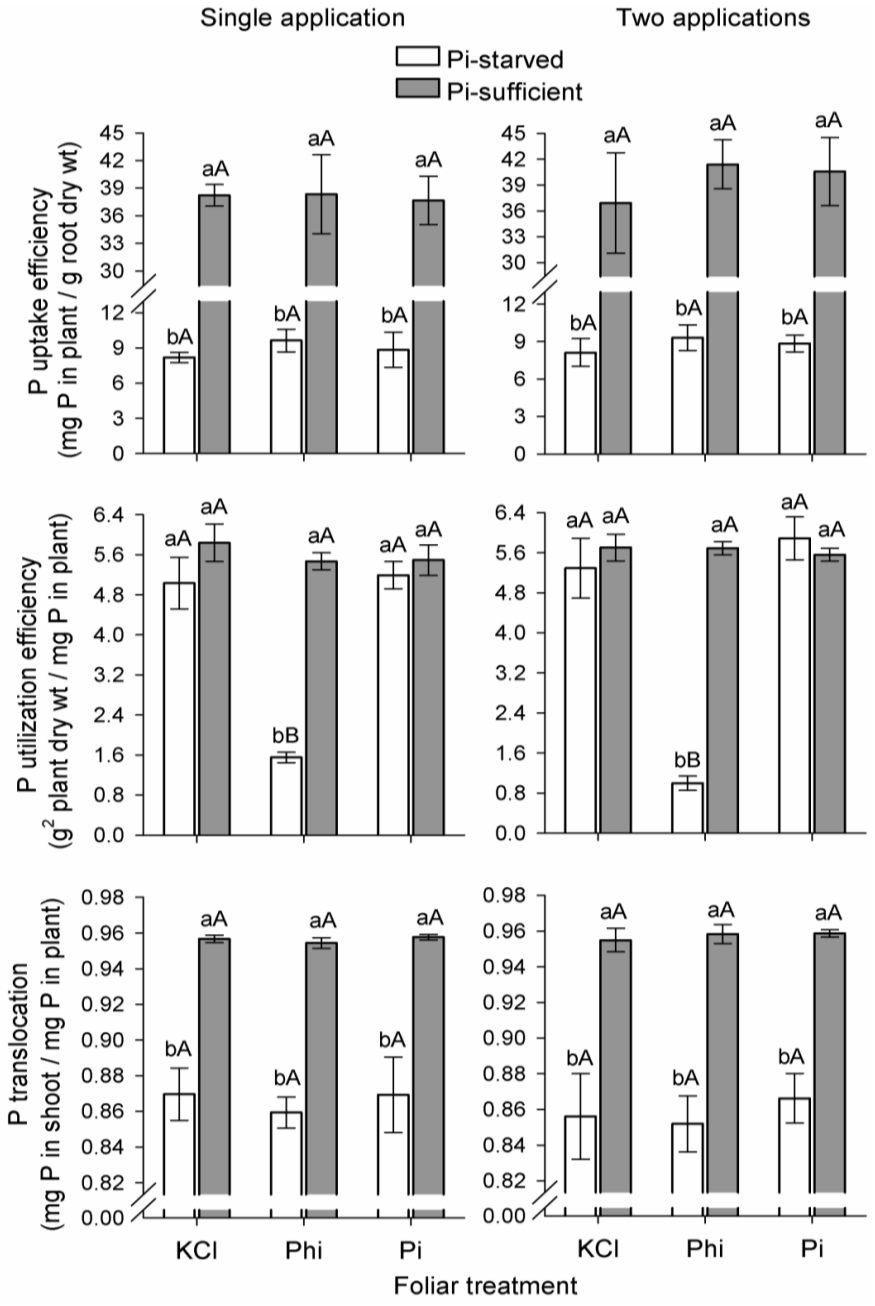

Figure 3. P uptake efficiency, P utilization efficiency, P translocation in common bean grown in Oxisol under 2 phosphate levels (Pi-starved and Pi-sufficient), 3 nutrient sources (KH_2PO_3, KH_2PO_4, and KCl), and 2 foliar supplied via foliar application application numbers (single and two applications). Averages followed by the same lowercase letter within soil phosphate levels and uppercase letter among foliar application for each phosphate level, do not differ among themselves by the Tukey test at 5% of probability. The bars represent the mean standard error.

in shoot of phosphate-starved plant, whereas for others nutrients the foliar treatment effects were not significant ($p > 0.05$). In general, foliar-applied phosphate has no effect on nutrient concentrations and accumulations in shoot. Hu et al. (2008) also did not find alterations in leaf P concentrations of maize plants submitted to foliar NPK applications. In this study the concentrations of nutrients in roots (data not shown) were not affected by application of foliar potassium phosphate and phosphite as well as by foliar application numbers, whereas the limiting phosphate availability in soil increased concentration and decreased accumulation of some nutrients.

Table 2. Concentrations of nutrients in common bean shoot grown in Oxisol under 2 phosphate levels (Pi-starved and Pi-sufficient), 3 nutrient sources supplied via foliar application (KH_2PO_3, KH_2PO_4, and KCl), and 2 foliar application numbers (single and two applications).

Application numbers	Soil P status	Foliar treatments	Macronutrients (g kg^{-1})					Micronutrients (mg kg^{-1})				
			N	K	Ca	Mg	S	B	Zn	Cu	Mn	Fe
A single foliar application timing	Pi-starved	KCl	47^{bA}	19^{bA}	13^{aA}	6^{bA}	2^{aA}	32^{abA}	57^{aA}	6^{bA}	61^{bA}	347^{bA}
		Phi	57^{aA}	22^{aA}	15^{aA}	9^{aA}	2^{aA}	37^{aA}	61^{aA}	8^{aA}	77^{aA}	511^{aA}
		Pi	46^{bA}	18^{bA}	14^{aA}	6^{bA}	2^{aA}	30^{bA}	58^{aA}	5^{bA}	58^{bA}	381^{bA}
	Pi-sufficient	KCl	33^{aB}	17^{aA}	9^{aB}	4^{aB}	1^{aB}	17^{aB}	30^{aB}	4^{aB}	39^{aB}	131^{aB}
		Phi	33^{aB}	17^{aB}	9^{aB}	4^{aB}	1^{aB}	17^{aB}	29^{aB}	3^{aB}	42^{aB}	183^{aB}
		Pi	31^{aB}	18^{aA}	8^{aB}	3^{aB}	1^{aB}	16^{aB}	35^{aB}	4^{aB}	37^{aB}	167^{aB}
Two foliar application timings	Pi-starved	KCl	46^{bA}	20^{bA}	14^{aA}	6^{bA}	2^{aA}	31^{abA}	52^{aA}	5^{bA}	55^{bA}	334^{bA}
		Phi	55^{aA}	23^{aA}	16^{aA}	8^{aA}	2^{aA}	36^{aA}	53^{aA}	7^{aA}	73^{aA}	559^{aA}
		Pi	45^{bA}	19^{bA}	13^{aA}	6^{bA}	2^{aA}	29^{bA}	51^{aA}	5^{bA}	62^{abA}	310^{bA}
	Pi-sufficient	KCl	29^{aB}	18^{aA}	9^{aB}	3^{aB}	1^{aB}	17^{aB}	32^{aB}	4^{aB}	40^{aB}	186^{aB}
		Phi	34^{aB}	19^{aB}	8^{aB}	4^{aB}	1^{aB}	16^{aB}	34^{aB}	3^{aB}	38^{aB}	176^{aB}
		Pi	32^{aB}	19^{aA}	7^{aB}	4^{aB}	1^{aB}	16^{aB}	36^{aB}	3^{aB}	41^{aB}	148^{aB}
Source of variation:												
Foliar application numbers (A)			ns	ns	ns	ns	ns	ns	ns	ns	ns	Ns
Soil P status (B)			***	***	***	***	***	***	***	***	***	***
Foliar treatments (C)			***	*	ns	***	ns	**	ns	***	*	***
A × B			ns	ns	ns	ns	ns	ns	ns	ns	ns	Ns
A × C			ns	ns	ns	ns	ns	ns	ns	ns	ns	Ns
B × C			*	*	ns	**	ns	*	ns	***	*	***
A × B × C			ns	ns	ns	ns	ns	ns	ns	ns	ns	Ns

In each number of foliar application (a single application timing and two application timings), lower case compare the foliar application products (KCl, Phi and Pi) for each soil phosphate level (Pi-starved and Pi-sufficient), and upper case compare the soil phosphate levels for each foliar application product. Means followed by same letter are not different by Tukey's test ($p \leq 0.05$). *, **, ***, and ns corresponding to $p \leq 0.05$, $p \leq 0.01$, $p \leq 0.001$, and non-significant, respectively, by F test.

Conclusion

Common bean growth under limiting phosphate availability in soil exhibited lower biomass yield and higher concentration of nutrients in shoot tissues, which may be due to concentration effect since accumulation of nutrients in shoot was not increased. Either one or two foliar sprays of potassium phosphate were not sufficient to affect the growth and nutrition of the common bean, regard-less of soil P status. However, the results exhibit foliar-applied potassium phosphite causes harmful effects in phosphate-starved common bean, but no effect is observed in phosphate-sufficient common bean, confirming earlier

investigations with other plant species. Our results indicate phosphite anion may not be recommended as a P source for nutrition of common bean, but it is suitable to be used for other purposes that requires an optimum soil phosphate status.

ACKNOWLEDGEMENTS

The authors are grateful to the CNPq, CAPES and FAPEMIG, all from Brazil, for the financial support. F.W. Ávila also thanks CNPq for a postgraduate fellowship.

REFERENCES

Akhtar MS, Oki Y, Adachi T (2008). Genetic variability in phosphorus acquisition and utilization efficiency from sparingly soluble p-sources by *Brassica* cultivars under P-stress environment. J. Agron. Crop Sci., 194(5): 380-392.

Albrigo LG (1999). Effects of foliar applications of urea or Nutriphite on flowering and yields of Valencia orange trees. Proc. Fla. State Hort. Soc., 112(1): 1-4.

Alvarez VVH, Novais RF, Dias LE, Oliveira JA (2000). Determination and phosphorus use available. Boletim Informativo da Sociedade Brasileira de Ciência do Solo, 25(1): 27-32.

Anne A (1945). Sur le dosage rapide du carbone organique des sols. Ann. Agron., 2(1): 161-172.

Clarkson DT (1985). Factors affecting mineral nutrient acquisition by plants. Ann. Rev. Plant Physiol., 36(1): 77-115.

Barbara: University of California, California. Agric. Exp. Stat. Bull., 766: 1956.

Contee CAM, Boaretto AE (2001). Foliar fertilization of bean with nutrients, b1 vitamin and methionine. Sci. Agraria, 2(1): 117-121.

Cook PJ, Landschoot PJ, Schlossberg MJ (2009). Inhibition of *Pythium* spp. and suppression of Pythium Blight of turfgrasses with phosphonate fungicides. Plant Dis., 93(8): 809-814.

Crusciol CAC, Arf O, Soratto RP, Mateus GP (2008). Grain quality of upland rice cultivars in response to cropping systems in the Brazilian Tropical Savanna. Sci. Agrícola, 65(5): 468-473.

Danova-Alt R, Dijkema C, Dewaard P, Köck M (2008). Transport and compartmentation of phosphite in higher plant cells-kinetic and ^{31}P nuclear magnetic resonance studies. Plant Cell Environ., 31(10): 1510-1521.

Day PR (1965). Particle fractionation and particle-size analysis. In: Black CA (ed.). Methods of soil analysis, Part 1, Madison, Wisconsin, USA: Am. Soc. Agron., pp. 545-566.

Deliopoulos T, Kettlewell PS, Hare MC (2010). Fungal disease suppression by inorganic salts: A review. Crop Prot., 29(10): 1059-1075.

Embrapa-Empresa Brasileira de Pesquisa Agropecuária (1997). Methods of soil analysis. 2 Ed. Centro Nacional de Pesquisa de Solos/EMBRAPA, Rio de Janeiro, RJ, Brazil.

Ferreira DF (2008). Sisvar: a program for statistical analysis and teaching. Revista Sympos., 6(1): 36-41.

Girma K, Martin KL, Freeman KW, Mosali J, Teal RK, Raun WR, Moges SM, Arnall DB (2007). Determination of optimum rate and growth stage for foliar-applied phosphorus in corn. Commun. Soil Sci. Plant Anal., 38(9): 1137-1154.

Hu Y, Burucs Z, Schmidhalter U (2008). Effect of foliar fertilization application on the growth and mineral nutrient content of maize seedlings under drought and salinity. Soil Sci. Plant Nutr., 54(1): 133-141.

Johnson CM, Ulrich A (1959). Analytical methods for use in plant analysis. California Agric. Exp. Station Bull., p. 766.

Kannan S (1990). Role of foliar fertilization on plant nutrition. In: Baligar VC, Duncan RR (eds.). Crops as enhancers of nutrient use. Academic Press, San Diego, USA. pp. 313-348.

Klug HP, Alexander LE (1974). X-ray diffraction procedures for polycrystalline and amorphous materials, John Wiley and Sons, New York, NY, USA.

Lee TM, Tsai PF, Shyu YT, Sheu F (2005). The effects of phosphite on phosphate starvation responses of *Ulva lactuca* (Ulvales, chlorophyta). J. Phycol., 41(5): 975-982.

Lovatt CJ (1990). Foliar phosphorus fertilization of citrus by foliar application of phosphite. In: Citrus Research Advisory Committee (ed.). Summary of Citrus Research. University of California, Riverside, USA, pp. 25-26.

Lovatt CJ (1990). A definitive test to determine whether phosphite fertilization can replace phosphate fertilization to supply P in the metabolism of 'Hass' on 'Duke 7'. California Avocado Society Yearbook, 74(1): 61-64.

Marschner H (1995). Mineral nutrition of higher plants. Academic Press, London, England.

McDonald AE, Grant BR, Plaxton WC (2001). Phosphite (Phosphorous acid): Its relevance in the environment and agriculture and influence on plant phosphate starvation response. J. Plant Nutr., 24(10): 1505-1519.

Mehra OP, Jackson ML (1960). Iron oxide removal from soils and clays by a dithionite-citrate system buffered with sodium bicarbonate. Clays Clay Miner., 7(1): 317-327.

Moor U, Põldma P, Tõnutare T, Karp K, Starast M, Vool E (2009). Effect of phosphite fertilization on growth, yield and fruit composition of strawberries. Sci. Hortic., 119(2): 264-269.

Mosali J, Desta K, Teal RK, Freeman KW, Martin KL, Lawles JW, Raun WR (2006). Effect of foliar application of phosphorus on winter wheat grain yield, phosphorus uptake, and use efficiency. J. Plant Nutr., 29(12): 2147-2163.

Murphy J, Riley HP (1962). A modified single solution method for the determination of phosphate in natural waters. Anal. Chim. Acta, 27(1): 31-36.

Ohtake H, Wu H, Imazu K, Anbe Y, Kato J, Kuroda A (1996). Bacterial phosphonate degradation, phosphite oxidation and polyphosphate accumulation. Resour. Conserv. Recycl., 18(1): 125-134.

Raghothama KG (1999) Phosphate acquisition. Annu. Rev. Plant Physiol., Plant Mol. Biol., 50(1): 665-693.

Rickard DA (2000). Review of phosphorus acid and its salts as fertilizer materials. J. Plant Nutr., 23(2): 161-180.

Schenk MK (2006). Nutrient efficiency of vegetable crops. Acta Hortic., 700(1): 21-34.

Schroetter S, Angeles-Wedler D, Kreuzig R, Schnug E (2006). Effects of phosphite on phosphorus suplly and growth of corn (*Zea mays*). Landbauforsch Völkenrode, 56(1): 87-99.

Schwertmann U (1964). Differenzierung der eisenoxide des bondes durch extraktion mit ammonium-oxalat-losung. Zeitschrift Pflanzenernähr Düng Bodenkd, 105(1): 194-202.

Shearer BL, Fairman RG (2007) A stem injection of phosphite protects *Banksia* species and *Eucalyptus marginata* from *Phytophthora cinnamomi* for at least four years. Australas Plant Pathol., 36(1): 78-86.

Siddiqi MY, Glass ADM (1981). Utilization Index: A modified approach to the estimations and comparison of nutrient utilization efficiency in plants. J. Plant Nutr., 4(3): 289-302.

Swiader JM, Chyan Y, Freiji FG (1994). Genotypic differences in nitrate uptake and utilization efficiency in pumpkin hybrids. J. Plant Nutr., 17(10): 1687-1699.

Thao HTB, Yamakawa T, Shibata K, Sarr PS, Myint AK (2008). Growth response of komatsuma (*Brassica rapa* var. peruvirids) to root and foliar applications of phosphate. Plant Soil, 308(1): 1-10.

Thao HTB, Yamakawa T, Shibata K (2009). Effect of phosphite-phosphate interaction on growth and quality of hydroponic lettuce (*Lactuca sativa* L.). J. Plant Nutr. Soil Sci., 172(3): 378-384.

Thao HTB, Yamakawa T (2009). Phosphite (phosphorous acid): Fungicide, fertilizer or bio-stimulator? Soil Sci. Plant Nutr., 55(2): 228-234.

Ticconi CA, Delatorre CA, Abel S (2001). Attenuation of phosphate starvation responses by phosphite in Arabidopsis. Plant Physiol., 127(3): 963-972.

Thomas GW (1982). Exchangeable cations. In: Page AL, Miller RH and Keeney DR (eds.). Methods of soil analysis, Part 2, Madison,

Wisconsin, USA: American Society of Agronomy, Soil Sci. Soc. Am., pp. 159-165.
Vance CP, Uhde-Stone C, Allan DL (2003). Phosphorus acquisition and use: critical adaptations by plants for securing a nonrenewable resource. New Phytol., 157(3): 423-447.
Varadarajan DK, Karthikeyan AS, Matilda PD, Raghothama KG (2002). Phosphite, an analog of phosphate suppresses the coordinated expression of genes under phosphate starvation. Plant Physiol., 129(3): 1232-1240.
Vettori L (1969). Methods of soil analysis. Ministério da Agricultura, Rio de Janeiro, RJ, Brazil, p. 24.
Watanabe K (2005). A new fertilizer for foliar application, phosphite fertilizer. Fertilizer, 101(1): 91-96.
Wilkinson CJ, Holmes JM, Dell B, Tynan KM, Mccomb JA, Shearer BL, Orbović V, Syvertsen JS, Bright D, Van Clief DL, Graham JH (2008). Citrus seedling growth and susceptibility to root rot as affected by phosphite and phosphate. J. Plant Nutr., 31(4): 774-787.

Scientific Research and Essays Vol. 7(25), pp. 2205-2212, July 2012
Available online at http://www.academicjournals.org/SRE
DOI: 10.5897/SRE11.2012
ISSN 1992-2248 ©2012 Academic Journals

Full Length Research Paper

Effects of short term exposure of layer-type breeder eggs to magnetic field on hatchability and hatching parameters

Shafey T. M.[1]*, M. A. Alodan[1], M. M. Ghannam[2], M. A. K. Abdelhalim[2] and M. M. Mady[2]

[1]Department of Animal Production, College of Food and Agriculture Sciences, King Saud University, P. O. Box 2460, Riyadh 11451, Saudi Arabia.
[2]Department of Physics, College of Sciences, King Saud University, P. O. Box 2460, Riyadh 11451, Saudi Arabia.

Accepted 25 April, 2012

Two trials were conducted to investigate the effects of short term exposure of layer-type breeder eggs to magnetic field (MF) of 7.5 Gauss (0.75 mT) at 50 Hz, for 0, 20, 40 and 60 min before incubation on the characteristics of egg contents, egg weight loss, embryonic growth and hatching time (Trial 1) and hatchability of eggs (Trials 1 and 2). 384 and 240 Leghorn and Baladi eggs were used in trials 1 and 2, respectively. Treatments were replicated 4 times in the two trials. Exposing Leghorn eggs to MF did not influence weight of egg contents, eggshell thickness, albumen and yolk heights, embryo weight, hatching time and hatchability of eggs. Eggs exposed to MF for 40 and 60 min had higher weight loss percentage and chick hatching weight when expressed on the basis of absolute value. It can be concluded that short term exposure of layer-type breeder eggs to MF of 7.5 Gauss (0.75 mT) at 50 Hz, for up to 60 min before incubation did not influence the characteristics of egg contents, embryonic growth, hatching time, and hatchability of eggs. MF exposure of eggs for 40 and 60 min increased egg weight loss during incubation, and chick weight at hatch day.

Key words: Magnetic field, layer eggs, embryonic growth, hatchability.

INTRODUCTION

The use of electrical devices around us has resulted in a great interest in the biological effects of the electromagnetic fields (EMF) radiated from these devices. Magnetic field (MF) is part of the electromagnetic spectrum. All living organisms (almost) are exposed to MF from various sources. MF affects various biological functions of living organisms, for example, DNA synthesis and transcription (Phillips et al., 1992), as well as ion transportation through cell membranes (Liburdy et al., 1993). The geomagnetic field on the surface of the earth is approximately 0.50 to 0.75 Gauss (0.05 to 0.075 mT) at 50 Hz in strength. The detectable limit of interaction between higher animals and a stationary MF is 80 to 100 Gauss (8 to 10 mT) (Ketchen et al., 1978).

The body of birds is formed by many cells that communicate with the environment through information transfer carried out by electric impulses or chemical substances. The body EMFs from the biological structures are characterized by certain specific frequencies that can be interfered with by the EMF radiation, through induction and causing modification in their biological responses, and capable of morphological change and metabolism, growth and reproduction (Hyland, 2000). Animals exposed to the EMF can suffer a deterioration of health, changes in behaviour (Marks et al., 1995; L'oscher and K'as, 1998), and reproductive

*Corresponding author. E-mail: tmshafey@ksu.edu.sa. Tel: 966-1-4678785. Fax: 966-1-4678474.

success (Doherty and Grubb, 1996; Fernie et al., 2000). EMF exposure affected the reproductive success of kestrels (*Falco sparverius*), increasing fertility, egg size, embryonic development and fledging success but reduced hatching success (Fernie et al., 2000). Birds are especially sensitive to MFs (Liboff and Jenrow, 2000). Grigoriew (2003) reported a high mortality rate of chicken embryos subjected to the radiation from a cell phone when compared with those of the control group. Exposing chicken embryos to pulsed MFs increased mortality (Youbicier-Simo and Bastide, 1999) and morphological abnormalities, especially of the neural tube (Ubeda et al., 1983, 1994; Farrell et al., 1997). Recently, Shafey et al. (2011) found that exposing meat-type breeder eggs to MF of 18 Gauss (1.8 mT) at 50 Hz for up to 75 min did not influence the hatchability of eggs and chick weight at hatch. However, hatched chicks from eggs exposed to MF for 60 and 75 min had lower weight gain and feed intake than those of the non-exposed treatment at 39 days of age.

There is lack of information regarding the effects of MF on the hatchability traits of layer type breeder eggs. The objectives of this study were to examine the effects of MF before incubation of layer-type breeder eggs on the characteristics of eggs, embryonic development, hatchability, hatching time and chick weight at hatch day.

MATERIALS AND METHODS

The effects of exposure of fertile eggs to MF before incubation on the characteristics of egg contents, embryonic growth and hatchability of layer-type breeder eggs were investigated in 2 trials. A total of 384 freshly laid eggs produced by a layer-type breeder flock (Leghorn, King Saud University), at 50-weeks of age were used in trial 1. Birds were fed a standard breeder ration (16% CP, 2866 kcal/kg of ME per kg, 3.4% calcium, 0.45% available phosphorus) and reared under standard husbandry conditions. A photoperiod of 14 h commenced when the birds were caged at 22 weeks of age and was maintained throughout the trials. Eggs were numbered, weighed individually, distributed into weight classes and assigned into 16 replicates of 24 eggs each. Four replicates were randomly assigned to each of the four experimental treatments. The treatments were non-exposed control (MF0) or exposed to MF of 7.5 Gauss (0.75 mT) at 50 Hz for 20, 40 and 60 min (MF20, MF40 and MF60) before incubation. Twelve eggs from each treatment were selected at random to investigate the effects of MF on the quality and characteristics of egg contents. Eggs were broken, albumen and yolk separated, weighed and then percentage of albumen and yolk were calculated (percent albumen = albumen weight/egg weight*100, and percent yolk = yolk weight/egg weight*100, respectively). Egg shells were washed with water, dried at room temperature of 25°C with paper towels, weighed and then percent eggshell was calculated (percent eggshell = eggshell weight/egg weight*100). Three eggshell thickness measurements were taken from each eggshell with a micrometer (Ames, Waltham, MA, USA). Measurements of eggshell weight and eggshell thickness were done with the membranes intact. The remaining eggs were incubated and four eggs per treatment were removed for egg weight loss and embryo weight measurements on day 7, 14, and 18 of incubation. Eggs were weighed, broken open, and embryos were separated and weighed individually after removing the yolk sac and placing it on a paper tissue to dry. Percents of egg weight loss and embryonic weight were calculated (percent egg weight loss = (1-egg weight after incubation/egg weight before incubation)*100, and percent embryo = embryo weight/egg weight before incubation*100, respectively). Measurements were made of egg contents and characteristics (weight of albumen, yolk, and eggshell, eggshell thickness, and height of albumen and yolk), embryonic growth and egg weight loss during incubation, percents of hatchability and hatchability failures (pips with live embryos, pips with dead embryos, dead embryos), and hatching time.

The incubation trial was repeated with different strain of eggs. A total of 240 eggs produced by a layer-type breeder flock (Baladi, King Saud University), at 53-week of age were used in this trial. Husbandry conditions of the flock were similar to those of the Leghorn flock. Eggs were evenly assigned into 16 replicates of 15 eggs of equal weight per each replicate. Replicates were assigned to the four treatments as in trial 1. Measurements were made of percentages of hatchability and hatchability failures (pips with live embryos, pips with dead embryos, dead embryos).

Magnetic field

A homogenous MF was generated by four solenoids of 270 turns each of electrically insulated copper coil of 2.2 mm, wound around a parallel double walled cylindrical chamber from copper of 2 mm thick and internal and external diameter of 45 and 55 cm, respectively (Figure 1). The four coils are connected in parallel to minimize the total impedance of the wire and to get a homogeneous MF within the chamber volume. The coils are connected to a variac fed from the main power outlet (220 V_{pp} and 50 Hz). The strength of MF was controlled and varied by the variac. The MF inside the chamber is measured at different locations in order to find out the most homogenous zone inside the chamber. A hand-held Gauss/Tesla Meter Model 4048, with probe T-4048-001 (USA) of accuracy ± 2% is used to calibrate the MF. Homogeneity of MF under different field intensities is shown in Figure 2.

The space between the double walled cylindrical chamber was sealed with an inlet and outlet to permit water flow between the two cylinders in order to keep the temperature of the chamber constant during the exposure period. The temperature of the flowing cooling water at the outlet of the jacket and the temperature inside the irradiation chamber were constantly measured through the use of thermocouple thermometer, which can give reading for the temperature variations within ± 0.1°C. There was no difference in temperature between the room and the chamber.

Incubation of eggs

Eggs were set in a Maino, force-draft incubator (Model II, Maino Enrico, Co., Rome, Italy) and incubated at 99.5°F (37.5°C) and 55% relative humidity. Eggs were transferred to separate compartments in the hatching tray on 19 days of incubation, for chick identification at hatch. The hatching tray was divided into individual hatching compartments using thin sheets of wire mesh. Incubation procedures were similar to those published previously (Shafey et al., 2005b), in which eggs were examined by candling at days 6 and 14 of incubation, and clear eggs and eggs containing dead embryos were removed. Early dead embryos were counted from days 1 to 14 of incubation. The hatcher condition was 98.6°F (37°C) and 65% relative humidity until the end of day 21 of incubation, at which time chicks, pips (unhatched eggs with live or dead chicks) and late dead embryos (unhatched eggs with unbroken shell) were counted. Late dead embryos were counted from day 14 to the end of day 21,

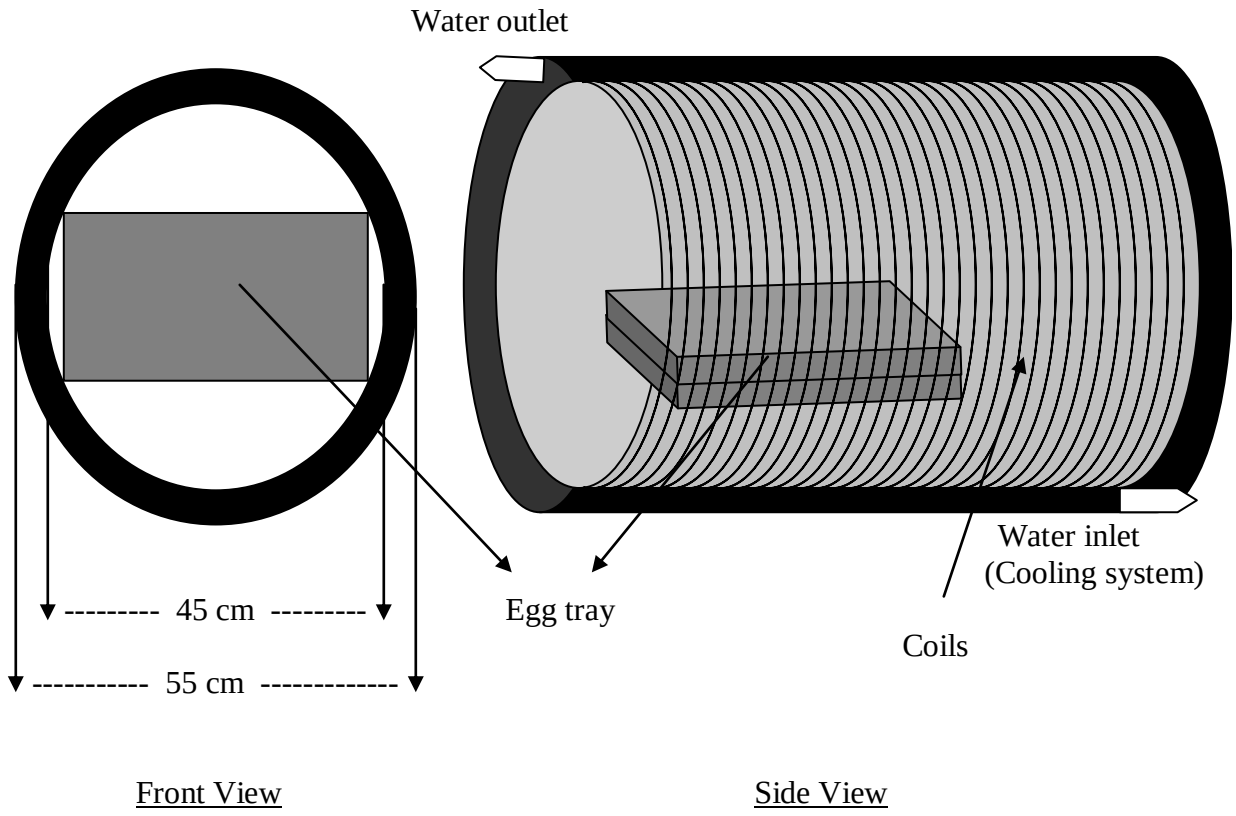

Figure 1. Magnetic field.

when incubation ended. Percentage of hatchability was calculated on the basis of the number of hatched chicks as a per cent of the number of fertile eggs per treatment. Hatching time was recorded every 24 h in the first trial. Chicks were removed every 24 h intervals from 432 to 504 h of incubation and hatching weight were recorded by scale with 0.1 g accuracy. Percent of hatched chicks over each interval of 24 h was calculated as percentage of the total number of hatched chicks over the whole incubation period.

Data on egg contents, and characteristics, and chick hatching weight (trial 1), hatchability (trials 1 and 2) were subjected to a one-way ANOVA. Data on egg weight loss, and embryonic weight were arranged in 4 × 3 factorials with four levels of treatments [0 (non-exposed eggs, control), 20, 40, and 60 min of MF] and three days of incubation (days 7, 14 and 18) as main effects and their two-way interactions fitted into the model. All percent data were transformed using arc sine square root percentage transformation before analysis. When significant variance ratios were detected, differences between treatment means were tested using the least significant difference (LSD) procedure. All statistical analysis was performed using the Statistical Analysis System (SAS Institute, 1985).

RESULTS

The effects of exposing layer-type breeder eggs to MF of 7.5 Gauss (0.75 mT) for up to 60 min before incubation on the characteristics of egg contents, weight of embryos, egg weight loss, hatchability and hatchability failures (early or late dead embryos and pips with live or dead chicks), chick hatching weight and length of incubation are shown in Tables 1 to 4, respectively (trial 1). There were no significant differences in the percentage of albumen, yolk, eggshell, and embryo weights in the egg, eggshell thickness, egg albumen, and yolk heights, and percentages of hatchability and hatchability failures, and incubation period. Eggs of MF40 and MF60 had significantly ($P < 0.05$) higher weight loss percentage during incubation and chick weight when expressed on the basis of absolute value (g) than those of MF0, whilst percent of egg weight loss and chick hatching weight (g) of MF20 were intermediate. Age of embryo significantly ($P < 0.01$) influenced percent of egg weight loss and embryo weight. Embryos at older age had higher percent of egg weight loss and body weight when compared with those of younger age (18 days < 14 days < 7 days). Percent of chick hatching weight of MF40 was significantly ($P < 0.05$) higher than those of MF0, whilst percent of chick hatching weight of MF20 and MF60 was intermediate. Percent of hatched chicks of MF40 and MF60 was higher at 456 h of incubation and lower at 480 h of incubation than those of MF0 and MF20 (trial 1).

The effects of exposing Baladi eggs to MF of 7.5 Gauss

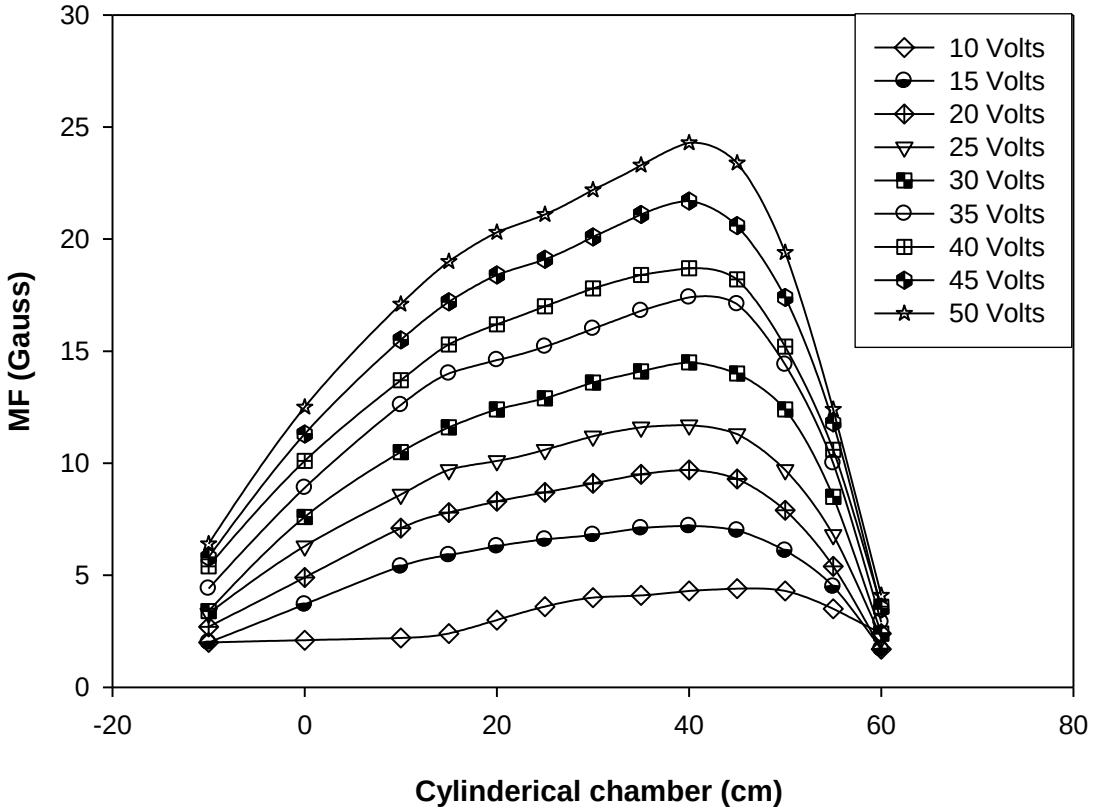

Figure 2. Homogeneity of magnetic field (MF) inside the cylindrical chamber under different field intensities.

(0.75 mT) for up to 60 min before incubation on hatchability and hatchability failures are shown in Table 5 (trial 2). Exposing Baladi eggs to MF did not significantly influence percents of hatchability and hatchability failures of eggs.

DISCUSSION

Results from this study indicated that exposing layer-type breeder eggs to MF of 7.5 Gauss (0.75 mT) for up to 60 min before incubation did not influence the egg contents and its characteristics, embryonic growth, hatchability, hatchability failures and incubation period (trial 1). Eggs exposed to MF for 40 and 60 min had higher weight loss per cent during incubation and chick hatching weight when expressed on the basis of absolute value than those of the non-exposed treatment by approximately 10.4 and 1.2, and 14.4 and 1.2%, respectively (trial 1). The effects of MF on the chicken embryo weight and chick weight at hatch day are in agreement with Koch and Koch (1991) who reported no effects for MF of pulsed waveforms and 50 Hz sinusoidal fields on embryos. Similarly, Cox et al. (1993) reported no effect on the development of chicken embryos when eggs were exposed to MF of 10 µT, 50 Hz in the first 52 h of incubation. The effect of MF on chick weight was in agreement with Pierra et al. (1992) who reported an increase in chick weight at hatch day. In contrast, several studies reported that MF affected early development of chicken embryos, and increased malformation (Delgado et al., 1982; Juutilainen, 1986; Juutilainen and Saali, 1986; Juutilainen et al., 1986, 1987; Farrell et al., 1997), and hatchability of chicken eggs exposed to MF before incubation, and reduced hatchability and chick weight from eggs exposed to MF during incubation (Toman et al., 2002), and had no affect on chick hatching weight (Veicsteinas et al., 1996; Shafey et al., 2011). These studies on the effects of MF on chicken embryos, hatchability and chick hatching weight have been reported in the literature, but evaluation of the consistency of the findings is difficult due to the varying methods, periods of exposures, approaches used in different studies and strain of bird.

The increase in chick weight at hatch day in this experiment may have resulted, partly from the difference in egg weight loss during incubation. Shafey et al. (2005a, 2007) reported that incubation of eggs under the influence of electric field of 30 Kv/m at 60 Hz significantly increased the percentage of egg weight loss and chick-

Table 1. Egg contents, eggshell thickness and albumen and yolk heights of layer-type breeder (Leghorn) eggs exposed to magnetic field (MF) of 7.5 Gauss before incubation for up to 60 min (Trial 1) [1].

MF treatment (min)	Egg weight (g)	Albumen weight (%)[2]	Yolk Weight (%)[2]	Shell weight (%)[2]	Shell thickness* 100 (mm)	Albumen height*10 (mm)	Yolk height *10 (m m)
0	55.4 ± 1.80	59.7 ± 0.80	30.7 ± 0.91	9.5 ± 0.21	38.7 ± 1.32	80.2 ± 2.27	53.0 ± 2.81
20	55.9 ± 1.61	58.5 ± 1.46	31.9 ± 1.21	9.6 ± 0.45	37.4 ± 1.69	73.7 ± 2.85	52.3 + 3.50
40	55.1 ± 2.02	59.5 ± 0.74	30.6 ± 0.68	9.8 ± 0.11	39.2 ± 0.25	76.7 ± 3.00	52.4 + 2.84
60	55.7 ± 1.78	58.8 ± 1.51	31.8 ± 1.68	9.4 ± 0.26	39.0 ± 1.58	72.4 ± 6.53	52.4 + 3.42
Probability	NS	NS	NS	NS	NS	NS	NS

[1], Values are means ± SE of 12 eggs; [2], As a percentage of egg weight; NS= Not significant (P > 0.05).

Table 2. Mean percent of egg weight loss, and embryo weight of layer-type breeder eggs (Leghorn) exposed to magnetic field (MF) of 7.5 Gauss before incubation for up to 60 min (Trial 1) [1].

Treatment	Egg weight (g)	Egg weight loss (%)[2]	Embryo weight (%)[2]
MF (T) (min)			
0 (18)	55.24 ± 0.95	9.04 ± 0.72[b]	18.41 ± 3.76
20 (18)	55.39 ± 0.83	9.64 ± 0.79[ab]	18.80 ± 3.88
40 (18)	54.90 ± 0.82	9.98 ± 0.89[a]	18.73 ± 3.84
60 (18)	54.34 ± 1.07	10.34 ± 1.06[a]	19.72 ± 3.80
Embryonic age (day)			
7 (24)	55.33 ± 0.84	5.58 ± 0.17[c]	1.13 ± 0.04[a]
14 (24)	54.3 ± 0.67	10.04 ± 0.28[b]	15.96 ± 0.31[b]
18 (24)	55.32 ± 0.86	13.63 ± 0.45[a]	38.87 ± 0.74[a]
T	NS	P < 0.05	NS
Age	NS	P < 0.0001	P < 0.0001
T × Age	NS	P < 0.05	NS

[1], Values are means ± SE of the number of replicates given in parentheses; [2], As a percentage of egg weight. [a,b,c], Means within column followed by different superscripts are significantly different (P < 0.05); NS= Not significant (P > 0.05).

hatching weight of Baladi eggs by approximately 18.4 and 1.7%, respectively. Egg weight loss during incubation is very important for embryonic growth and development (Rahn and Ar, 1974; Rahn et al., 1981), and consequently, hatchability (Meir et al., 1984). However, it seems that the increase in egg weight loss during incubation of MF treated eggs was not enough to influence hatchability and hatchability failures of eggs (Romanoff, 1930; Peebles and Brake, 1985). MF exposure of eggs for 20, 40 and 60 min reduced albumen height by approximately 8.1, 4.4 and 9.7% (Table 1), respectively, albeit non-significantly, may indicate that MF exposure of eggs before incubation tended to increase the liquefaction of albumen of eggs and consequently vital gas exchange. Meuer and Baumann (1988) and Brake et al. (1993) suggested that thick albumen might interfere with gas exchange during early incubation. In this study, eggs of comparable weights, contents, and eggshell thickness were used (Table 1). This finding may suggest that MF exposure of eggs before incubation increased the evaporation rate of water from eggs and consequently increased egg weight loss. The improvement of evaporation rate of water from the incubated egg may improve the capacity of eggshell to vital gas exchange and consequently, support oxygen consumption of the embryo.

Results indicated exposure of eggs to MF for 40 and 60 min before incubation increased percent of hatching chicks within 456 h of incubation by approximately 85.7 and 98.6%, respectively and reduced percent of hatching chicks within 480 h of incubation by approximately 29.7 and 15.6%, respectively, without any significant effect on the length of incubation when compared with those of the control (Table 4). It appears that exposing layer-type eggs to MF for 40 and 60 min increased egg weight loss, chick hatching weight (g), and hatching rate of chicks at456 h of incubation and tended to increase chick weight percentage and liquefaction of albumin, albeit non-

Table 3. Mean percent of hatchability, hatchability failures, egg weight and chick hatching weight express on an absolute and percentage basis (chick hatching weight*100/egg weight) of layer-type breeder eggs (Leghorn) exposed to magnetic field (MF) of 7.5 Gauss before incubation for up to 60 min (Trial 1)[1].

MF treatment (min)	Hatch of fertile (%)[2]	Early dead embryo (%)	Late dead embryo (%)	Pipped with live embryos (%)	Pipped with dead embryos (%)	Egg weight (g)	Chick weight (g)	Chick weight (%)
0	84.48 ± 2.04	1.39 ± 1.39	11.27 ± 0.16	1.47 ± 1.47	1.39 ± 1.39	55.44± 0.51	36.88 ± 0.37[b]	66.41 ± 0.28[b]
20	87.17 ± 4.97	4.33 ± 2.80	8.50 ± 3.63	0.00 ± 00.00	0.00 ± 00.00	55.33 ± 0.47	36.85 ± 0.32[ab]	66.63 ± 0.26[ab]
40	80.15 ± 3.91	10.05 ± 5.03	8.41 ± 3.66	1.39 ± 1.39	0.00 ± 00.00	55.32 ± 0.49	37.31 ± 0.38[a]	67.45 ± 0.32[a]
60	85.78 ± 2.45	5.71 ± 0.16	8.50 ± 2.61	0.00 ± 00.0	0.00 ± 00.00	55.46 ± 0.59	37.31 ± 0.50[a]	67.23 ± 0.41[ab]
Probability	NS	NS	NS	NS	NS	NS	P < 0.05	P < 0.05

[1], Values are means ± SE of 4 replicates with 21 eggs in each replicate. There was no significant difference in the percentage of fertile eggs (mean ± SE) between treatments (95.8 ± 1.39, 98.6 ± 1.39, 97.2 ± 2.78, and 98.6 ± 1.39, for eggs exposed to MF for 0, 20, 40 and 60 min, respectively, NS= Not significant (P > 0.05).

Table 4. Incubation period of layer-type breeder eggs (Leghorn) exposed to magnetic field (MF) of 7.5 Gauss before incubation for up to 60 min (Trial 1)[1].

MF treatment (min)	Incubation period (h)	Hatching distribution over the incubation period (%)		
		Incubation period (h)		
		456	480	504
0	475.0 ± 2.99	21.0 ± 12.46[b]	79.0 ± 12.46[a]	0.0 ± 0.00
20	475.5 ± 2.52	21.8 ± 9.01[b]	75.3 ± 7.60[a]	2.9 ± 1.71
40	471.9 ± 0.86	39.0 ± 5.05[a]	55.5 ± 6.72[b]	5.4 ± 1.86
60	472.7 ± 0.47	41.7 ± 4.81[a]	47.1 ± 11.35[b]	11.2 ± 6.57
Probability	NS	P < 0.0201	P < 0.0031	NS

[1] Values are means ± SE of hatching hour; NS= Not significant (P > 0.05).

Table 5. Mean percent of hatchability and hatchability failures of layer-type breeder eggs (Baladi) exposed to magnetic field (MF) of 7.5 Gauss before incubation for up to 60 min (Trial 2)[1].

MF treatment (min)	Hatch of fertile (%)[2]	Early dead embryo (%)	Late dead embryo (%)	Pipped with live embryos (%)	Pipped with dead embryos (%)
0	87.48 ± 3.41	6.39 ± 1.69	3.66 ± 1.63	2.47 ± 1.68	0.00 ± 0.00
20	85.17 ± 4.18	4.33 ± 1.91	6.50 ± 2.31	2.50 ± 1.25	1.50 ± 1.500
40	83.15 ± 3.98	5.05 ± 3.09	8.41 ± 2.79	1.31 ± 1.31	2.08 ± 2.08
60	86.78 ± 2.44	6.50 ± 1.96	5.51 ± 2.61	1.21 ± 1.09	0.00 ± 00.00
Probability	NS	NS	NS	NS	NS

[1] Values are means ± SE of 4 replicates with 15 eggs in each replicate. There was no significant difference in the percentage of fertile eggs (mean ± SE) between treatments (97.6 ± 1.32, 98.4 ± 1.79, 96.9 ± 2.13, and 97.9 ± 1.89, for eggs exposed to MF for 0, 20, 40 and 60 min, respectively; NS= Not significant (P > 0.05).

significantly. These results may suggest that exposure of eggs to MF for 40 and 60 min improved the characteristics of egg contents leading to increased eggshell conductance and gas exchange (Christensen et al., 1996), and increased the efficiency of transfer of nutrients from the eggs, and consequently enhanced nutrient utilization by embryos.

It can be concluded that MF exposure of eggs to MF of 7.5 Gauss at 50 Hz for up to 60 min for layer breeder eggs did not influence the characteristics of egg contents, hatchability and hatchability failures of eggs. MF of 7.5 Gauss at 50 Hz exposure of eggs for 40 and 60 min increased egg weight loss during incubation, and hatching weight of chickens.

ACKNOWLEDGEMENTS

The authors extend their appreciation to the Deanship of Scientific Research at King Saud University for funding the work through the research group project No RGP-VPP-121. The authors would like to thank E.O.S. Elkordy for his technical assistance.

REFERENCES

Brake J, Walsh TJ, Vick SV (1993). Relationship of egg storage time, storage conditions, flock age, eggshell and albumen characteristics, incubation conditions, and machine capacity to broiler hatchability-Review and model synthesis. Zootec. Int., 16: 30-41.

Christensen VL, Davis GS, Lucore LA (1996). Eggshell conductance and other functional qualities of ostrich eggs. Poult. Sci., 75: 1404-1410.

Cox FC, Brewer LJ, Raeman CH, Schryver CA, Child SZ, Carstensen EL (1993). A test for teratological effect of power frequency magnetic fields on chick embryos. IEEE T. Bio-Med. Eng., 40: 605-610.

Delgado JMR, Leal J, Montagudo JL, Gracie G (1982). Embryological changes induced by weak, extremely low frequency electromagnetic fields. J. Anat., 134: 533-551.

Doherty PF, Grubb TC (1996). Effects of high-voltage power lines on birds breeding within the power lines' electromagnetic. Sialia, 18: 129-134.

Farrel JM, Litovitz TL, Penafiel M (1997). The effect of pulsed and sinusoidal magnetic fields on the morphology of developing chick embryos. Bioelectromagnetics, 18: 431-438.

Fernie KJ, Bird DM, Dawson RD, Lague PC (2000). Effects of electromagnetic fields on the reproductive success of American kestrels. Physiol. Biochem. Zool., 73: 60–65.

Grigoriew JG (2003). Influence of the electromagnetic field of the mobile phones on chickens embryo, to the evaluation of the dangerousness after the criterion of this mortality. J. Radiat. Biol., 5: 541-544.

Hyland GJ (2000). Physics and biology of mobile telephony. Lancet, 356: 1-8.

Juutilainen J (1986). Effects of low frequency magnetic fields on chick embryos: Dependence on incubation temperature and storage of the eggs. Z. Naturforsch. A, 41c: 1111-1115.

Juutilainen J, Saali K (1986). Development of chick embryos in 1 Hz to 100 kHz magnetic fields. Radiat. Environ. Biophys., 25:135-140.

Juutilainen J, Harri M, Saali K, Lahtinen T (1986). Effect of 100-Hz magnetic fields with various waveforms on the development of chick embryos. Radiat. Environ. Biophys., 25:65-74.

Juutilainen J, Laara E, Saali K (1987). Relationship between field strength and abnormal development in chick embryos exposed to 50 Hz magnetic fields. Int. J. Radiat. Biol., 52: 787-793

Ketchen EE, Porter WE, Bolton NE (1987). The biological effects of magnetic fields on man. Am. Ind. Hyg. Assoc. J., 39: 1-11.

Koch WE, Koch BA (1991). Exposure of chicken embryos to selected magnetic fields. J. Bioelectricity, 10: 65–80.

Liboff AR, Jenrow KA (2000). New model for the avian magnetic compass. Bioelectromagnetics, 21: 555-565.

Liburdy RP, Callahan DE, Harland J, Dunham E, Sloma TR, Yaswen P (1993). Experimental evidence for 60 Hz magnetic fields operating through the signal transduction cascade: effects on calcium influx and c-MYC mRNA induction. FEBS Lett., 334: 301-308.

L'oscher W, K'as G (1998). Conspicuous behavioural abnormalities in a dairy cow herd near a tv and radio transmitting antenna. Prac. Vet. Surg., 29: 437-444.

Marks TA, Ratke CC, English WO (1995). Stray voltage and developmental, reproductive and other toxicol. problems in dogs, cats and cows: a discussion. Vet. Hum. Toxicol., 37: 163-172.

Meir M, Ar A, Nir A (1984). Preincubation dipping of turkey eggs. Does it affect eggshell conductance? Poult. Sci., 63: 2475-2478.

Meuer HJ, Baumann R (1988). Oxygen pressure in intra- and extra-embryonic blood vessels of early chick embryos. Resp. Physiol. 71:331-342.

Peebles ED, Brake J (1985). Relationship of eggshell porosity to stage of embryonic development in broiler breeders. Poult. Sci., 64: 2388-2391.

Phillips JL, Haggren W, Thomas WJ, Ishida-Jones T, Adey WR (1992). Magnetic field- induced changes in specific gene transcription. Biochim. Biophys. Acta., 112: 140-144 .

Pierra V, Rodriquez A, Cobos A, Torrente M, Cobos P (1992). Influence of continuos electromagnetic fields on the stage, weight and stature of chick embryo. Acta Anat. Base, 145: 302-306.

Rahn H, Ar A (1974). The avian egg: Incubation time and water loss. Condor, 76: 147-152.

Rahn H, Christensen VL, Eden FW (1981). Changes in egg conductance, pores, and physical dimensions of egg and shell during the first breeding cycle of turkey hens. Poult. Sci., 60: 2536-2541.

Romanoff AL (1930). Biochemistry and biophysics of the development hen's egg. Memoir. by Cornell University. Agricultural Experiment Station, 132: 1-27.

SAS Institute (1985). SAS User's Guide: Statistics (Cary, NC, SAS Institute Inc.).

Shafey TM, Al-Batshan HA, Al-Hassan MJ, Al-Haidary AA, Al-Faraj A, Ghannam, MM (2005a). Embryonic growth of chicks under the influence of electric field. Int. J. Poult. Sci., 11: 872-878.

Shafey TM, Al-Batshan HA, Ghannam MM (2007). Effects of electric field on hatchability performance of a layer-type breeder eggs. Br. Poult. Sci., 48: 145-153.

Shafey, TM, Al-Batshan, HA, Ghannam MM, Al-ayed MS (2005b). Effect of intensity of eggshell pigment and illuminated incubation on hatchability of brown eggs. Br. Poul. Sci., 46: 190-198

Shafey TM, Aljumaah RS, Swillam SA, Al-mufarrej, SI, Al-abdullatif AA, Ghannam MM (2011). Effects of short term exposure of eggs to magnetic field before incubation on hatchability and post-hatch performance of meat chickens. Saudi J. Biol. Sci., 18: 381-386.

Toman R, Jedlicka J, Broucek J (2002). The influence of a temporary magnetic field on chicken hatching. J. Environ. Sci. Health. A, 37: 969-974.

Ubeda AJ, Leal MA, Trillo MA, Jimenez MA, Delgado JMR (1983). Pulse shape of magnetic fields influences chick embryogenesis. J. Anat., 137: 513-536.

Ubeda A, Trillo MA, Chacon L, Blanco MJ, Leal J (1994). Chick embryo development can be irreversibly altered by early exposure to weak extremely-low-frequency magnetic fields. Bioelectromagnetics, 15: 385-398.

Veicsteinas A, Bellerii M, Cinquetti A, Parlini S, Barbato G, Molinari Tosatti MP (1996). Development of chicken embryos exposed to an intermittent horizontal sinusoidal 50 Hz magnetic field.

Bioelectromagnetics, 17: 411-424.
Youbicier-Simo, BJ, Bastide M (1999). Pathological effects induced by embryonic and postnatal exposure to EMFs radiation by cellular mobile phones. Radiat. Prot., 1: 218-223.

Scientific Research and Essays Vol. 7(25), pp. 2213-2217, 5 July, 2012
Available online at http://www.academicjournals.org/SRE
DOI: 10.5897/SRE11.1876
ISSN 1992-2248 ©2012 Academic Journals

Full Length Research Paper

Aortic branch variations: An anatomical study in 900 subjects

Federico Mata-Escolano[1], Luis Aparicio-Bellver[2], Vicente Martinez-Sanjuan[1] and Juan A. Sanchis-Gimeno[2]*

[1]Eresa General University Hospital of Valencia, Spain.
[2]Department of Anatomy and Human Embryology, Faculty of Medicine, University of Valencia, Spain.

Accepted 11 June, 2012

The anatomic variations in the branches arising from the aortic arch in 900 Caucasian subjects and the exact origin of the right subclavian artery, the right common carotid artery, the left common carotid artery, the left subclavian artery, the right vertebral artery, and the left vertebral artery were analyzed by means of angio-computerized tomography. Seven hundred and thirty-four subjects (81.55%) had three branches arising from the aortic arch, 126 subjects (14%) had 2 branches and 40 subjects (4.44%) had 4 branches. In addition, the following anatomic variations were found: The left common carotid was observed arising from the brachiocephalic trunk in 80 subjects (8.88%); the left carotid and the brachiocephalic trunk arose from a common stem, which in turn arose directly from the aortic arch in 46 subjects (5.11%); the right common carotid and the right subclavian artery (arteria lusoria) arose directly from the aortic arch in 30 (3.33%) and 4 subjects (0.44%), respectively; the left vertebral artery and the right vertebral artery arose directly from the aortic arch in 16 (1.77%) and 2 subjects (0.22%), respectively. The study revealed that more than 20% of the Caucasian subjects had anatomical variations in the aortic arch branches.

Key words: Aortic arch, arteries, vessels.

INTRODUCTION

Theoretically, human body anatomy is very well known as should be the case of the number of branches arising directly from the human aortic arch. Normally, three branches arise directly from the human aortic arch, these being the brachiocephalic trunk (BCT), the left common carotid artery (LCCA), and the left subclavian artery (LSA). It is considered as normal that the right common carotid artery (RCCA) and the right subclavian artery (RSA) arise from the BCT. Moreover, the right vertebral artery (RVA) arises from the right subclavian artery (RSA) and the left vertebral artery (LVA) from the left subclavian artery (LSA).

Currently, the development of modern imaging techniques makes it possible to study the human aortic arch branches *in vivo*. The use of imaging techniques is increasing the knowledge of the anatomy of the branches that arise from the aortic arch (Lemke et al., 1999; Goray et al., 2005; Natsis et al., 2009; Fawcett et al., 2010). The exact anatomy of an aortic arch malformation and its relationship to adjacent structures can be accurately defined by computerized tomography (CT) and magnetic resonance (MR). Both methods allow excellent delineation of all patent vessels by contrast enhanced angiography (angio-CT and angio-MR) with comparable image quality and the possibility of 3-D display of the malformation (Kellenberger, 2010).

In the light of the aforementioned, we present the largest study, to our knowledge, carried out on

*Corresponding author. E-mail: juan.sanchis@uv.es. Tel: + 34 96 3983518. Fax: + 34 96 3864815.

Abbreviations: BCT, Brachiocephalic trunk; **LCCA,** left common carotid artery; **LSA,** left subclavian artery; **RCCA,** right common carotid artery; **RSA,** right subclavian artery; **RVA,** right vertebral artery; **LVA,** left vertebral artery.

Figure 1. Angio-CT showing the 'normal' three branches arising from the aortic arch. From left to right: the BCT, the LCCA, and the LSA.

Caucasians using angio-CT that analyzes the variations in the number of branches arising directly from the human aortic arch. In addition, we also analyzed the exact origin of the RSA, the RCCA, the LCCA, the LSA, the RVA, and the LVA.

MATERIALS AND METHODS

We carried out a four-year prospective study in order to quantify the number of branches arising directly from the human aortic arch. We analyzed a large sample of 900 Caucasian volunteers. The mean age of the 900 subjects was 62.84 ± 15.04 years old (range, 18 to 88 years). There were 400 women (44.44%) and 500 men (55.55%). All protocols were approved by the Committees of Ethics and Research of the Faculty of Medicine, University of Valencia. The work was performed in accordance with the World Medical Association's Declaration of Helsinki and written informed consent was obtained from all subjects. Subjects who were diagnosed with cardiovascular pathology before the study were excluded. No subjects had either clinical symptoms of cardiovascular pathology during the study. We analyzed these kinds of subjects because we wanted to study variations of the anatomical normality in asymptomatic subjects.

We quantified the number of branches arising directly from the aortic arch and analyzed the exact origin of the RSA, RCCA, LCCA, LSA, RVA, and LVA arteries by means of angio-CT. The angio-CT study was carried out with a LightSpeed ultra CT (General Electric Medical Systems, Milwaukee, WI, USA). The device used can make 16 slices per second; the slice thickness was 0.63 mm. Iopamidol 300 (Bracco UK. Ltd, High Wycombe, Bucks, UK) intravenous contrast medium was administered during the study (100 ml). Image reconstructions were made with Voxar 3D software (Barco, Kortrijk, Belgium).

RESULTS

Of the 900 subjects examined, 734 (81.55%) presented 3 branches (for example, BCT, LCCA, and LSA, in that order) arising directly from the human aortic arch (Figure 1). In that typical branching pattern, the RCCA and the RSA arose from the BCT, the RVA arose from the RSA and the LVA arose from the LSA. Nevertheless, we also found 126 subjects (14%) that presented 2 branches and 40 subjects (4.44%) that presented 4 branches that arose from the aortic arch (Figures 2 and 3).

In addition, we found the following anatomic variations in the origin of the arteries: the LCCA was observed arising from the BCT in 80 subjects (8.88%); the LCCA and the BCT arose from a common stem, which in turn arose directly from the aortic arch in 46 subjects (5.11%); the RCCA and the RSA (aberrant RSA or arteria lusoria) arose directly from the aortic arch in 30 (3.33%) and 4 subjects (0.44%), respectively; the LVA and the RVA arose directly from the aortic arch in 16 (1.77%) and 2

Figure 2. Angio-CT showing only two branches arising from the aortic arch. From left to right: the BCT and the LSA. The LCCA was observed arising from the BCT.

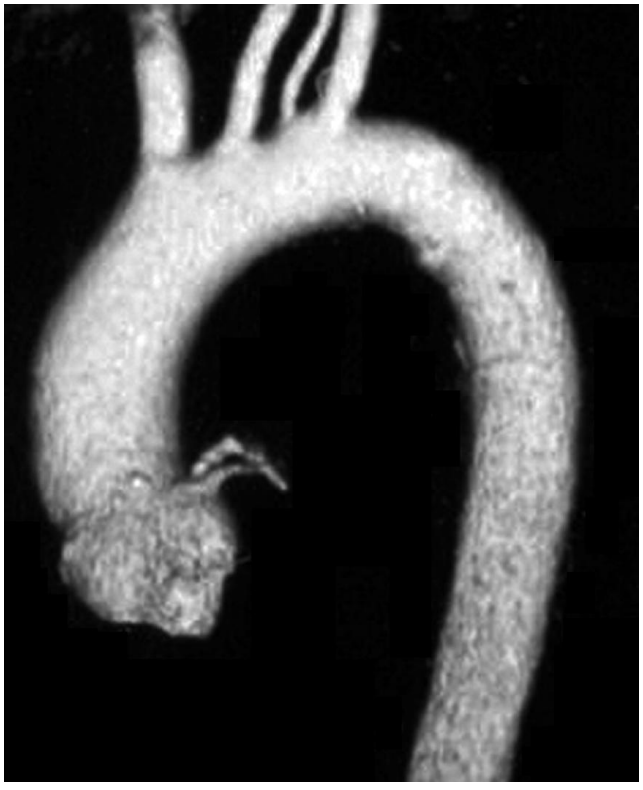

Figure 3. Angio-CT showing four branches arising from the aortic arch. From left to right: the BCT, the LCCA, the LVA and the LSA.

subjects (0.22%), respectively.

DISCUSSION

We have analyzed the number of branches arising directly from the human aortic arch and the exact origin of the RSA, the RCCA, the LCCA, the LSA, the LVA, and the RVA in a large sample of Caucasian subjects. The exact anatomy of an aortic arch malformation and its relationship to adjacent structures can be accurately defined by CT (Kellenberger, 2010); thus we used this technique to study the aortic arch branches. Moreover, we used angio-CT because it has the great advantage of making a hospital stay unnecessary. Another of the most important points of the study is the large cohort we analyzed with this technique. In addition, angio-CT makes it possible to obtain anatomic images *in vivo* simulating a "virtual dissection", thus similar results can be obtained to those acquired when performing cadaveric human dissections.

Natsis et al. (2009) in an angiographic study carried out on 633 subjects, described eight types (I to VIII) of the aortic arch; Type I being the most common type (83%), that is, the "normal" aortic arch giving rise to three branches: the BCT (or innominate artery), which then branches into the RSA and RCCA, the LCCA and the LSA. We also found the same normal pattern. Similar results were found in the classic study carried out on cadavers by Thomson (1893) and in the cadaveric studies carried out by Grande et al. (1995) and by Shin et al. (2008). However, Williams et al. (1932) and McDonald and Anson (1940) observed that only approximately 50% of Afro-Americans have the most common type of aortic arch. More recently, Nelson and Spark (2001) and Nayak et al. (2006) observed that more than 90% of the American-Japanese and Indian cadavers they studied have the most common type of the aortic arch. Aortic arch anomalies are usually incidental findings on imaging studies (Kellenberger, 2010). These anatomical anomalies of the aortic arch are usually asymptomatic (Poultsides et al., 2004; Chahwan et al., 2006; Natsis et al., 2009) as was the case in the subjects we analyzed.

We also found the presence of an aberrant RSA or arteria lusoria in 0.44% of the subjects we analyzed. Arteria lusoria is the most common anomaly of the aortic arch, occurring in 0.5 to 2.5% of individuals (Myers et al., 2010). Arteria lusoria is usually asymptomatic because the aberrant artery does not form a complete vascular ring around the esophagus and trachea, and is most often discovered during the course of evaluation of other mediastinal anomalies (Myers et al., 2010). Although these variations are often asymptomatic, they have been described as being the cause of a condition called "dysphagia lusoria". This situation is characterized by difficulty in swallowing and pain in some cases, due to the pressure applied by the artery onto the wall of the esophagus (Natsis et al., 2009).

Results obtained in the present study are of special importance for surgeons. Preoperative angio-CT can be ideal for studying the anatomy of the aortic branches. Surgeons can obtain an idea of what they are going to find before performing surgery. In addition, the results of this kind of study may be of interest to surgeons when they cannot carry out radiologic studies before surgery (that is emergency surgery on a patient in a critical condition) because, as was described in this study, the anatomy of aortic branches is different in approximately 20% of subjects and knowing this can help to anticipate possible complications during surgery. Moreover, we have found variations in the aortic branches. An explanation for the variations in the aortic arch has been thought to be related to a different development of the aortic branches during the embryonic period (Barry, 1951). Nevertheless, ethnicity may be another cause for the differences, as has been suggested by other authors (Williams et al., 1932; McDonald and Anson, 1940). Based on this, we analyzed a large sample exclusively made up of Caucasian subjects.

In conclusion, the present study has shown that approximately 20% of subjects have a 'non normal' anatomy of the aortic branches, if we take into account that a normal anatomy has three branches arising directly from the aortic arch: The BCT, the LCCA and the LSA.

REFERENCES

Barry A (1951). The aortic arch derivatives in human adult. Anat. Rec., 111(2): 221-238.

Chahwan S, Miller MT, Kim KA, Mantell M, Kirksey L (2006). Aberrant right subclavian artery associated with a common origin of carotid arteries. Ann. Vasc. Surg., 20(6): 809-812.

Fawcett SL, Gomez AC, Hughes JA, Set P (2010). Anatomical variation in the position of the BCT (innominate artery) with respect to the trachea: a computed tomography-based study and literature review of Innominate Artery Compression Syndrome. Clin. Anat., 23(1): 61-69.

Goray VB, Joshi AR, Garg A, Merchant S, Yadav B, Maheshwari P (2005). Aortic arch variation: a unique case with anomalous origin of both vertebral arteries as additional branches of the aortic arch distal to left subclavian artery. Am. J. Neuroradiol., 26(1): 93-95.

Grande NR, Costa e Silva A, Pereira AS, Aguas AP (1995). Variations in the anatomical organization of the human aortic arch. A study in a Portuguese population. Bull. Assoc. Anat. Nancy, 79(244): 19-22.

Kellenberger CJ (2010). Aortic arch malformations. Pediatr. Radiol., 40(6): 876-884.

Lemke AJ, Benndorf G, Liebig T, Felix R (1999). Anomalous origin of the right vertebral artery: review of the literature and case report of right vertebral artery origin distal to the left subclavian artery. Am. J. Neuroradiol., 20(7): 1318-1321.

McDonald JJ, Anson BJ (1940). Variations in the origin of arteries derived from the aortic arch, in American whites and negroes. Am. J. Phys. Anthropol., 27(1): 91-107.

Myers PO, Fasel JH, Kalangos A, Gailloud P (2010). Arteria lusoria: developmental anatomy, clinical, radiological and surgical aspects. Ann. Cardiol. Angeiol. Paris, 59(3): 147-154.

Natsis KI, Tsitouridis IA, Didagelos MV, Fillipidis AA, Vlasis KG, Tsikaras PD (2009). Anatomical variations in the branches of the human aortic arch in 633 angiographies: clinical significance and literature review. Surg. Radiol. Anat., 31(5): 319-323.

Nayak RS, Pai MM, Prabhu LV, D'Costa S, Shetty P (2006). Anatomical organization of aortic arch variations in the India: embryological basis and review. J. Vasc. Bras., 5(2): 95-100.

Nelson ML, Sparks CD (2001). Unusual aortic arch variation: distal origin of common carotid arteries. Clin. Anat., 14(1): 62-65.
Poultsides GA, Lolis ED, Vasquez J, Drezner AD, Venieratos D (2004). Common origins of carotid and subclavian arterial systems: report of a rare aortic arch variant. Ann. Vasc. Surg., 18(5): 597-600.
Shin IY, Chung YG, Shin WH, Im SB, Hwang SC, Kim BT (2008). A morphometric study on cadaveric aortic arch and its major branches in 25 korean adults: the perspective of endovascular surgery. J. Korean Neurosurg. Soc., 44(2): 78-83.
Thomson A (1893). Third Annual Report of Committee of Collective Investigation of Anatomical Society of Great Britain and Ireland for the Year 1891-92. J. Anat. Physiol., 27(Pt 2): 183-194.
Williams GD, AFF HM, Schmeckebier M, Edmonds HW, Graul EG (1932). Variations in the arrangement of the branches arising from the aortic arch in American whites and negroes. Anat. Rec., 54(2): 247-251.

Scientific Research and Essays Vol. 7(25), pp. 2218-2224, 5 July, 2012
Available online at http://www.academicjournals.org/SRE
DOI: 10.5897/SRE11.2261
ISSN 1992-2248 ©2012 Academic Journals

Full Length Research Paper

Anthropometric measures as predictors for the occurrence of insulin resistance among obese Jordanians

Khalid M. Abu khadra[1] and Ahmad Aljaberi[2]*

[1]Department of Biology, Faculty of Science, Yarmouk University, Irbid, Jordan.
[2]Department of Pharmaceutical Sciences and Pharmaceutics, Faculty of Pharmacy, Applied Science University, Amman, Jordan.

Accepted June 18, 2012

A total of 210 overweight and obese participants were recruited to investigate the association between various obesity parameters with insulin resistance (IR) in Jordanians. Weight, height, waist circumference (WC) and hip circumference were measured, and the corresponding body mass index (BMI), waist to hip ratio (WHR), and waist to height ratio (WHtR) were calculated. HOMA-IR was calculated from the corresponding fasting blood sugar and plasma insulin levels for each participant. The correlation as well as the prediction ability of obesity parameters for the occurrence of insulin resistance was evaluated statistically. Pearson and point-biserial correlation coefficients revealed that only BMI, WC and WHtR correlated with insulin resistance. However, the strength of correlation appeared to be gender-dependent. Logistic regression and ROC curve analysis showed that BMI is the best parameter to predict insulin resistance in the male population followed by WHtR. In females however, WHtR appeared to be a better classifier than BMI. In conclusion, BMI and WHtR were found to be the most significant obesity parameters for predicting insulin resistance in Jordanians male and female populations, respectively.

Key words: Obesity, body mass index, waist circumference, waist to height ratio, insulin resistance.

INTRODUCTION

Insulin resistance is a pathophysiological condition characterized by an impaired response to the presence of insulin. The exact mechanism behind the development of this condition is complex and not well understood. Several factors have been thought to play a major role in the development of insulin resistance. At the top of the list is obesity-associated exposure of tissues to elevated dietary nutrients and the resultant accumulation of toxic metabolic by-products (Kahn et al., 2006; Muoio and Newgard, 2008). The high association between obesity and insulin resistance was recognized among both males and females, and it appeared across all ethnic groups (Khan and Flier, 2000).

On the other hand, obesity is considered as an independent risk factor to type 2 diabetes mellitus (T2DM) (Carey et al., 1997; Chan et al., 1994). This association depends basically on the aforementioned link between obesity and the risk of developing insulin resistance. Insulin resistance was found to be a reputable finding among obese patient with T2DM, and considered by some authors to be the basic etiology for T2DM as most of T2DM patients shows this resistance (Reaven, 1988; Taylor, 1999; Wellen and Hotamisligil, 2005). Accordingly, obesity and insulin resistance could be used

*Corresponding author. E-mail: aljaberi@asu.edu.jo. Tel: +962-6-560-9999. Ext: 1141. Fax: +962-6-523-2899.

Abbreviations: BMI, Body mass index; **HOMA,** homeostatic model assessment; **IR,** insulin resistance; **ROC,** receiver-operating characteristic; **T2DM,** type 2 diabetes mellitus; **WC,** waist circumference; **WHR,** waist to hip ratio; **WHtR,** waist to height ratio.

Table 1. Baseline characteristics of study participants.

Characteristic	Men	Women	All participants
Participants (n)	91	119	210
Age (years)	32.82 ± 11.99	33.53 ± 11.79	33.22 ± 11.86
Weight (kg)	103.30 ± 23.69	81.03 ± 14.76	90.68 ± 22.07
Height (m)	1.73 ± 0.07	1.60 ± 0.05	1.66 ± 0.09
BMI (kg/m^2)	34.51 ± 6.7	31.55 ± 5.51	32.83 ± 6.22
WC (cm)	108.09 ± 14.73	97.66 ± 10.39	102.18 ± 13.46
WHR (kg/m)	0.92 ± 0.05	0.90 ± 0.06	0.91 ± 0.06
WHtR (kg/m)	0.63 ± 0.08	0.61 ± 0.08	0.62 ± 0.07
Fasting blood glucose level (mg/dl)	90.56 ± 11.00	88.45 ± 10.76	89.37 ± 10.89
Insulin level (mU/L)	14.11 ± 9.53	10.46 ± 6.50	12.04 ± 8.14
Insulin resistance	3.23 ± 2.43	2.32 ± 1.52	2.72 ± 2.02

used as strong predictors for the development of T2DM.

Investigation of obesity and fat accumulation as a risk factor for chronic diseases relies on obesity parameters and measurable indicators such as body mass index (BMI), waist circumference (WC), waist to hip ratio (WHR) and waist to height ratio (WHtR). Considerable attention has been given to the BMI as a universal measurable indicator of overall obesity. On the other hand, WC was found to be directly associated with the increase of the risk of insulin resistance as well as cardiovascular diseases and mortality (Koike et al., 2009; Schneider et al., 2007; 2010). The remaining two parameters, WHR and WHtR, were less investigated as compared to BMI or WC. Nevertheless, all parameters appear to increase the incidence of insulin resistance, and they are considered independent risk factors for T2DM (Kawada et al., 2010). However, the parameter that has the most predictive power of insulin resistance as well as other obesity-related health problems is not known. Apparently, the most predictive parameter is still a matter under dispute. In addition to this, many authors found that the different parameters are equally predictive with no significant difference between them (Janghorbania and Amini, 2010; Qiao and Nyamdorj, 2010; Sargeant et al., 2001; Stevens et al., 2001).

Worldwide, most researchers focused on investigating the association between obesity parameters and the incidence of T2DM as well as cardiovascular diseases (Carey et al., 1997; Schneider et al., 2007, 2010; Stevens et al., 2001). Few attempted to specifically characterize the association of these parameters with the increased risk of developing insulin resistance. To our knowledge, none has reported on the association between obesity parameters and insulin resistance in the Arab world although the prevalence of T2DM and the metabolic syndrome is high and increasing in Jordan and other Arab countries (Ajlouni et al., 2008; Khader et al., 2007). Moreover, the environmental and dietary factors which are major risk factor for diabetes-obesity end point related disease are different between Western and Arab societies. Therefore, the current work was undertaken to investigate the association between obesity parameters and insulin resistance in Jordanians as a representative Arabic community. The correlation and the ability to predict insulin resistance of BMI, WC, WHR and WHtR as reliable and measurable anthropometric obesity parameters were explored. We hope that the findings of this work will shed light on the obesity-diabetes dogma as a major public health problem and establish a simple, yet robust obesity parameter that can be used to predict and monitor obesity-related diseases in Arabic communities.

MATERIALS AND METHODS

Study subjects

This study was conducted in the Faculty of Science, Yarmouk University, Irbid, Jordan, during the period of March to September 2010. A total of 210 overweight and obese individuals were recruited for this study in order to test the relationship between insulin resistance and various obesity indicators. Participants were considered to be overweight if they have a BMI ≥ 25 and obese if their BMI was ≥ 30, according to the WHO definition of obesity and overweight. In this study group, 43% were males and 57% were females aged from 18 to 50 years and 52% of them were married. The base line characteristics of the study participants are shown in Table 1. The study was approved by the ethical and research committee of Yarmouk University and informed written consents were obtained from all participants. Medical history was taken from all individuals recruited in this study to rule out any possibility of chronic diseases. Patients who were previously diagnosed of diabetes or individuals whose fasting blood sugar was above 120 mg/dl were excluded, and they were not part of the study.

Measurements

For anthropometric measurements, participants stood and dressed in light clothing without shoes. Body weight were measured with a calibrated balance beam scale to the nearest 0.5 kg, and height with a vertical ruler to the nearest 0.5 cm. Waist and hip circumference was measured in accordance with WHO standards with a tape to the nearest 0.5 cm. WC was measured midway between lower rib margin and the iliac crest in the horizontal plane.

Table 2. The Pearson and point-biserial correlation coefficients between various anthropometric measurements and insulin resistance.

Measurement	Men		Women		All participants	
	Pearson R^2	Point-biserial R^2	Pearson R^2	Point-biserial R^2	Pearson R^2	Point-biserial R^2
BMI	0.320**	0.238*	0.228*	0.349**	0.318**	0.325**
WC	0.359**	0.181	0.173	0.329*	0.347**	0.303**
WHR	0.133	-0.155	-0.51	0.100	0.075	-0.059
WHtR	0.307**	0.185	0.221*	0.370**	0.286**	0.301**

**Correlation is significant at the 0.01 level (2-tailed); *Correlation is significant at the 0.05 level (2-tailed).

Hip circumference was measured at the point yielding the maximum circumference over the buttocks.

All participants fasted for 10 to 12 h before blood sample were collected into vacuum tubes containing no preservative. Serum was separated by centrifugation at 4°C within 1 h. Fasting blood glucose was directly measured by the hexokinase method, and the rest of the serum was stored in freezer at -20°C for insulin level determination as well as any possible extra laboratory analysis. Fasting insulin level was measured by Enzyme Linked Immuno Sorbant Assay (ELISA) according the kit instructions provided by the supplier using standard laboratory procedures. The insulin resistance was quantified using the Homeostatic Model Assessment (HOMA) as glucose (mg/dl) × insulin (mU/L)/405 (Matthews et al., 1985). A cutoff value of 1.4 to indicate if the participant is insulin resistant or not, was used based on the common practice of endocrinologists in Jordan (Dr. Nadima Shuqom, internal medicine and endocrinologist, personal communication).

Statistical analysis

The relationship between the various obesity parameters with the HOMA insulin-resistance was systematically studied using standard statistical tests. The analysis was performed with SPSS 17 (Statistical Package for social sciences). The correlation between obesity parameters and insulin resistance was evaluated by calculating the Pearson and point-biserial correlation coefficients. The insulin-resistance predicting power of these obesity parameters was evaluated by logistic regression and three models for male participants, female participants, as well as all participants were obtained. Finally, a receiver-operating characteristic (ROC) curve analysis was used to examine the discriminatory power of the various obesity parameters. The sensitivity (true positive) and specificity (true negative) for all possible cutoff points for each parameter were simultaneously measured by performing ROC curve analysis. The ROC curves were constructed by plotting sensitivity against 1–specificity for each obesity parameters. The areas under the curve (AUCs) for each ROC curve were calculated to assess the overall performance of each anthropometric test for detecting insulin resistance.

RESULTS

The current work involved 210 overweight and obese individuals whose base line characteristics are summarized in Table 1. In this sample group, the relationship between four obesity parameters, namely BMI, WC, WHR and WHtR, with insulin resistance was evaluated. Table 2 shows the correlation between the obesity anthropometric parameters and the dependent variable under the study, the insulin resistance. The results revealed a positive correlation between BMI, WC and WHtR and the dependent variable under evaluation when the analysis was conducted for all the participants regardless of the gender. When Pearson correlation coefficient was calculated, WC was found to be more correlated with insulin resistance than BMI and WHtR. The fourth parameter on the other hand, WHR, appears to be poorly correlated with insulin resistance for that same group. However, the dependent variable in this work is dichotomous, i.e., it is categorical with only two categories as the participant is either insulin resistant or not. HOMA insulin resistance was categorized such as those values less than 1.4 indicate no insulin resistance and ≥ 1.4 indicate insulin resistance. Therefore, the relationship between the obesity parameters and insulin resistance is better investigated using the point-biserial correlation coefficient. When this correlation coefficient was calculated, BMI was the parameter that was most correlated with insulin resistance in the all participants group.

To assess the effect of the gender, the same evaluation was carried out for male and female participants separately. Strikingly, different results were obtained than those discussed before when the correlation was investigated for all the participants. In the male population, only BMI appears to be significantly correlated with insulin resistance as indicated by the point-biserial correlation coefficients calculation. Surprisingly, the other obesity parameters were poorly correlated in spite of the significant correlation shown by the Pearson correlation coefficients for these parameters when insulin resistance is treated as a continuous variable than a discrete dichotomy. Analysis of the female population on the other hand shows BMI and WHtR to be the parameters that are most correlated with insulin resistance. However, the WHtR parameter correlated better with insulin resistance than BMI as indicated by the point-biserial correlation coefficients of these two parameters shown in Table 2.

Logistic regression was also applied to find the factors (age and gender) and obesity parameters that significantly predict the incidence of insulin resistance among the various populations in the study. To start with, logistic regression for all participants was performed in

Table 3. Logistic regression analysis of insulin resistance as a function of the various obesity parameters..

Participant	Predictor	B	SE	Significance	e^B	95% CI for e^B
Men	BMI	0.179	0.064	0.005	1.196	1.056 - 1.355
	Constant	- 3.962	1.955	0.043	0.019	NA
Women	WHtR	0.154	0.041	0.000	1.167	1.078 - 1.263
	Constant	- 8.635	2.405	0.000	0.000	NA
All participant	BMI	0.138	0.062	0.027	1.148	1.016 - 1.296
	WHtR	0.209	0.089	0.019	1.232	1.035 - 1.467
	Gender	1.604	0.531	0.003	4.972	1.757 - 14.064
	Constant	- 7.081	1.920	0.000	0.001	NA

Nagelkerke R^2, Hosmer and Lemeshow χ^2 were 0.195 and 8.007, 0.203 and 5.475, 0.276 and 12.828, for male, female and all participants' models, respectively.

the backward stepwise method for insulin resistance as a function of age, gender, BMI, WC and WHtR. A significant model was obtained in which BMI, WHtR and gender were significant variables in the model (Table 3). The odd ratios (e^B) suggest that gender, as a categorical variable, has a profound effect on the model. To assess that effect, logistic regression models for individual male and female populations were constructed, and again significant models could be obtained. For the male population, BMI remained as the most significant obesity parameter for developing insulin resistance; while on the other hand, WHtR appears to be the most significant predictor in the female population.

Similar to logistic regression, the ROC curve analysis is an excellent diagnostic tool that is commonly used to establish the usefulness of particular obesity parameters for distinguishing populations with particular diseases or metabolic syndrome. The ability of the parameters to predict the response in question is classified according to the magnitude of the area under the ROC curve. The area under the ROC curve should usually range from 0.5 to 1.0 with larger values being indicative of better fit. ROC curves illustrating the performance of each obesity parameter as explained in the method section are presented in Figure 1. The calculated areas under the ROC curves (AUCs) and their 95% confidence intervals are summarized in Table 4.

In agreement with the analysis of the point-biserial correlation coefficient as well as the logistic regression for the male population, the ROC curves of BMI had the largest AUC and thus, it appears to be the most predictive obesity parameters for the development of insulin resistance in men. In the female population on the other hand, equal AUCs for BMI and WHtR were obtained indicating comparable predictive capabilities of these two parameters for the development of insulin resistance. It is worth mentioning that, in theory, no realistic classifier should have an AUC less than 0.5. Otherwise, the performance of this classifier would be worse than random guessing represented by the diagonal line between points (0,0) and (1,1) in Figure 1. The performance of the obesity parameter WHR was an example of such behavior. Clearly, WHR offers no information about the possibility of developing insulin resistance. On the contrary, this parameter may be said to predict insulin resistance incorrectly and in a reverse manner where the larger the WHR and the more obese the person is the less likely he or she might develop insulin resistance. Lastly, the ROC curve analysis for the all participant group revealed a similar pattern to that obtained by logistic regression modeling. Specifically, both parameters, BMI and WHtR are excellent classifiers with a slight superior predicting ability for BMI (AUC = 0.73) over WHtR (AUC = 0.72).

DISCUSSION

Insulin resistance gained more attention recently as researchers tried to understand the pathogenesis mechanisms of T2DM and metabolic syndrome from the insulin-resistance point view. Insulin resistance together with beta cell dysfunction leads to the appearance and gradual progression of type 2 diabetes. Accordingly, insulin resistance can be targeted to reduce the risk of diabetes and many other chronic diseases. However, HOMA insulin resistance as calculated parameter depends on two laboratory tests, fasting blood glucose and serum insulin level, which are costly and time consuming. In contrast, obesity parameters are simple and associated with fewer measurement errors and could be used as precious markers and exemplary indicators for the occurrence of insulin resistance.

Therefore, clinicians are encouraged to target obesity as a manageable health problem to prevent or delay the onset of diabetes through lifestyle intervention approaches such as weight reduction and increasing physical activity (National Institutes of Health, 2000; Qiao and

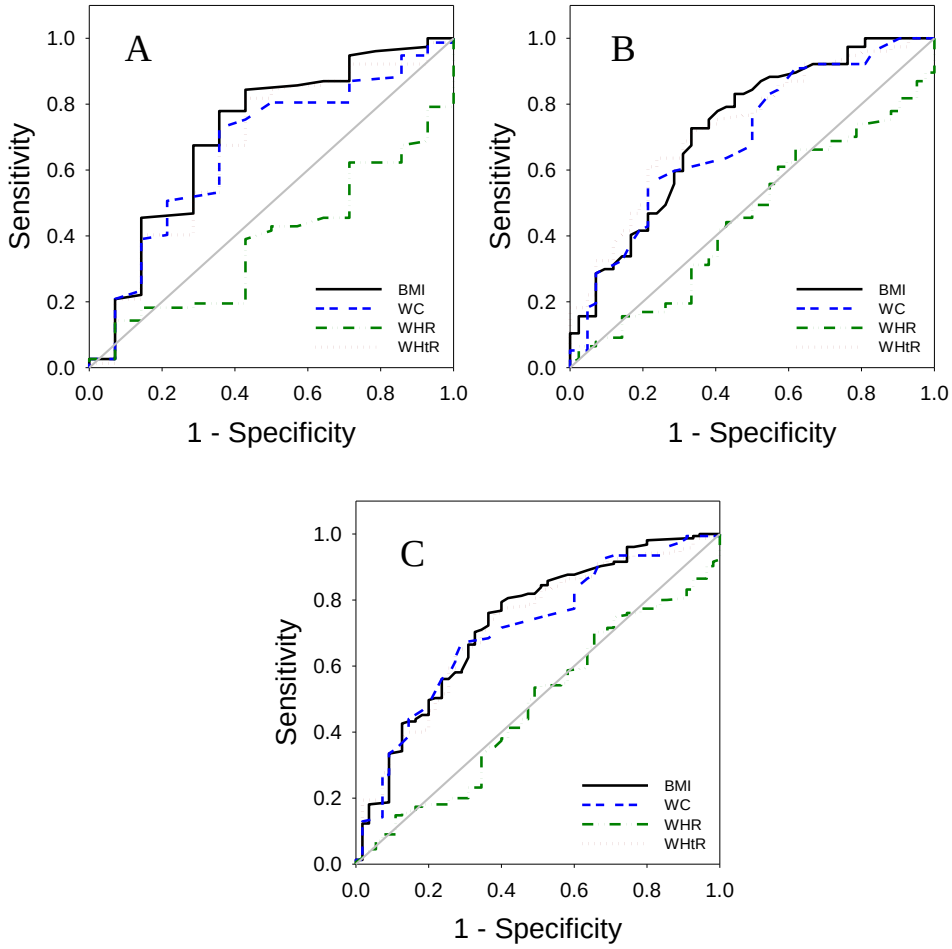

Figure 1. Receiver operating characteristic (ROC) curves to predict insulin resistance from various anthropometric measurements in (A) men, (B) women and (C) all participants.

Table 4. Areas under the receiver operating characteristic curves to predict insulin resistance from various obesity parameters.

Measurement	Men		Women		All participants	
	AUC (95% CI)	Significance	AUC (95% CI)	Significance	AUC (95% CI)	Significance
BMI	0.71 (0.55 – 0.87)	0.013	0.73 (0.63 – 0.83)	0.000	0.73 (0.65 – 0.81)	0.000
WC	0.67 (0.51 – 0.82)	0.051	0.70 (0.60 - 0.80)	0.000	0.71 (0.63 – 0.79)	0.000
WHR	0.38 (0.24 – 0.52)	0.167	0.46 (0.35 – 0.57)	0.446	0.48 (0.39 – 0.56)	0.599
WHtR	0.67 (0.51 -0. 84)	0.044	0.73 (0.64 – 0.83)	0.000	0.72 (0.64 – 0.80)	0.000

and Nyamdorj, 2010; Zimmeta et al., 2011). As mentioned previously, continuous findings for the indicative strength of various obesity parameters left clinicians nearly confused on which obesity parameter should be considered. In the Arabic and Middle Eastern societies, the situation is even vaguer as the association and the predictability of obesity parameters to the risk of insulin resistance has never been investigated.

This work presents a cross-sectional study that investigated the association between obesity parameters, namely BMI, WC, WHR and WHtR, with insulin resistance in eastern Arab society. Most of the previous studies on obesity and insulin resistance were taken in the western societies and Japan. However, dietary patterns and individual's lifestyle for eastern Arab society are different from those of the aforementioned societies. These factors directly affect the weight status and fat distribution demonstrated by the various obesity

parameters. Therefore, the aim of this study was to delineate the relationship between obesity parameters with insulin resistance in Jordanian society. To this end, 210 overweight and obese individuals were recruited, and their anthropometric measurements were taken. The participant's glucose and insulin levels were measured, and the subsequent insulin resistance was calculated. The obesity parameters were statistically investigated and modeled to identify which parameter is better related to insulin resistance and thus, should be used as a predictor for the development of T2DM.

The current data suggests that BMI and WHtR are more significantly associated and correlated with the development of insulin resistance in Jordanians than WC or WHR. Estimation of correlation coefficients, logistic regression and ROC curve analysis were applied to assess the relationship between these obesity parameters and the occurrence of insulin resistance. BMI, WC and WHtR were positively correlated with insulin resistance as indicated by Pearson as well as point-biserial correlation coefficients calculated for the whole population under study. Nevertheless, when the latter correlation coefficient was calculated for the individual male and female populations, the strength of these markers appeared to be gender-dependent. While BMI was the only significantly correlated parameter with insulin resistance in males, WHtR and to a less degree BMI were the most correlated parameters with insulin resistance in females. These findings were further investigated by modeling insulin resistance as a function of age, gender, BMI, WC and WHtR using logistic regression. In agreement with correlation calculation, gender was found to have significant effect on the incidence of insulin resistance when this dependent variable was modeled in all participants. Moreover, BMI and WHtR were found to be the most significant parameters for predicting insulin resistance in the male and female populations, respectively. The goodness of fit as well as the outcome of the three logistic regression models obtained were evaluated and validated by performing ROC curve analysis. The calculated AUCs agree with the findings discussed above regarding BMI being the best obesity parameters to predict the occurrence of insulin resistance in men. In women however, both WHtR and BMI resulted in similar AUCs and thus, they are predicted to have equal classifier performance by this statistical tool.

The gender-specific behavior obtained is expected due to the vast differences in body composition between men and women. However, the combined population was always subjected to analysis in this work. This was in an attempt to explore the possibility of establishing a universal obesity parameter that has the strongest correlation and the prediction ability of insulin resistance in both genders. Apparently, this quest was not satisfactorily successful as different parameters were consistently associated with each gender.

It is also worth mentioning that our conclusions are restricted to the inability to include certain confounding factors that could affect the dependent variable under study. Such factors include individual variations in the lifestyle pattern and the nutritional habits of our participants. Limitations of resources and many social barriers are the main reasons that restricted our conclusions to include and study these factors. In conclusion, the current findings suggest that BMI and WHtR are better indicative markers for insulin resistance than other obesity parameters such as WC or WHR. Therefore, BMI in men and WHtR in women are promoted to be used as obesity parameters for many risk conditions related to insulin resistance. Moreover, clinicians in eastern Arab societies are encouraged to use them to monitor obese and diabetic patients' response to body weight reduction treatments.

ACKNOWLEDGEMENTS

The authors gratefully acknowledge Mrs. Argelia El Abed for her cooperation and help, and Ms. Ruba Sinjilawi for her technical assistance.

REFERENCES

Ajlouni K, Khader YS, Batieha A, Ajlouni H, El-Khateeb M (2008). An increase in prevalence of diabetes mellitus in Jordan over 10 years. J. Diab. Complic., 22: 317-324.

Carey VJ, Walters EE, Colditz GA, Solomon CG, Willet WC, Rosner BA, Speizer FE, Manson JE (1997). Body fat distribution and risk of non-insulin-dependent diabetes mellitus in women. The Nurses' Health Study. Am. J. Epidemiol., 145: 614-619.

Chan JM, Rimm EB, Colditz GA, Stampfer MJ, Willett WC (1994). Fat distribution and weight gain as risk factors for clinical diabetes in men. Diab. Care, 17: 961-969.

Janghorbania M, Amini M (2010). Comparison of body mass index with abdominal obesity indicators and waist-to-stature ratio for prediction of type 2 diabetes: The Isfahan diabetes prevention study. Obes. Res. Clin. Pract., 4: e25-e32.

Kahn SE, Hull RL, Utzschneider KM (2006). Mechanisms linking obesity to insulin resistance and type 2 diabetes. Nature, 444: 840-846

Kawada T, Otsuka T, Inagaki H, Wakayama Y, Li Q, Li YJ, Katsumata M (2010). Insulin resistance, as expressed by HOMA-R, is strongly determined by waist circumference or body mass index among Japanese working men. Obes. Res. Clin. Pract., 4: e9-e14.

Khader YS, Batieha A, El-Khateeb M, Als-shaikh A, Ajlouni K (2007). High prevalence of the metabolic syndrome among Northern Jordanians. J. Diab. Complic., 21: 214-219.

Khan BB, Flier JS (2000). Obesity and insulin resistance. J. Clin. Invest., 106: 473-481

Koike T, Miyamoto M, Oshida Y (2009). Waist circumference is positively associated with insulin resistance but not with fasting blood glucose among moderately to highly obese young Japanese men. Obes. Res. Clin. Pract., 3: 109-114.

Matthews DR, Hosker JP, Rudenski AS, Naylor BA, Treacher DF, Turner RC (1985). Homeostasis model assessment: insulin resistance and beta-cell function from fasting plasma glucose and insulin concentrations in man. Diabetologia, 28: 412–419.

Muoio DM, Newgard CB (2008). Mechanisms of disease: molecular and metabolic mechanisms of insulin resistance and beta-cell failure in type 2 diabetes. Nat. Rev. Mol. Cell. Biol., 9: 193-205.

National Institutes of Health (2000). The Practical Guide: Identification, Evaluation, and Treatment of Overweight and Obesity in Adults waist circumference or waist-to-hip ratio stronger than that with body

mass index? Eur. J. Clin. Nutr., 64: 30–34.
Reaven GM (1988). Role of insulin resistance in human disease. J. Diab., 37: 1595-1607.
Sargeant LA, Bennett FI, Forrester TE, Cooper RS, Wilks RJ (2002). Predicting incident diabetes in Jamaica: the role of anthropometry. Obes. Res., 10: 792–798.
Schneider HJ, Friedrich N, Klotsche J, Pieper L, Nauck M, John U, Dörr M, Felix S, Lehnert H, Pittrow D, Silber S, Völzke H, Stalla GK, Wallaschofski H, Wittchen H (2010). The predictive value of different measures of obesity for incident cardiovascular events and mortality. Clin. Endocrinol. Metab., 95: 1777-1785.
Schneider HJ, Glaesmer H, Klotsche J Böhler S, Lehnert H, Zeiher AM, März W, Pittrow D, Stalla GK, Wittchen H (2007). For the DETECT Study group accuracy of anthropometric indicators of obesity to predict cardiovascular risk. Clin. Endocrinol. Metab., 92: 589-594.
Stevens J, Couper D, Pankow J, Folsom AR, Duncan BB, Neito FJ, Jones D, Tyroler HA (2001). Sensitivity and specificity of anthropometrics for the prediction of diabetes in a biracial cohort. Obes. Res., 9: 696–705.
Taylor SI (1999). Deconstructing type 2 diabetes. Cell, 97: 9-12.
Wellen KE. Hotamisligil GS (2005). Inflammation, stress and diabetes J. Clin. Investig., 115: 1111-1119.
Zimmeta P, Campbelld L, Toomathg R, Twiggh S, Wittertj G, Proiettol J (2011). Bariatric surgery to treat severely obese patients with type 2 diabetes: A consensus statement. Obes. Res. Clin. Pract., 5: 71-78.

Scientific Research and Essays Vol. 7(25), pp. 2225-2229, 5 July, 2012
Available online at http://www.academicjournals.org/SRE
DOI: 10.5897/SRE11.1150
ISSN 1992-2248 ©2012 Academic Journals

Full Length Research Paper

Effects of cold stratification and sulphuric acid pre-treatments on germination of pomegranate (*Punica granatum* L.) seeds in greenhouse and laboratory conditions

Askin Gokturk*, Zafer Olmez, Banu Karasah and Hilal Surat

Faculty of Forestry, Artvin Coruh University, 08000 Artvin, Turkey.

Accepted 8 June, 2012

This study was carried out to determine the effects of some pretreatments including soaking in concentrate (98%) H_2SO_4 for 10, 20, 30, 40 and 50 min and cold stratification (at 4±1°C) for 15, 30, 45 and 60 days followed by soaking in H_2SO_4 for 10, 20, 30, 40 and 50 min on seed germination and to investigate how to overcome dormancy of *Punica granatum* L. seeds. The seeds were sown in polyethylene pots in the greenhouse and sown at 22±1°C under darkness in laboratory conditions. The statistical approach was a randomized complete block design with three replications. Germinated seeds were observed periodically during 50 days to determine germination percentages and germination rates. Soaking in H_2SO_4 for 30 min with cold stratification for 45 days gave the highest germination percentage (60.7%) in the laboratory while, the highest germination percentage (85.5%) was obtained from soaking in H_2SO_4 for 40 min with 30 day cold stratification pre-treatment although there were not any significant differences for germination percentages between pre-treatments in the greenhouse. In addition, the best germination rate (21 days) was obtained from the seeds which were soaked in H_2SO_4 for 30 min with 45 day cold stratification and soaked in H_2SO_4 for 40 min with cold stratification for 45 days pre-treatments in the greenhouse.

Key words: Dormancy, germination, pre-treatment, *Punica granatum*, seed.

INTRODUCTION

Vegetation cover is one of the most important factors in preventing and controlling soil erosion. It gives long-term soil surface protection by providing leaf cover that reduces rain-drop effects. In addition, it helps better soil structure development through establishing a root system, thereby increasing infiltration and soil stability (Pritchett and Fisher, 1987; Balci, 1996).

Punica granatum is believed to have originated from Southern Caspian belt and Northeast Turkey, and the Mediterranean basin is an important diversification center of the plant (Halilova and Yildiz, 2009). Pomegranate is one of the oldest subtropical species cultivated in Turkey and surrounding areas. The country has very rich pomegranate genetic resources mostly found in semi-arid and arid areas (Halilova and Yildiz, 2009). *P. granatum* is a drought tolerant tree suitable for arid and semi-arid zone afforestation. This species is important in soil erosion control and is planted along rivers to stabilize banks. Pomegranate leaf litter decomposes slowly and is suitable for mulching. It is also used as an ornamental plants in many countries (Orwa et al., 2009).

Seeds of many woody plant species cannot germinate even if they are sown under optimal moisture, oxygen and soil conditions (Dirr and Heuser, 1987; Landis et al., 1996; Urgenç, 1998; Yahyaoglu and Olmez, 2005). This

*Corresponding author. E-mail: askingokturk@hotmail.com. Tel: +90 466 215 1106. Fax: +90 466 215 1034.

problem is called dormancy and their causes are a hard and impermeable seed coat, immature or dormant embryo, absence of endosperm, or thick, fleshy seed cover (ISTA, 1966, 1993). There is a great deal of variation in germination ability of seeds even within the same species. Poulsen (1996) reported that dormancy among and within seed lots of the same species varies with provenance, crop year, and individual trees.

There are various germination obstacles in *Punica* seeds (Ellis et al., 1985; Olmez et al., 2007a, b; Yucedag and Gultekin, 2009; Rawat et al., 2010) resulting in propagation difficulties.

Generally pre-treatments such as submersion in hot water, mechanical or chemical scarification, and hot aeration are used for seed coat dormancy while the cold and warm stratifications are usually applied to dormancy caused by restrictions at the embryo level (Landis et al., 1996). Among these methods and techniques, especially cold stratification and submersion in concentrated H_2SO_4 are used to increase germination percentage of *P. granatum* seeds (Riley, 1981; Piotto et al., 2003; Olmez et al., 2007a, b; Yucedag and Gultekin, 2009; Rawat et al., 2010).

Olmez et al. (2007a) obtained both the highest germination percentage (84.4%) and the best germination rates (30 and 36 days) in seeds pre-treated with soaking in H_2SO_4 for 15 min followed by cold stratification for 60 days. Olmez et al. (2007b) achieved 11.2% germination in seeds that were cold stratified for 60 days in greenhouse conditions. Yucedag and Gultekin (2009), obtained best germination percentage (71.8%) in seeds that were cold stratified for 45 days. Ravat (2010) stated that stratification for 30 days at 5°C showed highest germination percentage (91.7%). Pioto et al. (2003) recommended 28 to 56 days cold stratification *for P. granatum* seeds.

The aim of this study was to examine the influence of cold stratification and submersion in sulphuric acid pre-treatments on breaking dormancy of *P. granatum* seeds sown both in the laboratory and in the greenhouse conditions.

MATERIALS AND METHODS

Ripe fruits were collected from *P. granatum* individuals in September 2007, in Artvin region located in the North-Eastern part of Turkey. The seeds were separated from the fruit material, rinsed with tap water, dried in the shade, and stored at 5±1°C in plastic bags.

The following pre-treatments were applied to determine their effects on germination percentage (GP) and germination rate (GR) of *P. granatum* seeds:

i) Submersion in concentrated (98%) sulphuric acid for 10, 20, 30, 40 and 50 min.
ii) Cold stratification (CS) for 15, 30, 45 and 60 days.
iii) Submersion in concentrated (98%) sulphuric acid for 10, 20, 30, 40 and 50 min + CS for 15, 30, 45 and 60 days.
iv) Control.

The seeds were stratified at 4±1°C by putting layers of moistened sand and seeds on top of each other in the closed boxes. Since there was a risk of some of the seeds being mixed with the sand because of their small size, linen cloth was placed between the sand and the seeds. The moisture of the sand and the seeds were checked regularly so that the seeds would not get mouldy.

The seeds were sown in polyethylene pots in the greenhouse and into the petri dishes on filter paper at 22±1°C under darkness in laboratory, in April 2008. The polyethylene pots were filled with growing medium composed of forest soil, creek sand, and cattle manure (3:1:1). The experimental design was a randomized complete block with three replications (30 seeds in each replication) for each treatment.

Numbers of germinated seeds [evaluation done according to ISTA Rules (1993)] were recorded for 7th, 10th, 14th, 21st, 28th, 35th and 42nd days after the sowing.

The GP and GR values were determined for each pre-treatment. The formula used in determining GR (Pieper, 1952) and GP values is as follows

$$GR = \frac{(n1 \times t1) + (n2 \times t2) + (n3 \times t3) + ... + (ni \times ti)}{T}$$

Where; *GR:* Germination rate, *n:* Number of days for each counting of germinated seeds, *t:* Number of germinated seeds at each counting day, *T*: Total number of germinated seeds.

$$GP = \frac{T}{TS} \times 100$$

Where; GP*:* Germination percentage, *T*: Total number of germinated seeds, *TS:* Total seeds.

The whole experiment lasted for about 50 days when it was observed that the seeds stopped germinating. Data from the pre-treatments were analyzed using the SPSS statistical software after arc-sinus transformation was applied to GP values to meet ANOVA assumptions. The ANOVA and Duncan tests were used to compare treatment groups to find out whether they showed any statistically significant differences with significance level (α) set at 0.05.

RESULTS AND DISCUSSION

Statistical analyses showed that the pre-treatments used in this study affected seed GP and GR in the laboratory and seed GR only in the greenhouse conditions significantly. While the GPs of the seeds varied between 0.7 and 60.7% in the laboratory, the GPs in the greenhouse ranged from 61.0 to 85.5%. The highest GP in the greenhouse (85.5%) was obtained from the seeds which were soaked in H_2SO_4 for 40 min with CS for 30 days although there were not any significant differences for GP between pre-treatments. On the other hand, the highest GP (60.7%) was obtained from submersion in H_2SO_4 for 30 min with CS for 45 days pre-treatment in the laboratory (Tables 1 and 2). No germination was acquired in seeds soaked in H_2SO_4 for 50 min followed by CS for60 days in laboratory condition. When concentrated H_2SO_4 was used with cold stratification method, GPs resulted in an increase both in the greenhouse and laboratory comparing to using H_2SO_4 alone (Tables 1 and 2). Previous studies that used CS application reported

Table 1. Results of statistical analyses showing the relationship of the germination percentage and rate with different pre-treatments for laboratory conditions (Means in column with the same letter are not significantly different at α=0.05).

Pre-treatment	F-ratio	GP (%)	F-ratio	GR (days)
50 min H_2SO_4 + 60-day cold stratification		0.0^{a}		0^{a}
50 min H_2SO_4		0.7^{a}		12^{ab}
40 min H_2SO_4 + 60-day cold stratification		2.0^{a}		9^{ab}
30 min H_2SO_4 + 60-day cold stratification		3.3^{a}		26^{cde}
20 min H_2SO_4 + 60-day cold stratification		3.3^{a}		19^{bcde}
40 min H_2SO_4		4.0^{a}		31^{de}
Control		4.7^{ab}		28^{de}
30 min H_2SO_4		4.7^{ab}		29^{de}
20 min H_2SO_4		4.7^{ab}		32^{de}
10 min H_2SO_4 + 60-day cold stratification		6.0^{ab}		9^{ab}
10 min H_2SO_4		7.3^{ab}		28^{de}
30 min H_2SO_4 + 15-day cold stratification		28.7^{bc}		27^{de}
10 min H_2SO_4 + 15-day cold stratification	9.99*	36.0^{cd}	3.21*	25^{cde}
20 min H_2SO_4 + 15-day cold stratification		36.7^{cd}		26^{cde}
50 min H_2SO_4 + 45-day cold stratification		38.0^{cd}		24^{cde}
40 min H_2SO_4 + 15-day cold stratification		44.7^{cd}		26^{cde}
40 min H_2SO_4 + 30-day cold stratification		46.7^{cd}		18^{bcde}
20 min H_2SO_4 + 30-day cold stratification		46.7^{cd}		25^{cde}
50 min H_2SO_4 + 30-day cold stratification		48.0^{cd}		18^{bcd}
20 min H_2SO_4 + 45-day cold stratification		50.7^{cd}		22^{bcde}
10 min H_2SO_4 + 30-day cold stratification		54.7^{d}		24^{cde}
50 min H_2SO_4 + 15-day cold stratification		56.0^{d}		22^{bcde}
30 min H_2SO_4 + 30-day cold stratification		57.3^{d}		24^{bcde}
40 min H_2SO_4 + 45-day cold stratification		58.7^{d}		22^{bcde}
10 min H_2SO_4 + 45-day cold stratification		60.0^{d}		21^{bcde}
30 min H_2SO_4 + 45-day cold stratification		60.7^{e}		20^{bcde}

* VS: Pre-treatments, significantly different at α= 0.05

successful outcomes to overcome dormancy of *P. granatum* seeds (Riley, 1981; Piotto et al., 2003; Yucedag and Gultekin, 2009; Rawat et al., 2010). Riley (1981) reported that CS pre-treatment at 1 to 5°C for 30 to 60 days gave good GPs that varied between 91 and 96% for *P. granatum* seeds. Rawat et al. (2010) implied that the highest GP (91.7%) was determined from the seeds stratified for 30 days at 5°C and sown in the laboratory. In addition, Yucedag and Gultekin (2009) obtained the highest GP (71.8%) from CS treatment for 45 days and sown in open field conditions. On the contrary, Olmez et al. (2007b) stated that the highest GP in the greenhouse was 11.2% for the seeds cold stratified for 60 days. In addition, scarification with H_2SO_4 for 15 min followed by CS for 60 days were suggested by Olmez et al. (2007a) for *P. granatum* seeds, and the highest GPs determined from their study were 32.0 and 84.8% for the open field and the greenhouse conditions, respectively.

Dormancy among and within seed lots of the same species varies with provenance, crop year, and individual trees like Poulsen (1996)'s explanation. In addition, provenance differences in seed germination have been explained by the conditions of the site of origin for several species (Olmez et al., 2007c, 2009; Wang et al., 2010).

In general, the present results for *P. granatum* seeds showed that soaking in H_2SO_4 followed by CS resulted in early, uniform and high GP in the greenhouse. Therefore, the results indicated that greenhouse conditions can be preferably used to improve germination of the seeds.

The best germination rate (21.3 and 20.7 days) was determined in seeds soaked in H_2SO_4 for 30 or 40 min followed by 45-day CS pre-treatments and sown in the greenhouse. In addition, the GR was 22.3 days for the highest GP (85.5%) that were obtained from submersion in H_2SO_4 for 40 min with CS for 30 days pre-treatment in the greenhouse condition (Table 2). The GR was 19.7 days for the highest GP in the laboratory conditions (Table 1). The difference of GP and GR in the greenhouse and laboratory conditions could have resulted from germination conditions. Geisel (2004) stated that the medium in which the seeds are sown should be loose

Table 2. Results of statistical analyses showing the relationship of the germination percentage and rate with different pre-treatments for the greenhouse conditions (means in column with the same letter are not significantly different at α=0.05).

Pre-treatment	F-ratio	GP (%)	F-ratio	GR (days)
Control		61.0		28^{h}
20 min H_2SO_4 + 30-day cold stratification		68.0		23^{abcd}
10 min H_2SO_4		68.7		28^{gh}
10 min H_2SO_4 + 45-day cold stratification		68.7		24^{bcdef}
30 min H_2SO_4 + 30-day cold stratification		71.7		22^{ab}
20 min H_2SO_4 + 15-day cold stratification		72.7		26^{efg}
30 min H_2SO_4 + 45-day cold stratification		72.8		21^{a}
30 min H_2SO_4		74.8		26^{fgh}
20 min H_2SO_4		76.1		28^{gh}
10 min H_2SO_4 + 15-day cold stratification		76.7		25^{defg}
50 min H_2SO_4 + 30-day cold stratification	0.43^{NS}	77.0	7.11*	23^{abcde}
40 min H_2SO_4		77.8		26^{efg}
10 min H_2SO_4 + 45-day cold stratification		78.6		25^{cdef}
50 min H_2SO_4		78.8		25^{defg}
50 min H_2SO_4 + 15-day cold stratification		79.5		23^{abcd}
40 min H_2SO_4 + 45-day cold stratification		79.8		21^{a}
20 min H_2SO_4 + 45-day cold stratification		81.0		23^{abcd}
50 min H_2SO_4 + 45-day cold stratification		81.4		23^{abcd}
30 min H_2SO_4 + 15-day cold stratification		81.5		25^{cdefg}
40 min H_2SO_4 + 15-day cold stratification		82.7		25^{cdefg}
40 min H_2SO_4 + 30-day cold stratification		85.5		22^{abc}

* VS: Pre-treatments, significantly different at α= 0.05, NS: not significant.

and well during germination is limited or reduced, germination can be severely retarded or inhibited. Greenhouse conditions were well aerated than laboratory conditions, so the differences could be derived from aeration.

Conclusions

Consequently, among all the pre-treatments applied to the *P. granatum* seeds, submersion in H_2SO_4 for 30 min with 45 day-CS in the laboratory and submersion in H_2SO_4 for 40 min with 30 day-CS resulted in the highest GPs, 60.7 and 85.5%, respectively. The results indicated that CS with submersion in H_2SO_4 pre-treatments gave higher GP values both in the greenhouse and in the laboratory than H_2SO_4 pre-treatment alone to improve germination dormancy of *P. granatum* seeds.

ACKNOWLEDGEMENTS

The authors would like to thank the Kafkas University for its financial support of this research (2007-OF-019).

REFERENCES

Balci AN (1996). Toprak koruma. Istanbul Universitesi, Istanbul, Turkey. Yayın. p 439.

Dirr MA, Heuser CW (1987). The reference manual of woody plant propagation: From seed to tissue culture. Varsity Press, Athens, GA.

Ellis RH, Hong TD, Roberts EH (1985). *Punicaceae*, handbook of seed technology for genebanks. Compendium of specific germination information and test recommendations. Handbooks for genebanks, International board for plant genetic resources (IBPGR), Rome. 2: 3.

Geisel PM (2004). Plant propagation, California Master Gardner Handbook [Dennis R. Pittenger (Ed.)]. University of California, ISBN: 1-879906-54-6. Agric. Nat. Resourc. p 3382.

Halilova H, Yildiz N (2009). Does climate change have an effect on proline accumulation in pomegranate (*Punica granatum* L.) fruits? Sci. Res. Essay, 4(12): 1543-1546.

ISTA (1993). Rules for testing seeds. Seed Sci. Technol., 21: 1-259.

ISTA (International Seed Testing Association) (1966). Internationale Vorschriften fur die Prufung von Saatgut, Wageningen, Netherland. p 31/4.

Landis TD, Barthell A, Loucks D, Webb S (1996). Seed treatments to overcome dormancy. Forest nursery notes, United States Department of Agriculture, Forest Service. July: 9-12.

Olmez Z, Gokturk A, Karasah B, Yilmaz H (2009). Effects of cold stratification, and sulphuric acid pretreatments on germination of three provenances of smoke-tree (*Cotinus coggygria* Scop.) seeds in greenhouse and laboratory conditions. Afr. J. Biotechnol., 8(19): 4964-4968.

Olmez Z, Gokturk A, Temel F (2007c). Effects of cold stratification, sulphuric acid, submersion in hot water and tap water pretreatments on germination of bladder-senna (*Colutea armena* Boiss. and Huet.) seeds. Seed Sci. Technol., 35: 266-271.

Olmez Z, Temel F, Gokturk A, Yahyaoglu Z (2007a). Effects of sulphuric acid and cold stratification pretreatments on germination of pomegranate (*Punica granatum* L.) seeds. Asian J. Plant Sci., 6(2): 427-430.

Olmez Z, Temel F, Gokturk A, Yahyaoglu Z (2007b). Effects of cold stratification treatments on germination of drought tolerant shrubs seeds. J. Environ. Biol., 28(2): 447-453.

Orwa C, Mutua A, Kindt R, Jamnadass R, Simons A (2009). *Punica granatum* L. agroforestree database: A tree reference and selection guide version 4.0. http://www.worldagroforestry.org/treedb2/AFTPDFS/Punica_granatum.pdf.

Pieper A (1952). Das Saatgut. P. Parey Verlag; Berlin, Hamburg, Germany.

Piotto B, Bartolini G, Bussotti F, Asensio A, García C, Chessa I, Ciccarese C, Ciccarese L, Crosti R, Cullum FJ, Noi AD, García P, Lambardi M, Lisci M, Lucci S, Melini S, Carlos J, Reinoso M, Murranca S, Nieddu G, Pacini E, Pagni G, Patumi M, Garcia FP, Piccini C, Rossetto M, Tranne G, Tylkowski T (2003). Fact sheets on the propagation of Mediterranean trees and shrubs from seed. In: Piotto B, Noi AD (eds.), Seed propagation of Mediterranean trees and shrubs. APAT I.G.E.R srl. Rome, Italy.

Poulsen K (1996). Case study: Neem (*Azadirachta indica* A. Juss.) seed research. In: Ouedraogos AS., Poulsen K, Stubsgaard F (eds.) Proceedings of an international workshop on improved methods for handling and storage of intermediate/recalcitrant tropical forest tree seeds. June 8-10. Humlebaek, Denmark.

Pritchett WL, Fisher RF (1987). Properties and management of forest soils. 2nd Edition, John Wiley and Sons. New York, USA.

Rawat JMS, Tomar YK, Rawat V (2010). Effect of stratification on seed germination and seeedling performance of wild pomegranate. J. Am. Sci., 6(5):97-99.

Riley JM (1981). Growing rare fruit from seed. California Rare Fruit Growers Yearbook, 13:1-47.

Urgenç S (1998). Genel plantasyon ve agaclandırma teknigi. Istanbul Universitesi, Orman Fakultesi, Istanbul, Turkey. Yayın p. 444.

Wang JH, Baskin CC, Chen W, Du GZ (2010). Variation in seed germination between populations of five sub-alpine woody species from Eastern Qinghai-Tibet Plateau following dry storage at low temperatures. Ecol. Res.. 25: 195-203.

Yahyaoglu Z, Olmez Z (2005). Tohum teknolojisi ve fidanlık teknigi. Kafkas Universitesi, Artvin Orman Fakultesi, Artvin. Yayın p. 1.

Yucedag C, Gultekin HC (2009). The effect of stratification and sowing time on germination of pomegranate (*Punica granatum* L.) seeds. AKU. Fen Bilimleri Dergisi, 1: 87-90.

Scientific Research and Essays Vol. 7(25), pp. 2230-2236, 5 July, 2012
Available online at http://www.academicjournals.org/SRE
DOI: 10.5897/SRE11.477
ISSN 1992-2248 ©2012 Academic Journals

Full Length Research Paper

Assessment of atherosclerosis in erectile dysfunction subjects using second derivative of photoplethysmogram

Yousef Qawqzeh[1]*, M. B. I. Reaz[1], M. A. M. Ali[1], Kok Beng Gan[2], Zulkifli S.Z.[3] and Noraidatulakma A.[3]

[1]Department of Electrical, Electronic and Systems Engineering, Universiti Kebangsaan Malaysia, 43600 UKM, Bangi, Selangor, Malaysia.
[2]Institute of Space Science (ANGKASA), Universiti Kebangsaan Malaysia, 43600 Bangi, Selangor Darul Ehsan, Malaysia.
[3]UKM Medical Molecular Biology Institute, Universiti Kebangsaan Malaysia, Cheras, Kuala Lumpur, Malaysia.

Accepted 7 June, 2012

Cardiovascular diseases are the main cause of death worldwide. Stiffing of the arterial wall is normally related with the beginning, or the progression of atherosclerosis. Atherosclerosis plays an important role in loss of the elastic properties of arteries walls. Thereby, atherosclerosis might cause harmful damage to arteries which in turn might cause cardiovascular disease and erectile dysfunction. Carotid intima-media thickness (CIMT) is used to measure atherosclerosis in parallel with the recording of Photoplethysmogram (PPG) from samples of erectile dysfunction subjects (68 patients). The results revealed PPG and clinical indices were correlated to CIMT. An index extracted from PPG 2nd derivative (b/a ratio) was found to be a good measure of high-risk of atherosclerosis in parallel with CIMT measurement. In addition, pulse pressure (PP) which is an indicator of arterial stiffness, was found to be positively correlated to CIMT. PP, b/a index and subject's height (H) were used to predict a high-risk of atherosclerosis by means of a logistic regression model. The developed model showed a sensitivity of 76.4% and specificity of 64.7% in the prediction of high-risk of atherosclerosis. In addition, the Nagelkerke R-square was better in backward logistic regression (0.372) compared to forward logistic regression (0.288). Thus increases in thickness of the intima and media of the carotid artery, as measured by CIMT, are directly associated with a decreased of b/a index values and increased of PP values. Thereby, PPG is recommended to be used as an assistant technique in the prediction of high-risk of atherosclerosis.

Key words: Photoplethysmogram (PPG), carotid intima-media thickness (CIMT), pulse pressure (PP), arterial stiffness and atherosclerosis.

INTRODUCTION

Coronary heart disease (CHD) or coronary artery disease (CAD) is generally caused by a condition called atherosclerosis, which occurs when fatty material and a substance called plaque builds-up on the walls of our arteries. Thickening and loss of elasticity of the coronary arteries occurs, leading to progressive insufficiency of the arteries and they start narrowing. Understanding the process of atherosclerosis would go a long way in helping to develop methods for prevention and treatment of such a disease. A marked increase in the incidence of coronary artery disease and death rates has been reported in both hemodialysis (HD) and diabetic

*Corresponding author. E-mail: ykchalacheh@gmail.com.

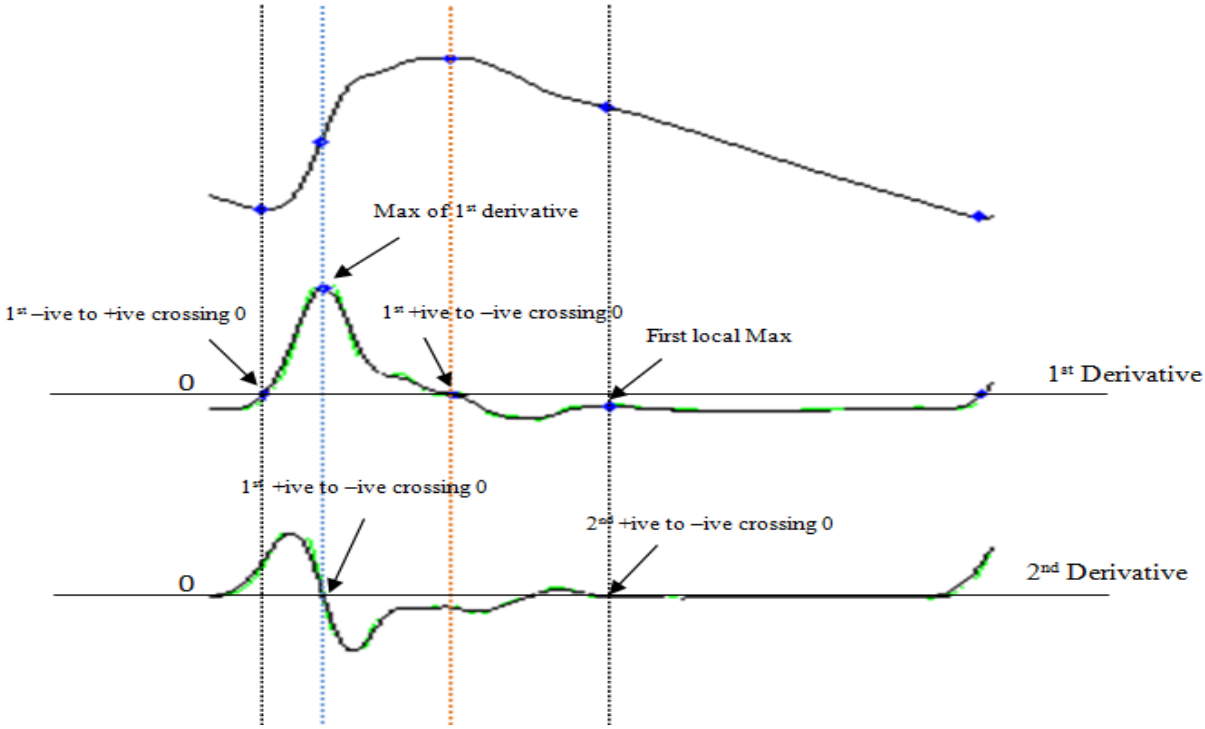

Figure 1. Description of the process of locating points of interest from PPG waveform and its 1st and 2nd derivatives (recorded PPG and its derivatives).

patients when compared with an age-matched general population (Koch et al., 1997). Atherosclerotic CVDs are a significant cause of morbidity and mortality for patients with end-stage renal disease (ESRD) (Fujisawa et al., 2000; Lindner et al., 1974; Dursuna et al., 2009). The major risk factors for atherosclerosis are serum lipid concentrations, smoking, and hypertension. Carotid intima-media thickness (CIMT) test is an established method for the measurement of atherosclerosis. The common carotid artery in the neck is accessed by an ultrasound probe, which in turn allows the measurement of the thickness of the inner two layers the carotid called the intima and media by high frequency sound waves. CIMT is costly and operator dependent which raises the desire of having an assistance tool which can be used to predict the high-risk of atherosclerosis in an easier, simple, operator independent, and low cost method. Photoplethysmogram (PPG) is an optoelectronic method for measuring and recording changes of blood volume of a body part. PPG signals have been applied in many different settings including clinical physiological monitoring, vascular assessment and autonomic function (Gonzalez et al., 2008). Atherosclerosis plays an important role in the propagation of blood stream since it accelerates blood velocity and harms the elastic properties of arteries.

The second derivative wave had characteristic contours that facilitated the interpretation of the original PPG (Takazawa et al., 1998). However, a sophisticated approach to contour analysis of the PPG has been developed by investigators in Japan (Takazawa et al., 1998; Takada et al., 1997). Imanaga et al. (1998) have proposed using the second derivative of PPG (SDPPG). This facilitates the distinction of five sequential waves called a, b, c, d and e waves. The relative heights of these waves (b/a, c/a, d/a and e/a ratios), have been related to age, arterial blood pressure, large artery stiffness and effects of vasoactive drugs. The indices calculated from the SDPPG waveforms are reported to correlate closely with both the distensibility of the carotid artery (Imanaga et al., 1998) and the central augmentation index (AIx) (Takazawa et al., 1998), suggesting the SDPPG indices may be a surrogate measure of arterial stiffness. Several previous studies showed that the SDPPG indices are associated with age (Hashimoto et al., 2005; Otsuka et al., 2006; Hashimoto et al., 2002; Ohshita et al., 2004), blood pressure (BP) (Hashimoto et al., 2005; Otsuka et al., 2006; Hashimoto et al., 2002), the estimated risk of coronary heart disease (Otsuka et al., 2006), and the presence of atherosclerotic disorders (Bortolotto et al., 2000). The dyslipidemia was independently associated with the b/a, Figure 1 illustrates PPG waveform, its 1st and 2nd derivatives, and the process of points locating.

Arterial stiffness is an independent risk factor of cardiovascular disease (Arnett et al., 1994), and pulse

pressure, a surrogate marker of increased arterial stiffness, is a powerful predictor of cardiovascular (CV) events (Franklin et al., 1999; Klocke et al., 2003). The aim of our work was to study the characteristics of PPG that can be used to predict high-risk atherosclerosis and to explore any relation between CIMT and PPG indices in these patients. We determined HRART as an indicator of atherosclerosis.

MATERIALS AND METHODS

Subjects and protocol

The study is conducted in Urology Clinic in the National University of Malaysia Medical Centre (PPUKM). PPUKM is a Teaching Medical Centre with 750 beds. The Medical Centre provides health services to most of the population around Kuala Lumpur as well the State of Selangor. The study was approved by the PPUKM ethics community review. Each patient was informed about the details of the study and their written consent was taken before the recordings were made. Patients were subject to obeying some inclusion criteria (high risks (hypertension, diabetes mellitus, dyslipidaemia, obesity, smoking, and significant family history) and no cardiovascular disease or risks at all) and to some exclusion criteria as well (establish cardiovascular disease, liver cirrhosis, renal failure, thyroid disease and spinal cord injuries and finger or having Raynauld's). PPG measurements were collected from the right and left index fingers of the 68 participants with ages ranging from 30 to 78 years and median age 56 years (all male). The samples were classified into two groups, 34 each (case group who had a CIMT value greater than 0.7 mm and control group who has CIMT value less than or equal to 0.7 mm). A written consent was taken from each participant. The data was recorded from a longitudinal study initially undertaken for the assessment of endothelium dysfunction in subjects presented with erectile dysfunction. The subjects were from three different races in Malaysia (Malay, Chinese and Indian).

Hardware and data acquisition

PPG pulse measurements collected simultaneously from the right and left index fingers to study and analyze arterial conditions. After subjects were rested for five minutes, PPG recordings was carried out for duration of 90 s. During the measurements, subjects were quiet, and breathed normally while resting in a supine position. PPG measurements were performed in hospital conditions at room temperature (24±1°C). A special National Instruments with Data Acquisition Board (NI cDAQ-9172) was used to digitize the signals locally and transmit the digital data to the personal computer with sampling rate of 5500 Hz. The recorded signals were analyzed off-line using customized algorithms developed in MATLAB (The MathWorks, Inc). These filters did not introduce phase delays or distortion to the waveforms (Edmond et al., 2007). Utilizing PPG derivatives, PPG's points of interest can be located and determined (Mustafa, 1997; Rubins et al., 2008; Qawqzeh et al., 2010).

Signal processing

A customized algorithm written in Matlab is used to analyze the contour of PPG signal. Contour or morphology analysis depends mainly on the detection of PPG's inflection peak (second peak or diastolic peak) since it tends to be less pronounced in most cases, especially aging and diabetic PPGs. However, among 12 variables extracted from PPG signal, an index derived from SDPPG (b/a ratio) is found to be a promising tool to assist the process of prediction high-risk atherosclerosis. The algorithm loads PPG data (txt file), PPG signals are down-sampled (275 Hz), de-trended for removing outliers, drifts, offset and any movement artifacts. Next PPG signals are band-pass filtered (0.6 to 15 Hz) for removing the effect of the respiratory rhythm and higher frequency disturbances. PPG 1st and 2nd derivatives are evaluated. PPG inflection point is determined as the first local maximum of PPG 1st derivative and it can be confirmed by the 2nd positive-to-negative crossing zero of SDPPG. In our study, b/a and c/a waves of SDPPG are evaluated and extracted. In real experiment, PPG wave is very sensitive to noise and artifacts, therefore, it needs good filtering and those unstable waveforms need to be excluded from any calculations, to avoid affecting the normal trend of the measurements. Basically, all unclean PPG waveforms are excluded (since their b/a ratios are inaccurate).

Statistical analysis

Descriptive analysis was summarized by means and standard deviations, while Pearson correlation test was used to assess the relationship between CIMT and PPG. Bland-Altman test was performed to know the degree of agreement between CIMT and PPG. The value of CIMT greater than (0.7 mm) is considered high-risk of atherosclerosis. A new index was derived from CIMT named as HRART is used to represent the presence or absence of atherosclerosis. CIMT value ≤ 0.7 represents 0 (No-Risk) and CIMT value > 0.7 represents 1 (High-Risk)). Predictive equations of high risk of atherosclerosis were produced by using stepwise multiple logistic regression analyses. MedCalc software version 11.4.4 is used to obtain receiver operating characteristics (ROC) curve and area under curve (AUC). P-value with less than 0.05 was interpreted as statistically significant. All analysis' were carried out by using Predictive Analytics Software (PASW, formerly known as SPSS) version 11.5 and MedCalc software version 11.4.2.0. HRART was taken as dependent variable.

RESULTS

The baseline characteristics of the study subjects are shown in Table 1. The mean age was 56.5±9.8 years. The comparison between b/a index (the relative height of b wave to a wave) and CIMT data showed a good agreement which raised the ability of using b/a index as assistance tool for the prediction of risk of atherosclerosis. CIMT was significantly correlated with age, b/a, max ejection time (MET), pulse pressure (PP), and subject's height (H). The rest of the variables showed no significance statistically.

Logistic regression is used to identify the factors that contributed to the risk of atherosclerosis. All the factors (BMI, SP, DP, MAP, Age, H, PT, MET, ST, DT, PPT, SI, MEV, PM, DM, RI, b/a and c/a) are tested one by one using (ENTER) method. Only (Age, b/a, H, and PP) is significant. In the multiple logistic regression, all the significant factors are included. Forward and backward stepwise procedures were performed to identify the risk factors and controlling for the confounding effect. In the forward stepwise procedure, only b/a and height are significant. The characteristics of forward method are shown in Table 2. In the other side, when (Backward: LR)

Table 1. Clinical and demographic characteristics of subjects.

Characteristic	N	Mean	Standard deviation
AGE	68	56.5	9.8
BMI	68	26	4.2
CIMT	68	0.84	.36
DP	68	82	7
H	68	167	6.4
MAP	68	101	7.3
PP	68	56	9
SP	68	138	10.6
Valid N (listwise)	68		

The values are expressed as mean±SD. H, subject's height; BMI, body max index; CIMT, carotid-intima-media thickness; DP, diastolic pressure; MAP, main arterial pressure; PP, pulse pressure; SP, systolic pressure.

Table 2. Forward: LR characteristics.

Factor-Model	B	S.E	Sig.	Exp (B)
b/a ratio	-5.465	1.9	0.006	0.004
H	-0.117	0.5	0.020	0.890
Constant	23.796	8.7	0.006	2.1025e+010
The Nagelkerke R^2 is 0.288				

Table 3. Backward: LR characteristics.

Factor-Model	B	S.E	Sig.	Exp (B)
b/a ratio	-4.758	2.00	0.019	0.009
H	-0.123	0.050	0.018	0.884
PP	0.066	0.037	0.040	1.069
Constant	20.696	8.90	0.020	9.7310e+008
The Nagelkerke R^2 is 0.372				

logistic regression is used, the model performed better. The characteristics of backward: LR is shown in Table 3.

In the forward: LR method, the Nagelkerke R-square was 0.288 which means that, b/a index and H contribute 28.8% to the risk of atherosclerosis, while other 71.2% are contributed by other factors that are not tested in this work.

However, backward: LR method gave better results since Nagelkerke R-square was 0.372 which means that, b/a index, H, and PP contribute 37.2% to the risk of atherosclerosis, while other 62.8% are contributed by other factors that are not tested in this work.

HRART was negatively correlated with b/a ratio. This indicated that, a reduction of b/a value may reflect the presence of high-risk atherosclerosis. In contrast, PP which is an indicator or atherosclerosis processes (Solonevich and Cobb, 1975), was positively correlated with HRART which in turn, confirm the association between hypertension and atherosclerosis. The implemented model showed a sensitivity of 76.5 and a specificity of 64.7 in the detection of true-positive and true-negative respectively. The receiver operating characteristics (ROC) curve for b/a ratio vs. HRART is shown in Figure 2. In addition, ROCs for all factors of the developed model are shown in Figure 3.

Mainly, our interest is to use the logistic model to predict the outcome for a new subject. When we have a new subject, the developed model can be used to predict the probability of having high-risk atherosclerosis. Let us say that, we have the inputs of b/a index, PP and H of an individual subject and the output is a number between 0 and 1 which denotes the probability of the subject to having high-risk atherosclerosis. Therefore, the predictive equation from the developed statistical model given by

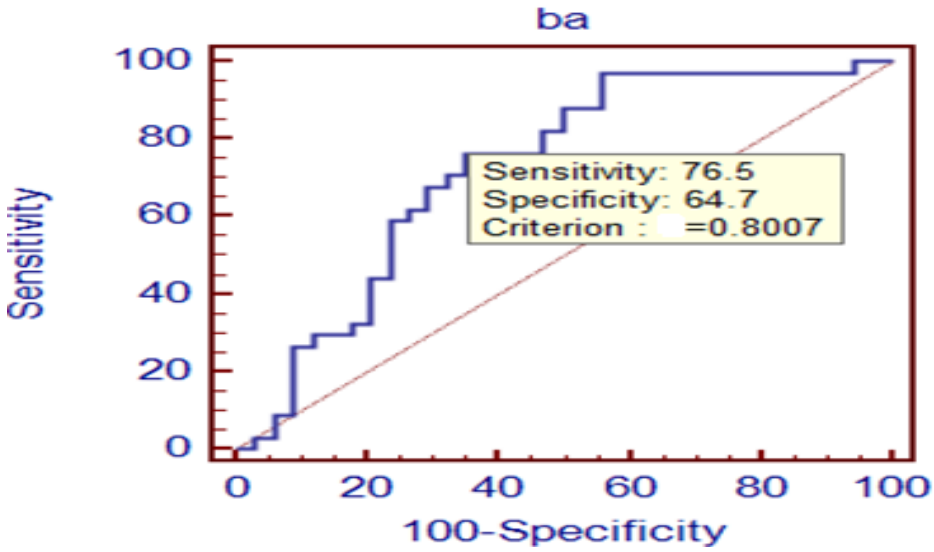

Figure 2. ROC curve of b/a ratio in the prediction of high-risk atherosclerosis.

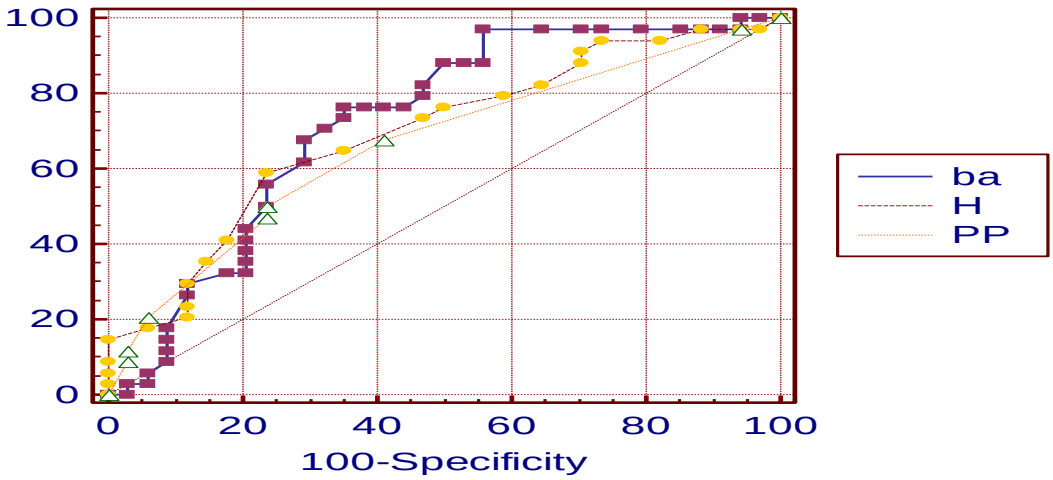

Figure 3. ROCs of all factors of the developed model in the prediction of high-risk atherosclerosis.

with Y (Model's outcome) = 20.696 – 4.758*b/a + 0.066*PP – 0.123*H. Therefore, the probability of having high-risk atherosclerosis can be calculated as with HRART = Exp (Y) / (1+Exp (Y)). This tells us that increasing b/a value decreases the risk of atherosclerosis. Moreover, increasing PP increases the chance of being under high-risk atherosclerosis. Finally, increasing height decreases the risk of atherosclerosis.

DISCUSSION

The novelty of this work is the evaluation of the independent determinants of the SDPPG (b/a ratio) among subjects with high-risk atherosclerosis as a factor for CVD by means of multiple logistic regression analysis.

In our study, we determined the presence of early sub clinical atherosclerosis in erectile dysfunction patients by measuring CIMT. CIMT represents a marker of structural atherosclerosis. We found a significant increase in CIMT compared to age, PP which is found to be a marker of arterial stiffness. An important finding in our study was the demonstration of a negative correlation between atherosclerosis as indicated by CIMT and b/a ratio. Based on our findings, we suggest the use of b/a ratio in addition to PP and subject's height as determinants of high-risk atherosclerosis in erectile dysfunction patients as an alternative method for the assessment of atherosclerosis. Figure 4 represents the grouping of b/a ratio based on HRART index.

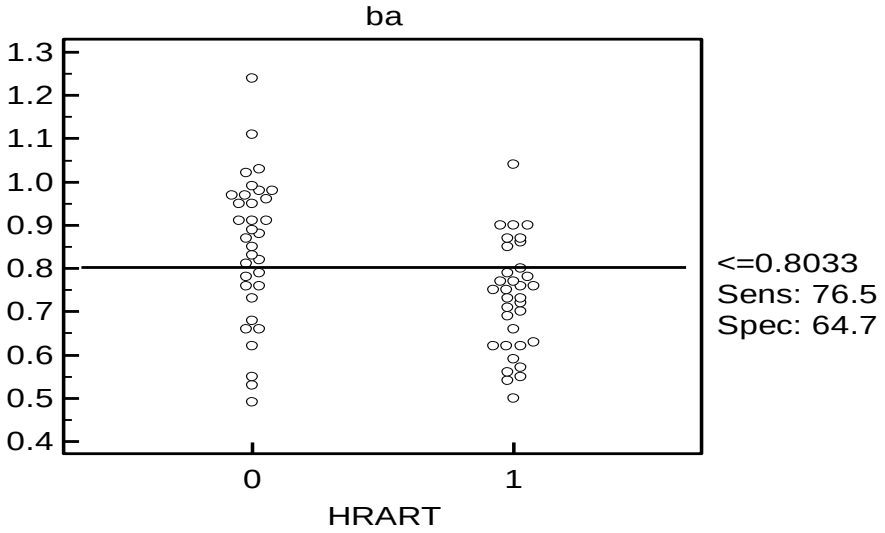

Figure 4. The interactive dot diagram of b/a index in the prediction of HRART.

Measuring the value of b/a ratio gives the opportunity to establish an alternative way of screening atherosclerosis. The fluctuations of PPG's morphology, observed by, normal PPG waveform, 1st PPG derivative waveform and 2nd PPG waveform, offer a window for screening the structural atherosclerosis. By its simple means, PPG (b/a) ratio therefore, can be utilized to track changes in the structural contents of atherosclerosis. Probably, the simplicity of running this proposed method encouraged further investigations to be implemented. As we are seeking to establish PPG technique, looking for its derivatives, relatively, gives a fruitful environment for more reliable and useful information for understanding changes to the structural atherosclerosis.

The major limitation of the study was the small size of the sample. The study is conducted to study and investigate the characteristics of PPG's indices that might yield better results in exploring the effects of atherosclerosis on erectile dysfunction patients. However, our study was the first study demonstrating a negative correlation between HRART and b/a ratio and a positive correlation between HRART and PP.

Conclusion

Atherosclerosis disturbances play an important role in the loss of elastic properties of arterial system, thereby, affecting the propagation of blood stream. CIMT used to screen carotid intima-media arteries in order to provide a window to the amount of hardening and stiffness of arteries. PPG is a non-invasive technique which reflects blood volume changes in arteries close to the skin. However, SDPPG is shown to be useful in explaining and understanding the characteristics of PPG waveform variations. The index b/a ratio is found to be useful in the assessment of the prediction of high-risk of atherosclerosis in parallel with CIMT. We concluded that, SDPPG's b/a ratio is a promising tool that might be used as a negative determinant of sub-clinical prediction of high-risk of atherosclerosis.

ACKNOWLEDGMENT

The authors would like to thank Universiti Kebangsaan Malaysia for sponsoring this work under the Research University Grant: UKM-AP-TKP-07-2009.

REFERENCES

Arnett D, Evans G, Riley W (1994). Arterial stiffness: A new cardiovascular risk factor? Am. J. Epidemiol., 140: 669-682.

Bortolotto L, Blacher J, Kondo T, Takazawa K, Safar M (2000). Assessment of vascular aging and atherosclerosis in hypertensive subjects: Second derivative of photoplethysmogram versus pulse wave velocity. Am. J. Hypertens., 13: 165-171.

Dursuna B, Dursunb E, Suleymanlarc G, Ozbend B, Capraze I, Ali Apaydine, Tomris Ozben (2009). The effect of hemodialysis on accelerated atherosclerosis in diabetic patients: correlation of carotid artery intima media thickness with oxidative stress. J. Diabetes Complicat., 23: 257-264.

Edmond Z, Kalaivani C, Mohd A, Harwant S (2007). Analysis of the Effect of Ageing on Rising Edge Characteristics of the Photoplethysmogram using a Modified Windkessel Model. Springer Sci. Bus. Media, pp. 172-181.

Franklin S, Khan S, Wong N, Larson M, Levy D (1999). Is pulse pressure useful in predicting risk for coronary heart disease? The Framingham heart study. Circular, 100: 354-360.

Fujisawa M, Haramaki R, Miyazaki H, Imaizumi T, Okuda S (2000). Role of lipoprotein (a) and TGF beta 1 in atherosclerosis of hemodialysis patients. J. Am. Soc. Nephrol., 11: 1889-1895.

Gonzalez R, Manzo A, Delgado J, Padilla J, Trenor B, Saiz J (2008). A computer based photoplethysmographic vascular analyzer through derivatives. Comput. Cardiol., 35: 177.

Hashimoto J, Watabe D, Kimura A, Takahashi H, Ohkubo T, Totsune K,

Imai Y (2005). Determinants of the second derivative of the finger photoplethysmogram and brachial ankle pulse wave velocity: The Ohasama study. Am. J. Hypertens., 18: 477-485.
Hashimoto J. Watabe D, Kimura A, Takahashi H, Ohkubo T, Totsune K, Imai Y. (2002). Pulse wave velocity and the second derivative of the finger photoplethysmogram in treated hypertensive patients: their relationship and associating factors. J. Hypertens., 20: 2415-2422.
Imanaga I, Hara H, Koyanagi S Tanaka K (1998). Correlation between wave components of the second derivative of plethysmogram and arterial distensibility. Jpn. Heart J., 39: 775-784.
Klocke R, Cockcroft J, Taylor G, Hall I Blake D (2003). Arterial stiffness and central blood pressure, as determined by pulse wave analysis, in rheumatoid arthritis. Ann. Rheum Dis., 62: 414-418.
Koch M, Gradaus F, Schoebel C, Leschke M, Grabensee B (1997). Relevance of conventional cardiovascular risk factors for the prediction of coronary artery disease in diabetic patients on renal replacement therapy. Nephrol. Dialysis Transplant, 12: 1187-1191.
Lindner A, Charra B, Sherrard J, Scribner BH (1974). Accelerated atherosclerosis in prolonged maintenance hemodialysis. New England J. Med., 290: 697-701.
Mustafa K (1997). A system for analysis of arterial blood pressure waveforms in humans. Comput. Biomed. Res., 30: 244-255.
Ohshita K, Yamane K, Ishida K, Watanabe H, Okubo M, Kohno N (2004). Post challenge hyperglycaemia is an independent risk factor for arterial stiffness in Japanese men. Diabet. Med., 21: 636-639.
Otsuka T, Kawada T, Katsumata M, Ibuki C (2006). Utility of second derivative of the finger photoplethysmogram for the estimation of the risk of coronary heart disease in the general population. Circ. J., 70: 304-310.
Qawqzeh Y, Mohd A, Mamun R, Maskon O (2010). Photoplethysmogram peaks analysis in patients presenting with erectile dysfunction. Proceedings of the International Conference on Electrical Computer Technology (ICECT), p. 165-168.
Rubins U, Grube J, Kukulis I (2008). Photoplethysmography analysis of artery properties in patients with cardiovascular diseases. IFMBE Proc., pp. 319-322.
Solonevich R, Cobb E (1975). Relationship between pulse pressure, arteriosclerosis a visual reversal phenomenon. Percept. Mot. Skills, Dec., 41: 939-949.
Takada H, Washino K, Harrel J, Iwata H (1997). Acceleration photoplethysmography to evaluate aging effect in cardiovascular system. Using new criteria of four wave patterns. Med. Prog. Technol., 21: 205-210.
Takazawa K, Tanaka N, Fujita Masami, Matsuoka O, Saiki T, Aikawa M, Tamura S, Ibukiyama C (1998). Assessment of vasoactive agents and vascular aging by the second derivative of photoplethysmogram waveform. Hypertens., 32: 365-370.

Scientific Research and Essays Vol. 7(25), pp. 2237-2241, 5 July, 2012
Available online at http://www.academicjournals.org/SRE
DOI: 10.5897/SRE11.192
ISSN 1992-2248 ©2012 Academic Journals

Full Length Research Paper

A pediatric oncology group pilot study on childhood cancers at the Chantal Biya Foundation Yaounde, Cameroon: Report of 350 cases

Enow-Orock G. E.[1]*, Pondy A.[2], Doumpe P.[2], Koki N.[2] and Lemerle J.[3]

[1]Pathology Service, General Hospital Yaounde, BP5408, Yaounde, Cameroon.
[2]Haemato-Oncology, GFAOP, Chantal Biya Foundation,Yaounde, Cameroon.
[3]Groupe Franco-Africaine d'Oncologie Pediatrique (GFAOP), Institut Gustave-Roussy, Villejuif, France.

Accepted 7 June, 2012

Cancer, especially in children is a public health problem in Cameroon. Suspected cases in the centre are biopsied and analysed in the Pathology Service of the Yaounde General Hospital. To find out the clinico-pathologic profile of patients seen at the centre, Clinical and Pathology registers of the two services were reviewed in this retrospective 3 years study from 2005 to 2007 and the data were analyzed. 350 specimens were analyzed in 3 years giving an annual average of 117.78.57% showed malignancy, 13.35% non-neoplastic diseases and 8.08% benign tumours. 55.7% were males, against 44.3% females. The predominant age group in both sexes was 5 to 14 years with peak at 5 to 9 years. The main diagnosis were Burkitt's lymphoma (40.86% of Acute lymphocytic leukemia (ALL) diagnosis, 52% of all malignancies and 54.79% of lymphomas). It is localised in the maxilllo-facial region (71%), abdomino-pelvic organs (17%) and eye (5%). Non Hodgkin lymphoma (NHL) (38.91%) was second commonest and the predominant type of NHL is non-Hodgkin's lymphoblastic lymphoma (26.29%). Among the cancers are rare malignancies that include nephroblastomas (0.73%), neuroblastomas (0.36%), Kaposi sarcoma (1.09%) hepatocellular carcinoma (0.36%) and soft tissue sarcomas (1.82%). Diagnosis was by fine-needle aspiration cytology (97.5%). The study reveal that childhood tumours are not rare in Cameroon. The commonest pathology seen at the Haemato-Oncology Service of the Chantal Biya Foundation is a lymphoma, mainly a Burkitt's. Late and adolescent childhood age groups are mostly affected. The pilot centre statistics reflect trends and patterns of pediatric cancers nationally. More indepth studies are recommended.

Key words: Acute lymphocytic leukemia (ALL) diagnosis, Cameroon, childhood cancers.

INTRODUCTION

In Africa, and Cameroon in particular, statistics on childhood malignancies are rare and fragmented (Lemerle et al., 2003). Malignant disease has been recognised in the past decades as a public health problem in near equal proportions to infectious diseases and malnutrition in developing countries (Abondo et al., 1994). In Cameroon, a sub-saharan country in the Central African sub-region, there have been many studies on neoplastic diseases. In most of the studies, lymphoproliferative malignancies in general and Burkitt's lymphoma in particular have been cited as predominant, especially in the children (Mbakop et al., 1996). The Groupe Franco-Africaine d'Oncologie pediatrique (GFAOP) Yaounde Pilot Centre in the Chantal Biya Foundation is a specialized pediatric oncology structure that serves as referral for childhood malignancies from all over Cameroon and the sub-region.

*Corresponding author. E-mail: enowrock24@yahoo.com. Tel: (237)77716045.

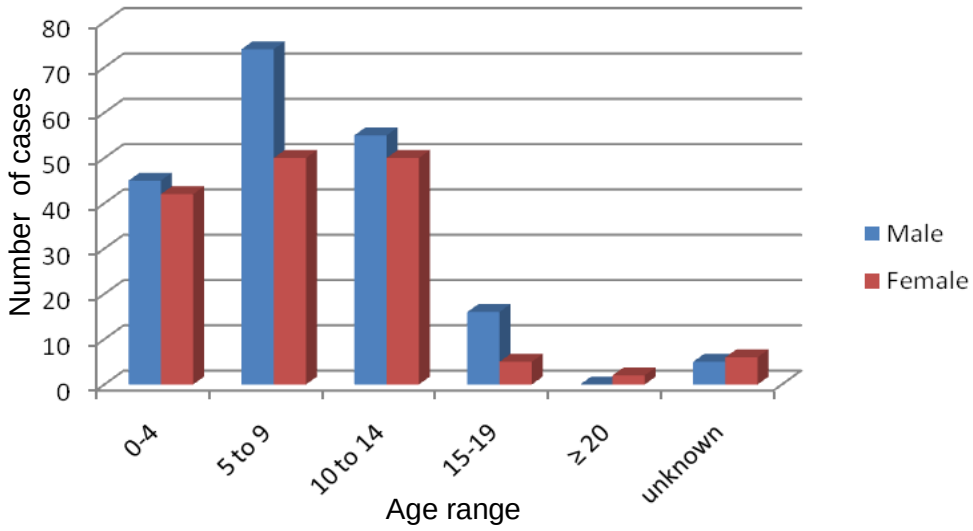

Figure 1. Age distribution by sex of cases seen at Chantal Biya Foundation between 2005 and 2007.

MATERIALS AND METHODS

Data from the registers of the Haemato-Oncology Service in the Chantal Biya Foundation Pilot Centre and the Pathology Service of the Yaounde General Hospital were consulted between 2005 and 2007. All patients with microscpically confirmed childhood cancers were recruited. The clinical and pathological data was analyzed. All cases out of the study period were rejected.

RESULTS

350 specimens were analyzed in 3 years giving an annual average of 117.78.57% showed malignancy, 13.35% non-neoplastic and 8.08% benign. 55.7% were males, against 44.3% females. The predominant age group in both sexes was 5 to 14 years with peak at 5 to 9 years. Main diagnosis were Burkitt's lymphoma at 40.86% of Acute lymphocytic leukemia (ALL) diagnosis, 52% of all malignancies and 54.79% of lymphomas. The tumour is localised in the maxilllo-facial region (71%), abdomino-pelvic organs (17%) and eye (5%) (Figure 2). Non-Hodgkin's (NH) lymphoma was the second commonest finding (30.6% of ALL diagnosis, 38.91% of all malignancies and 43% of lymphomas). In this last category NH lymphoblastic lymphoma (26.29%) was the commonest type. Rare malignancies include nephroblastomas (0.73%), neuroblastomas (0.36%), Kaposi sarcoma (1.06%), hepatocellular carcinoma (0.36%) and soft tissue sarcomas (1.82%). Diagnosis was by fine-needle aspiration cytology (97.5%).

Both non-Hodgkin's (NH) and Burkitt's lymphoma (BL) lymphomas are more prevalent in male than female children in late and adolescent childhood (> 5 years). BL is more common in males in late childhood (5 to 9 years), while NHL is more prevalent in the adolescent male compared to females of same age (14 to 19 years). In early childhood (<5 years), NHL and BL have no sex predeliction. Generally, BL is a disease of early childhood, while NHL is a disease of late childhood to adolescence. The incidence of both NHL and BL falls sharply after 10 years and decreases exponentially to 20 years.

DISCUSSION

Specimens from 350 patients in the GFAOP Yaounde Pilot Centre were analyzed in 3 years at the Pathology Service of the General Hospital Yaounde, giving an average incidence of 117.78.57% of the specimens analysed showed a malignant lesion. This is higher than reports from previous studies in this population (Abena Obama et al., 1989). Generally, pediatric malignancies show a slight male predominance (55.7%) in our series, similar to findings in earlier reports (Mbakop et al., 1996) (Figure 1). The patients were mainly children below 14 years (90.29%), and the predominant age group involved in both sexes was 5 to 14 years with peak at 5 to 9 years (43.41%) (Mbakop et al., 1996). The diagnosis was microscopically confirmed mainly by Fine-Needle Aspiration Cytology (FNAC) (97.5% against 2.5% by histology). No post-biopsy complication was reported. FNAC has been reported to be a cheap, rapid, non-invasive and reliable diagnostic method for tumour diagnosis in low-resource communities like ours (Brown and Coghill, 1992). The average duration of hospitalization of the patients was 14 days and only 8.0% of the patients had a post-therapeutic control FNAC. Malignant non-Hodgkin's lymphoma is the main childhood cancer in our community. The commonest type

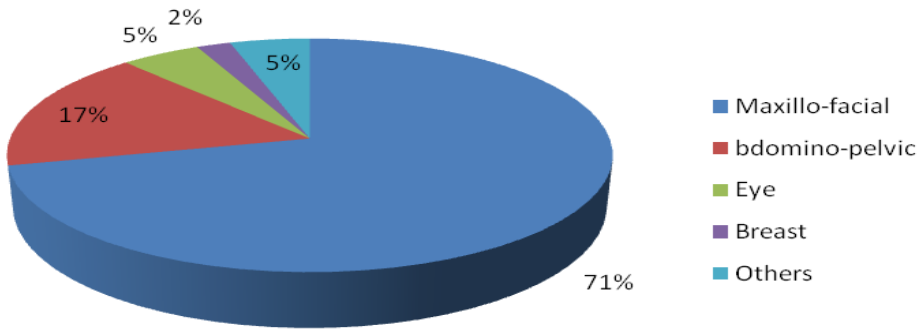

Figure 2. Localisation of Burkitt's lymphoma.

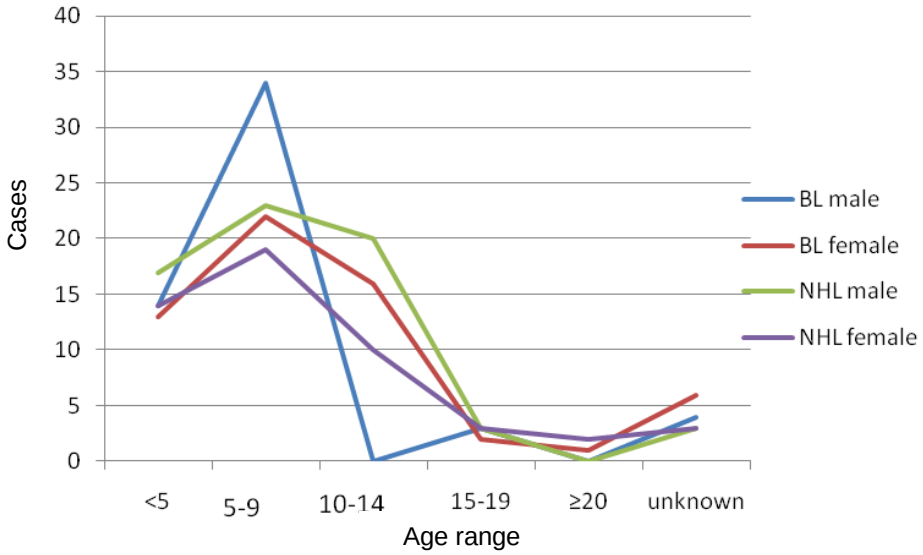

Figure 3. Distributon of BL and NHL by age and by sexes.

is Burkitt's lymphoma-BL (40.86% of all cases and 54.79% of lymphomas). It is predominant in the 5 to 9 years age range. Generally, and in each age group, BL is numerically more common in males than females, though with no statistically significant sex predilection (Figure 3). Lemerle et al. (2003) reported that BL is the most frequent cancer in children in subsaharan Africa, more than leucemias, and its preponderance in malaria endemic zones and relationship with Ebstein-Barr virus are established. They estimated about 8 to 12.000 new cases in 2004. The tumour is mainly localized in the maxilllo-facial region (71%), abdomino-pelvic organs (17%) and eye (5%). These findings were reported in some studies (Burkitt and O'connor, 1961) though others (Belly-Priso et al., 1999) observed an increasing abdomino-pelvic localization of the tumour especially in females.

The second most common tumour is NHL, particularly non-Hodgkin's lymphoblastic lymphoma (26.29% of all cases and 35.25% of all lymphomas). Other types of non-Hodgkin's lymphomas are rare (Table 2). Hodgkin's disease is not common in our study, accounting for only 2.80% of all lymphomas and 2.16% of all malignant lesions amongst the patients (Tables 1 and 2). This observation has been reported by Mbakop who observed that Hodgkin's disease is rare in both adults and children in Cameroon (Mbakop et al., 1991). Other rare malignancies in our series include nephroblastomas (0.73%), neuroblastomas (0.36%), Kaposi sarcoma (1.09%), hepatocellular carcinoma (0.36%) and soft tissue sarcomas (1.82%) (Table 1). This prevalence has been reported in earlier studies on this population. Although hepatoblastoma has been reported to be a common childhood liver tumour (Ishak and Glunz, 1967), in our series, hepatocellular carcinoma is more common, with a cytology similar to that found in adults (Weinberg and Finegold, 1983).

NH and BL show interesting trends among the various age groups in the 2 sexes. Both are more prevalent in male than female children in late and adolescent

Table 1. All malignant tumours by sex.

Diagnosis	Male	Female	Total cases	%
Hodgkin's lymphoma	3	3	6	2.18
Other NHL	61	46	107	38.91
Burkitt's lymphoma	79	64	143	52.00
Unspecified lymphoma	2	3	5	1.82
Nephroblastoma	1	1	2	0.73
Adenocarcinoma	1	1	2	0.73
Neuroblastoma	1	0	1	0.36
Hepatocellular carcinoma	1	0	1	0.36
Kaposi sarcoma	2	1	3	1.09
Soft tissue sarcoma	3	2	5	1.82
Total	154	121	275	100

Table 2. Distribution of lymphoma type by sex.

Diagnosis	Male	Female	Total cases	%
Burkitt	79	64	143	54.79
Lymphoblastic	52	40	92	35.25
Centroblastic	3	1	4	1.53
Lymphocytic	1	1	2	0.76
Lymphocytic/lymphoblastic	5	2	7	2.68
Lymphoma/leukemia	0	1	1	0.38
Hodgkin	3	3	6	2.30
Histiocytic	0	1	1	0.38
Unspecified	2	3	5	1.93
Total	145	116	261	100

Table 3. Non-malignant diagnosis by sex.

Diagnosis	Male	Female	Total	%
Leishmaniasis	0	1	1	1.6
Tuberculosis	4	4	8	12.9
Other Benign tumours	10	5	15	24.2
Reactive/inflammatory adenitides	17	10	27	43.6
Others	8	3	11	17.7
Total	39	23	62	100

childhood (>5 years). BL is more common in males in late childhood (5 to 9 years), while NHL is more prevalent in the adolescent male compared to females of same age (14 to 19 years) In early childhood (<5 years), NHL and BL have no sex predeliction (Figure 3). Generally, BL is a disease of early childhood, while NHL is a disease of late childhood and into adolescence. The incidence of both NHL and BL falls sharply after 10 years of age and decreases exponentially to 20 years in both sexes (Figure 3). These trends have been observed in past studies (Parkin et al., 1998). About 13.35% of all diagnosis in our study are non-neoplastic conditions like reactive or non-specific inflammatory adenitides and tuberculosis. In 8.08%, the disease was a benign tumour (Table 3).

Conclusion

Childhood tumours are not rare in Cameroon. The commonest pathology seen at the GFAOP Chantal Biya Foundation Pilot Centre is cancer, mainly NHL, and

predominantly a Burkitt's lymphoma. Other childhood cancers are rare. Late and adolescent childhood are the most commonly affected age group. At an annual incidence of 117, the centre receives pediatric oncology cases more than anywhere in the country. For their proper management, Fine Needle Aspiration Cytology has proven to be a reliable diagnostic procedure which not only distinguishes inflammatory from neoplastic but also between benign and malignant lesions. Further studies are recommended to find out trends in incidence, prevalence and disease outcome.

REFERENCES

Abena Obama MT, Befidi MR, Mbede J (1989). Childhood tumours, of 58 cases seen at the University Teaching Hospital Yaounde, Cameroon. Publ. Med. Afr., 2: 25-32.

Abondo A, Essomba R, Ngbangako M, Essame-Oyono JL, Mbakop A (1994). Cancer in Cameroon. Epidemiological aspects. Cahiers de l'I.M.P.M, 1: 5-40

Belly-Priso E, Mbakop A, Nkegoum B (1999). Anatomo-pathological aspects of ovarian Burkitt lymphoma. Report of 57 cases seen in Cameroon. Sem Hop Paris, 75: 31-32.

Brown LA, Coghill SB (1992). Cost effectiveness of a fine needle aspiration. Cl Cytopathol., 3: 275-280.

Burkitt D, O'connor GT (1961). Malignant lymphoma in African children. Cancer, 14: 258-269.

Ishak KG, Glunz PR (1967). Hepatoblastoma and hepatocellular carcinoma in infancy and childhood. Report of 47 cases. Cancer, 20: 396-422.

Lemerle J, Fouzia MA, Harif M, Kogum E, Ladjadj Y, Moreira C, Andriamparany RJ, Doumbe P (2003). Can childhood cancer be treated in Africa ? Action of the Franco African Pediatric Oncologie Group Med Ther, Ped., 6(3): 192-197.

Mbakop A, Doumbe P, Abena MT (1996). Childhood (0-15 years) cancer in Cameroon. Report of 179 cases seen in the Central Hospital , General Hospital and CHU Yaoundé. Sem Hop Paris, 72: 185-186.

Mbakop A, Essame-Oyono JL, Michel G, Owono D, Fewou A, Abondo A (1991). Hodgkin disease in Cameroon. Epidemiology and anatomo-clinical aspects. Arch. Anat. Cyto. Pathol., 39(3): 116-119.

Parkin DM, Kramarova E, Draper GJ, Masuyer E, Michaelis J, Neglia J, Qureshi S, Stiller CA (Eds) (1998). International Incidence of Childhood Cancer, Lyon, France: IARC Sci. Publ., 2: 144.

Weinberg AG, Finegold MJ (1983). Primary hepatic tumours of childhood. Human. Pathol., 14: 512-537.

Scientific Research and Essays Vol. 7(25), pp. 2242-2250, 5 July, 2012
Available online at http://www.academicjournals.org/SRE
DOI: 10.5897/SRE11.197
ISSN 1992-2248 ©2012 Academic Journals

Full Length Research Paper

Hybrid multiobjective evolutionary algorithm based technique for economic emission load dispatch optimization problem

A. A. Mousa[1,2]* and Kotb A. Kotb[2]

[1]Department of Basic Engineering Science, Faculty of Engineering, Menoufia University, Egypt.
[2]Department of Mathematics and Statistics, Faculty of Sciences, Taif University, Taif, El-Haweiah, P.O. Box 888, Zip Code 21974, Kingdom of Saudi Arabia (KSA).

Accepted 7 June, 2012

In this paper, we present a hybrid approach combining two optimization techniques for solving economic emission load dispatch (EELD) optimization problem. The proposed approach integrates the merits of both genetic algorithm (GA) and local search (LS), where it employs the concept of co-evolution and repair algorithm for handling nonlinear constraints, also, it maintains a finite-sized archive of non-dominated solutions which gets iteratively updated in the presence of new solutions based on the concept of ε-dominance. The use of ε-dominance also makes the algorithms practical by allowing a decision maker to control the resolution of the Pareto set approximation. To improve the solution quality, local search technique was implemented as neighborhood search engine where it intends to explore the less-crowded area in the current archive to possibly obtain more nondominated solutions. Several optimization runs of the proposed approach are carried out on the standard IEEE 30-bus 6-genrator test system. Simulation results with the proposed approach have been compared to those reported in literature. The comparison demonstrates the superiority of the proposed approach and confirms its potential to solve the multiobjective EELD problem.

Key words: Economic emission load dispatch, evolutionary algorithms, multiobjective optimization, local search.

INTRODUCTION

The purpose of economic emission load dispatch (EELD) problem is to figure out the optimal amount of the generated power for the fossil-based generating units in the system by minimizing the fuel cost and emission level simultaneously, subject to various equality and inequality constraints including the security measures of the power transmission/distribution. Various optimization techniques have been proposed by many researchers to deal with this multiobjective programming problem with varying degree of success.

Different techniques have been reported in the literature pertaining to economic emission load dispatch problem. In Brodesky and Hahn (1986) and Granelli et al. (1992), the problem has been reduced to a single objective problem by treating the emission as a constraint with a permissible limit. This formulation, however, has a severe difficulty in getting the trade-off relations between cost and emission. Alternatively, minimizing the emission has been handled as another objective in addition to usual cost objective.

A linear programming based optimization procedures in which the objectives are considered one at a time was presented in Farag et al. (1995). Unfortunately, the EELD problem is a highly nonlinear and a multimodal optimization problem. Therefore, conventional optimazation methods that make use of derivatives and gradients, in general, not able to locate or identify the global optimum. On the other hand, many mathematical

*Corresponding author. E-mail: a_mousa15@yahoo.com.

assumptions such as analytic and differential objective functions have to be given to simplify the problem. Furthermore, this approach does not give any information regarding the trade-offs involved.

In other research direction, the multiobjective EELD problem was converted to a single objective problem by linear combination of different objectives as a weighted sum (Chang et al., 1995; Dhillon et al., 1993; Xu et al., 1996; Zahavi and Eisenberg, 1985). The important aspect of this weighted sum method is that a set of Pareto-optimal solutions can be obtained by varying the weights. Unfortunately, this requires multiple runs as many times as the number of desired Pareto-optimal solutions. Furthermore, this method cannot be used to find Pareto-optimal solutions in problems having a nonconvex Pareto-optimal front.

In addition, there is no rational basis of determining adequate weights and the objective function so formed may lose significance due to combining non-commensurable objectives. To avoid this difficulty, the ε-constraint method for multiobjective optimization was presented in (Hsiao et al., 1994; Osman et al., 2004). This method is based on optimization of the most preferred objective and considering the other objectives as constraints bounded by some allowable levels. These levels are then altered to generate the entire Pareto-optimal set. The most obvious weaknesses of this approach are that it is time-consuming and tends to find weakly nondominated solutions.

Goal programming method was also proposed for multiobjective EELD problem (Kermanshahi et al., 1990. In this method, a target or a goal to be achieved for each objective is assigned and the objective function will then try to minimize the distance from the targets to the objectives. Although the method is computationally efficient, it will yield an inferior solution rather than a noninferior one if the goal point is chosen in the feasible domain. Hence, the main drawback of this method is that it requires a priori knowledge about the shape of the problem search space.

Heuristic algorithms such as genetic algorithm have been recently proposed for solving optimal power flow problem (Osman et al., 2004). The results reported were promising and encouraging for further research. Moreover the studies on heuristic algorithms over the past few years, have shown that these methods can be efficiently used to eliminate most of difficulties of classical methods (Abido, 2003a, Fonseca and Fleming, 1995). Since they are population–based techniques, multiple Pareto-optimal solutions can, in principle, be found in one single run.

In this paper, a hybrid multiobjective approach is proposed, which was based on concept of co-evolution and repair algorithm for handing constraints. ε-Dominance concept was implemented to maintains a finite-sized archive of non-dominated solutions which gets iteratively updated according to the chosen ε-vector. Also, local search method was introduced as neighborhood search engine where it intends to explore the less-crowded area in the current archive to possibly obtain more nondominated solutions.

MATERIALS AND METHODS

Here, we present a new technique combining two optimization techniques for solving economic emission load dispatch optimization problem (EELD).

Multiobjective optimization

Multiobjective optimization differs from the single objective case in several ways:

1. The usual meaning of the optimum makes no sense in the multiple objective case because the solution optimizing all objectives simultaneously is, in general, impractical; instead, a search is launched for a feasible solution yielding the best compromise among objectives on a set of, so called, efficient solutions;
2. The identification of a best compromise solution requires taking into account the preferences expressed by the decision-maker;
3. The multiple objectives encountered in real-life problems are often mathematical functions of contrasting forms.
4. A key element of a goal programming model is the achievement function; that is, the function that measures the degree of minimization of the unwanted deviation variables of the goals considered in the model. A general multiobjective optimization problem is expressed by:

Multiple objective programming (MOP):

$$\begin{aligned} \text{Min} \quad & \mathrm{F(x)} = (\mathrm{f_1(x), f_2(x), ..., f_m(x)})^{\mathrm{T}} \\ & \text{s.t.} \quad \mathrm{x} \in \mathrm{S} \\ & \mathrm{x} = (\mathrm{x_1, x_2, ..., x_n})^{\mathrm{T}} \end{aligned}$$

where $(f_1(x), f_2(x), ..., f_m(x))$ are the m objectives functions, $(x_1, x_2, ..., x_n)$ are the n optimization parameters, and $S \in R^n$ is the solution or parameter space.

Definition 1 (Pareto optimal solution): x^* is said to be a Pareto optimal solution of MOP if there exists no other feasible x (that is, $x \in S$) such that, $f_j(x) \le f_j(x^*)$ for all $j = 1, 2, ..., m$ and $f_j(x) < f_j(x^*)$ for at least one objective function f_j.

Definition 2 (Laumanns et al., 2002) (ε-dominance): Let $f : x \to R^m$ and $a, b \in X$. Then a is said to ε-dominate b for some ε > 0, denoted as $a \succ_\varepsilon b$, if and only if for $i \in \{1, ..., m\}$ $(1-\varepsilon) f_i(a) \le f_i(b)$ (Figure 1). Definition 3 (ε-approximate Pareto set): Let X be a set of decision alternatives and $\varepsilon > 0$. Then a set x_ε is called an ε-approximate Pareto set of X, if any vector $a \in x$ is ε-dominated by at least one

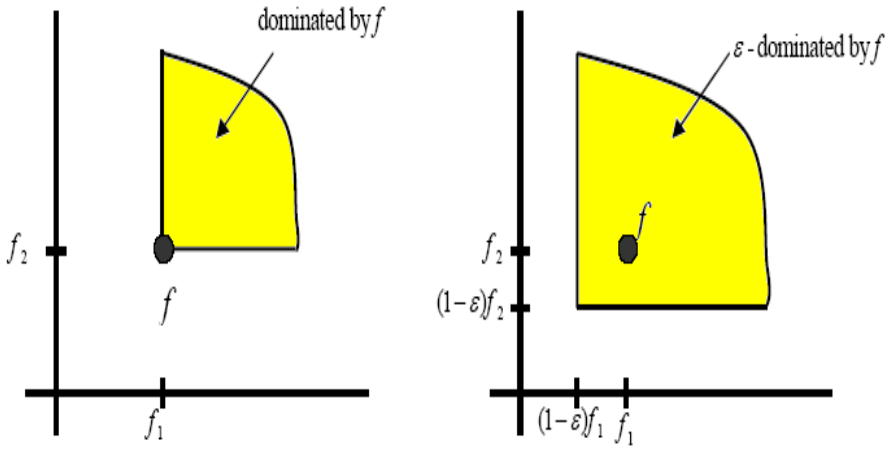

Figure 1. Graphs visualizing the concepts of dominance (left) and ε-dominance (right).

vector $b \in x_\varepsilon$, that is,

$$\forall a \in x : \exists b \in x_\varepsilon \; such \; that \; b \succ_\varepsilon a$$

According to definition 2, the ε value stands for a relative "tolerance" allowed for the objective values which was declared in Figure 1. This is especially important in higher dimensional objective spaces, where the concept of ε-dominance can reduce the required number of solutions considerably. Also, the use of ε-dominance also makes the algorithms practical by allowing a decision maker to control the resolution of the Pareto set approximation by choosing an appropriate ε value.

Economic emission load dispatch (EELD)

The economic emission load dispatch involves the simultaneous optimization of fuel cost and emission objectives which are conflicting ones. The deterministic problem is formulated as described subsequently.

Objective functions

Fuel cost objective: The classical economic dispatch problem of finding the optimal combination of power generation, which minimizes the total fuel cost while satisfying the total required demand can be mathematically stated as follows (Yokoyama et al., 1988):

$$f(\cdot) = C_t = \sum_{i=1}^{n} C_i(P_{Gi}) = \sum_{i=1}^{n} (a_i + b_i P_{Gi} + c_i P_{Gi}^2) \$/hr$$

where,

C: total fuel cost ($/hr), C_i: is fuel cost of generator i

a_i, b_i, c_i: fuel cost coefficients of generator i,

P_{Gi}: power generated (p.u)by generator i,

and n: number of generator.

Emission objective: The emission function can be presented as the sum of all types of emission considered, such as NO_x, SO_2, thermal emission, etc., with suitable pricing or weighting on each pollutant emitted. In the present study, only one type of emission NO_x is taken into account without loss of generality. The amount of NO_x emission is given as a function of generator output, that is, the sum of a quadratic and exponential function:

$$f_2(\cdot) = E_{NO_x} = \sum_{i=1}^{n} [10^{-2}(\alpha_i + \beta_i P_{Gi} + \gamma_i P_{Gi}^2) + \xi_i \exp(\lambda_i P_{Gi})] \; ton/hr$$

where, $\alpha_i, \beta_i, \gamma_i, \xi_i, \lambda_i$: coefficients of the *ith* generator's NO_x emission characteristic.

Constraints

The optimization problem is bounded by the following constraints:

Power balance constraint: The total power generated must supply the total load demand and the transmission losses.

$$\sum_{i=1}^{n} P_{Gi} - P_D - P_{Loss} = 0$$

where P_D : total load demand (*p.u.*), and P_{loss} : transmission losses (*p.u.*).

The transmission losses are given by (Hazarika and Bordoloi, 1991).

$$P_{Loss} = \sum_{i=1}^{n} \sum_{i=1}^{n} [A_{ij}(P_i P_j + Q_i Q_j) + B_{ij}(Q_i P_j - P_i Q_j]$$

where, n: number of buses, R_{ij}: series resistance connecting buses i

and j, V_i: voltage magnitude at bus I, δ_i : voltage angle at bus I, P_i: real power injection at bus i. Q_i: reactive power injection at bus i.

Maximum and minimum limits of power generation: The power generated P_{Gi} by each generator is constrained between its minimum and maximum limits, that is,

$$P_{Gi\min} \le P_{Gi} \le P_{Gi\max}, \qquad Q_{Gi\min} \le Q_{Gi} \le Q_{Gi\max},$$
$$V_{i\min} \le V_i \le V_{i\max}, \qquad i = 1,.....,n$$

where; $P_{Gi\min}$: minimum power generated, and $P_{Gi\max}$: maximum power generated.

Security constraints: A mathematical formulation of the security constrained EELD problem would require a very large number of constraints to be considered. However, for typical systems, the large proportion of lines has a rather small possibility of becoming overloaded. The EELD problem should consider only the small proportion of lines in violation, or near violation of their respective security limits which are identified as the critical lines. We consider only the critical lines that are binding in the optimal solution. The detection of the critical lines is assumed done by the experiences of the decision maker (DM). An improvement in the security can be obtained by minimizing the following objective function.

$$S = f(P_{Gi}) = \sum_{j=1}^{k} (|T_j(P_G)|/T_j^{\max})$$

where, $T_j(P_G)$ is the real power flow $T_j^{\max}$ is the maximum limit of the real power flow of the *j* th line and *k* is the number of monitored lines. The line flow of the *j th* line is expressed in terms of the control variables P_{Gs} , by utilizing the generalized generation distribution factors (GGDF) (Ng, 1981) and is as follows:

$$T_J(P_G) = \sum_{i=1}^{n} (D_{ji} P_{Gi})$$

where, D_{ji} is the generalized GGDF for line j, due to generator i

For secure operation, the transmission line loading S_l is restricted by its upper limit as

$$S_\ell \le S_{\ell\max}, \ell = 1,...., n_\ell$$

where n_ℓ is the number of transmission line.

Multiobjective formulation of EELD problem

The multiobjective EELD optimization problem is therefore formulated as:

$$Min \quad f_1(x) = C_t = \sum_{i=1}^{n} (a_i + b_i P_{Gi} + c_i P_{Gi}^2) \ \$/hr$$

$$Min \quad f_2(\cdot) = E_{NO_x} = \sum_{i=1}^{n} [10^{-2}(\alpha_i + \beta_i P_{Gi} + \gamma_i P_{Gi}^2) + \xi_i \exp(\lambda_i P_{Gi})] \ ton/hr$$

$$s.t. \quad \sum_{i=1}^{n} P_{Gi} - P_D - P_{Loss} = 0,$$
$$S_\ell \le S_{\ell\max}, \qquad \ell = 1,...., n_{Line},$$
$$P_{Gi\min} \le P_{Gi} \le P_{Gi\max} \qquad i = 1,.....,n$$
$$Q_{Gi\min} \le Q_{Gi} \le Q_{Gi\max} \qquad i = 1,.....,n$$
$$V_{i\min} \le V_i \le V_{i\max} \qquad i = 1,.....,n$$

The proposed algorithm

Recently, the studies on evolutionary algorithms have shown that these algorithms can be efficiently used to eliminate most of the difficulties of classical methods which can be summarized as:

1. An algorithm has to be applied many times to find multiple Pareto-optimal solutions.
2. Most algorithms demand some knowledge about the problem being solved.
3. Some algorithms are sensitive to the shape of the Pareto-optimal front.
4. The spread of Pareto-optimal solutions depends on efficiency of the single objective optimizer.

It is worth mentioning that the goal of a multiobjective optimization problem do not only guide the search towards Pareto-optimal front but also maintain population diversity.

Initialization stage

The algorithm uses two separate population, the first population $\boldsymbol{P}^{(t)}$ consists of the individuals which initialized randomly satisfying the search space (The lower and upper bounds), while the second population $\boldsymbol{R}^{(t)}$ consists of reference points which satisfying all constraints. However, in order to ensure convergence to the true Pareto-optimal solutions, we concentrated on how elitism could be introduced in the algorithm. So, we propose an archiving/selection (Laumanns et al., 2002) strategy that guarantees at the same time progress towards the Pareto-optimal set and a covering of the whole range of the non-dominated solutions. The algorithm maintains an externally finite-sized archive $\boldsymbol{A}^{(t)}$ of non-dominated solutions which gets iteratively updated in the presence of new solutions based on the concept of ε -dominance.

Repair algorithm

The idea of this technique is to separate any feasible individuals in a population from those that are infeasible by repairing infeasible individuals. This approach co-evolves the population of infeasible individuals until they become feasible. Repair process works as follows. Assume, there is a search point $\omega \notin \boldsymbol{S}$ (where $\boldsymbol{S}$ is the feasible space). In such a case, the algorithm selects one of the reference points (Better reference point has better chances to be selected), say $\boldsymbol{r} \in \boldsymbol{S}$ and creates random points $\bar{\boldsymbol{Z}}$ from the

segment defined between ω, r , but the segment may be extended equally on both sides determined by a user specified parameter $\mu \in [0,1]$. Thus, a new feasible individual is expressed as:

$$z_1 = \gamma.\omega + (1-\gamma).r, \quad z_2 = (1-\gamma).\omega + \gamma.r$$

where $\gamma = (1+2\mu)\delta - \mu$ and $\delta \in [0,1]$ is a random generated number

Local search (LS) stage

In this stage, we present modified local search technique (MLS) to improve the solution quality and to explore the less-crowded area in the external archive to possibly obtain more nondominated solutions nearby. We propose a MLS, which is a modification of Hooke and Jeeves (1961) method to be suitable for MOP. The general procedure of the MLS techniques can be described by the following steps.

Step1. Start with an arbitrary chosen point ($\left(X_n \in R^n\right) \in E^t$, and the prescribed step lengths Δx_i in each of the coordinate directions $u_i, i = 1,2,....,n.$ Set m = 0, assume that m is the size of E^t .

Step 2. Set *m = m + 1,* and *k = 1* where *k* is number of trial (*s.t.,* $k = 1,...,k_{\max}$) to obtain preferred solution than X_m .

Step 3. The variable x_i is perturbed about the current temporary base point X_m to obtain the new temporary base point $X_m^{'}$ as:

$$X_m^{'} = \begin{cases} X_m + \Delta x_i u_i & \text{if } f^+(\cdot) \succ f \\ X_m - \Delta x_i u_i & \text{if } f^-(\cdot) \succ \left(f(\cdot) \wedge f^+(\cdot)\right) \\ X_m & \text{if } f(\cdot) \succ \left(f^+(\cdot) \wedge f^-(\cdot)\right) \end{cases} \quad \forall i=1,2,...,n$$

Where, $f(\cdot) = f\left(X_m\right)$, $f^+(\cdot) = f\left(X_m + \Delta x_i u_i\right)$, and $f^-(\cdot) = f\left(X_m - \Delta x_i u_i\right)$. Assume $f(\cdot)$ is the evaluation of the objective functions at a point.

Step 4. If the point X_m unchanged. While the number of trial *k* is not satisfied, reduce the step length Δx_i . The following dynamic equation is presented to reduce Δx_i ,

$$\Delta x_i = \Delta x_i \left(1 - (r)^{\frac{k}{k_{\max}}}\right), \quad r \in [0,1]$$

and go to step 3.

Step 5. Else, if $X_m^{'}$ is preferred than X_m (that is, $f\left(X_m^{'}\right) \succ f\left(X_m\right)$), The new base point is $X_m^{'}$.

Step 6. With the help of the base points X_m and $X_m^{'}$, establish a pattern direction *S* as;

$$S = X_m^{'} - X_m$$

and find a point $X_m^{''}$ as $X_m^{''} = X_m^{'} + \lambda S$,Where λ is the step length, (taken as 1).

Step 7. If $f\left(X_m^{''}\right) \succ f\left(X_m^{'}\right)$ set $X_m = X_m^{'}$, $X_m^{'} = X_m^{''}$, and go to 6.

Step 8. If $f\left(X_m^{''}\right) \not\succ f\left(X_m^{'}\right)$ set $X_m = X_m^{'}$, and go to 4.

These steps is implemented on all nondominated solutions in A^t to get the true Pareto optimal solution and to explore the less-crowded area in the external archive. The following shows the pseudo code of the MLS algorithm.

MLS technique

Start with $X_m \in E^t$

Generate $X_m^{'}$

While $(f\left(X_m^{'}\right) \prec f\left(X_m\right)$ stopped criterion satisfied) DO

If $X_m^{'} = X_m$

Reduce $\Delta x_i \rightarrow$ Generate $X_m^{'}$

End

Establish a pattern direction $S \rightarrow$ Generate $X_m^{''}$

If $f\left(X_m^{''}\right) \succ f\left(X_m^{'}\right)$, set $X_m = X_m^{'}$, $X_m^{'} = X_m^{''}$

Set $S \rightarrow$ Generate $X_m^{''}$

Else if $f\left(X_m^{''}\right) \prec f\left(X_m^{'}\right)$

$X_m = X_m^{'}$

End

End

Basic algorithm

It uses two separate population, the first population $\boldsymbol{P}^{(t=0)}$ (where t is the iteration counter) consists of the individuals which initialized randomly satisfying the search space, while the second population $\boldsymbol{R}^{(t)}$ consists of reference points which satisfying all constraints. Also, it stores initially the Pareto-optimal solutions externally in a finite sized archive of non-dominated solutions $\boldsymbol{A}^{(0)}$. We use cluster algorithm (Das and Patvardhan, 1998) to create the next population $\boldsymbol{P}^{(t+1)}$, if $|\boldsymbol{P}^{(t)}| > |\boldsymbol{A}^{(t)}|$ (that is, the size of the

population $\boldsymbol{P}^{(t)}$ greater than the size of archive $\boldsymbol{A}^{(t)}$) then new population $\boldsymbol{P}^{(t+1)}$ consists of all individual from $\boldsymbol{A}^{(t)}$ and the population $\boldsymbol{P}^{(t)}$ are considered for the clustering procedure to complete $\boldsymbol{P}^{(t+1)}$, if $|\boldsymbol{P}^{(t)}| < |\boldsymbol{A}^{(t)}|$ then $|P|$ solutions are picked up at random from $A^{(t)}$ and directly copied to the new population $P^{(t+1)}$.

Since our goal is to find new nondominated solutions, one simple way to combine multiple objective functions into a scalar fitness function is the following weighted sum approach:

$$f(x) = w_1 f_1(x) + ... + w_i f_i(x) + ... + w_m f_m(x) = \sum_{j=1}^{m} w_j f_j(x)$$

where x is a string (that is, individual), $f(x)$ is a combined fitness function, $f_i(x)$ is the *ith* objective function. When a pair of strings is selected for a crossover operation, we assign a random number to each weight as follows.

$$w_i = \frac{random_i(.)}{\sum_{j=1}^{m} random_j(.)}, \quad i = 1,2,..,m$$

Calculate the fitness value of each string using the random weights w_i. Select a pair of strings from the current population according to he following selection probability $\beta(x)$ of a string x in the population $P^{(t)}$.

$$\beta(x) = \frac{f(x) - f_{\min}(P^{(t)})}{\sum_{x \in P^{(t)}} \{f(x) - f_{\min}(P^{(t)})\}},$$

where $f_{\min}(P^{(t)}) = \min\{f(x) \mid x \in P^{(t)}\}$

This step is repeated for selecting $|P|/2$ Paris of strings from the current populations. For each selected pair apply crossover operation to generate two new strings, for each strings generated by crossover operation, apply a mutation operator with a prespecified mutation probability. The system also includes the survival of some of the good individuals without crossover or selection. This method seems to be better than the others if applied constantly.

The proposed algorithm is shown as follows:

1. t □ 0
2. Create $P^{(0)}, R^{(0)}$
3. $A^{(0)} = \text{nondominated}(P^{(0)})$
3. *while* terminate $(A^{(t)}, t) = false$ do
4. $t = t + 1$
5. $P^{(t)} = \text{generate}(A^{(t-1)}, P^{(t-1)})$ {generate new point}
6. $A^{(t)} = \text{update}(A^{(t-1)}, P^{(t)})$ {update archive }
7. *end while*
8. $A^{(t)} = LS(A^{(t)})$
9. Output : $A^{(t)}$

The purpose of the function *generate* is to generate a new population in each iteration *t*, possibly using the contents of the old population $P^{(t-1)}$ and the old archive set $A^{(t-1)}$ in associated with variation (recombination and mutation). The function *update* gets the new population $P^{(t)}$ and the old archive set $A^{(t-1)}$ and determines the updated one, namely $A^{(t)}$ as indicated as shown as follows (Algorithm of select operator):

1. *INPUT* A,x
2. D={x′ ∈ A:box(x) ≻ box(x′))
3. if D ≠ ϕ *then*
4. $A' = A \bigcup \{x\} \setminus D$
5. *else if* $\exists x' : (box(x') = box(x) \wedge x \succ x')$*then*
6. $A' = A \bigcup \{x\} \setminus \{x'\}$
7. *else if* $\nexists x' : (box(x') \succeq box(x))$*then*
8. $A' = A \bigcup \{x\}$
9. *else*
10. $A' = A$
11. *endif*
12. *OUTPUT* A'

The function *Ls* is to explore the less-crowded area in the current archive to possibly obtain more nondominated solutions which is declared in pseudo code of the MLS algorithm.

The algorithm maintains a finite-sized archive of non-dominated solutions which gets iteratively updated in the presence of a new solutions based on the concept of ε-dominance, such that new solutions are only accepted in the archive if they are not ε-dominated by any other element in the current archive (Algorithm of select operator). The use of ε-dominance also makes the algorithms practical by allowing a decision maker to control the resolution of the Pareto set approximation by choosing an appropriate ε value.

Implementation of the proposed approach

The described methodology is applied to the standard IEEE 30-bus 6-generator test system to investigate the effectiveness of the proposed approach. The values of fuel cost and emission coefficients are given in Table 1. For comparison purposes with the reported results, the system is considered as losses and the security constraint is released. The techniques used in this study were developed and implemented on 1.7-MHz PC using MATLAB environment. Table 2 lists the parameter setting used in the algorithm for all runs.

RESULTS

Figure 2 shows well-distributed Pareto optimal nondominated solutions obtained by the proposed algorithm after 200 generations after and before applying local search technique. Tables 3 and 4 show the best fuel cost and best NO_x emission obtained by proposed algorithm as compared to nondominated sorting genetic algorithm (NSGA) (Abido, 2003a), niched pareto genetic algorithm (NPGA) (Abido, 2003b) and strength pareto

Table 1. Generator cost and emission coefficients.

Parameter		G1	G2	G3	G4	G5	G6
Cost	a	10	10	20	10	20	10
	b	200	150	180	100	180	150
	c	100	120	40	60	40	100
Emission	α	4.091	2.543	4.258	5.426	4.258	6.131
	β	-5.554	-6.047	-5.094	-3.550	-5.094	-5.555
	γ	6.490	4.638	4.586	3.380	4.586	5.151
	ζ	2.0E-4	5.0E-4	1.0E-6	2.0E-3	1.0E-6	1.0E-5
	λ	2.857	3.333	8.000	2.000	8.000	6.667

Table 2. GA parameters.

Population size (N)	60
No. of generation	200
Crossover probability	0.98
Mutation probability	0.02
Selection operator	Roulette wheel
Crossover operator	BLX-α
Mutation operator	Polynomial mutation
Relative tolerance ε	10e-6

evolutionary algorithm (SPEA) (Abido, 2003c).

DISCUSSION

The results declare that, implementing local search improve the solution quality for the same approach Also, for different approaches. Also, it can be deduced that the proposed algorithm finds comparable minimum fuel cost and comparable minimum NO_x emission to the three evolutionary algorithms.

In this part of the study a comparative study has been carried out to assess the proposed approach concerning large size problem of the Pareto-set, DM preference and computational time. On the first hand, evolutionary techniques suffer from the large size problem of the Pareto-set. Therefore the proposed approach has been used to reduce the Pareto-set to a manageable size. However, the goal is not only to prune a given set, but also to generate a representative subset, which maintains the characteristics of the general set and take the DM preference into consideration. Some proposed approaches have been developed using cluster analysis to reduce the size of the Pareto-set, but unfortunately it does not concern the DM preference.

On the other hand, evolutionary techniques suffer from the quality of the Pareto set. Therefore the proposed approach has been used to increase the solution quality by combing the two merits of two heuristic algorithms, genetic algorithm and local search techniques. Where, the proposed algorithm implements local search (LS) technique as neighborhood search engine such that it intends to explore the less-crowded area in the current archive to possibly obtain more nondominated solutions to improve the solution quality.

Another advantage is that the simulation results prove superiority of the proposed approach to those reported in the literature, where it completely covers and dominates all Pareto-set found by the other approaches. Finally, the reality of using the proposed approach to handle on-line problems of realistic dimensions has been approved due to small computational time.

Conclusions

The approach presented in this paper was applied to economic emission load dispatch optimization problem formulated as multiobjective optimization problem with competing fuel cost, and emission. The algorithm maintains a finite-sized archive of non-dominated solutions which gets iteratively updated in the presence of new solutions based on the concept of ε-dominance. Moreover, local search is employed to explore the less-crowded area in the current archive to possibly obtain more nondominated solutions. The following are the significant contributions of this paper:

(a) The proposed technique has been effectively applied to solve the EELD considering two objectives simultaneously, with no limitation in handing more than two objectives.
(b) Allowing a decision maker to control the resolution of the Pareto set approximation by choosing an appropriate ε value.
(c) The proposed approach is efficient for solving nonconvex multiobjective optimization problems where multiple Pareto-optimal solutions can be found in one simulation run.
(d) Local search method is employed to explore the less-

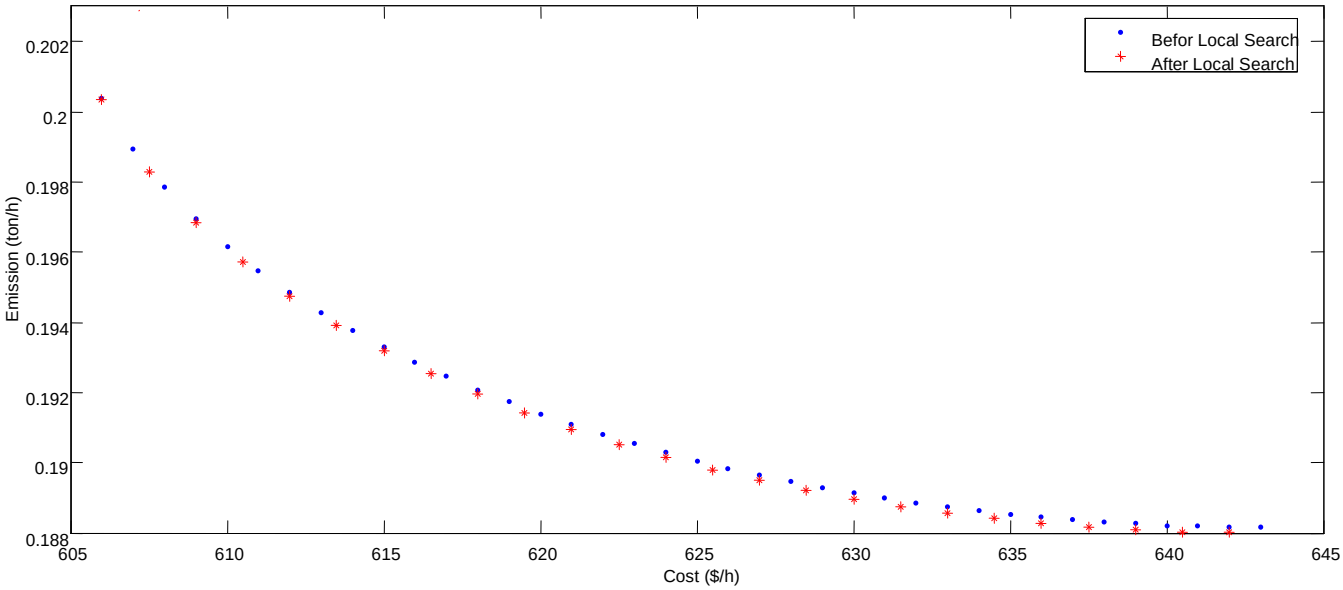

Figure 2. Pareto-optimal front of the proposed approach (before and after applying local search).

Table 3. Best fuel cost.

Parameter	NSGA	NPGA	SPEA	Proposed
P_{G1}	0.1168	0.1245	0.1086	0.1737
P_{G2}	0.3165	0.2792	0.3056	0.3568
P_{G3}	0.5441	0.6284	0.5818	0.5411
P_{G4}	0.9447	1.0264	0.9846	0.9890
P_{G5}	0.5498	0.4693	0.5288	0.4529
P_{G6}	0.3964	0.39993	0.3584	0.3705
Best cost	608.245	608.147	607.807	606.012
Corresponding emission	0.21664	0.22364	0.22015	0.20080

Table 4. Best NO_x Emission.

Parameter	NSGA	NPGA	SPEA	Proposed
P_{G1}	0.4113	0.3923	0.4043	0.3675
P_{G2}	0.4591	0.4700	0.4525	0.4904
P_{G3}	0.5117	0.5565	0.5525	0.5177
P_{G4}	0.3724	0.3695	0.4079	0.4512
P_{G5}	0.5810	0.5599	0.5468	0.5215
P_{G6}	0.5304	0.5163	0.5005	0.5304
Best cost	0.19432	0.19424	0.19422	0.1880
Corresponding emission	647.251	645.984	642.603	644.5346

crowded area in the current archive to possibly obtain more nondominated solutions.

(e) This work may be very valuable for on-line operation of power systems when environmental constraints are also needed to be considered. In addition to on-line operation, this work can be a part of an off-line planning tool when there are hard limits on how much emission is acceptable by a utility over a period of a month or a year.

For further work, we intend to solve large scale EELD problem with multiple dimension in a different vision using energy market which changes the role of dispatcher.

ACKNOWLEDGEMENTS

The authors are grateful to the anonymous reviewers for their valuable comments and helpful suggestions which greatly improved the paper's quality.

REFERENCES

Abido MA (2003a). A Niched Pareto Genetic Algorithm for Multiobjective Environmental/Economic Dispatch. Int. J. Elect. Pow., 25(2): 97-105.

Abido MA (2003b). A Novel Multiobjective Evolutionary Algorithm for Environmental/Economic Power Dispatch. Epsr., 65: 71-81.

Abido MA (2003c). Environmental/Economic Power Dispatch using Multiobjective Evolutionary Algorithms. IEEE T Power Syst., 18(4): 1529-1537.

Brodesky SF, Hahn RW (1986). Assessing the influence of power pools on emission constrained economic dispatch. IEEE Trans. Pow. Syst., 1(1): 57-62.

Chang CS, Wong KP, Fan B (1995). Security-constrained multiobjective generation dispatch using bicriterion global optimization. IEE Proc.-Gener. Transm. Distrib., 142(4) 406-414.

Das DB, Patvardhan C (1998). New Multi-Objective Stochastic Search Technique for Economic Load Dispatch. IEE Proc.-Gener. Transm. Distrib., 145(6): 747–752.

Dhillon JS, Parti SC, Kothari DP (1993). Stochastic economic emission load dispatch. EPSR., 26: 179-186.

Farag A, Al-Baiyat S, Cheng TC (1995). Economic load dispatch multiobjective optimization procedures using linear programming techniques. IEEE Trans. Power Syst., 10(2): 731-738.

Fonseca CM, Fleming PJ (1995). An overview of evolutionary algorithms in multiobjective optimization. Evol. Comput., 3(1): 1-16.

Granelli GP, Montagna M, Pasini GL (1992). Marannino P. Emission constrained dynamic dispatch. EPSR. 24: 56-64.

Hazarika D, Bordoloi PK (1991). Modified loss coefficients in the determination of optimum generation scheduling, IEE Proc., 138(2): 166-172.

Hooke R, Jeeves TA (1961). Direct search solution of numerical and statistical problems. J. ACM., 8(2): 212-229.

Hsiao YT, Chiang HD, Liu CC, Chen YL (1994). A computer package for optimal multi-objective VAR planning in large scale power systems, IEEE Trans. Power Syst., 9 (2): 668-676.

Kermanshahi BS, Wu Y, Yasuda, Yokoyama R (1990). Environmental marginal cost evaluation by non-inferiority surface, IEEE Trans. Power Syst. 5(4):1151-1159.

Laumanns M, Thiele L, Deb K, Zitzler E (2002). Archiving with Guaranteed Convergence And Diversity in Multi-objective Optimization. GECCO 2002: Proc. of the Genetic and Evolutionary Computation Conference, Morgan Kaufmann Publishers, New York, NY, USA., pp. 439-447.

Ng WY (1981). Generalized generation distribution factors for power system security evaluations. IEEE Trans. PAS. 100: 1001–1005.

Osman MS, Abo-Sinna MA, Mousa AA (2004). A Solution to the Optimal Power Flow Using Genetic Algorithm. AMC. 155: 391-405.

Xu JX, Chang CS, Wang XW (1996). Constrained multiobjective global optimization of longitudinal interconnected power system by genetic algorithm. IEE Proc.-Gener. Transm. Distrib. 143 (5):435-446.

Yokoyama R, Bae SH, Morita T, Sasaki H (1988). Multiobjective generation dispatch based on probability security criteria. IEEE Trans. Power Syst., 3(1): 317-324.

Zahavi J, Eisenberg L (1985). Economic-environmental power dispatch, IEEE Trans. Syst. Man, Cybern. SMC., 5(5): 485-489.

Related Journals: